Clinoforms and clinoform systems: Review and dynamic classification scheme for shorelines, subaqueous deltas, shelf edges and continental margins

Stefano Patruno[a,1], William Helland-Hansen[b,*]

[a] *PGS, Weybridge, United Kingdom*
[b] *University of Bergen, Norway*

ABSTRACT

Clinoforms are inclined and normally basinward-dipping horizons developed over a range of spatial and temporal scales in both siliciclastic and carbonatic systems. The study of clinoform successions underpins sequence stratigraphy and all efforts to reconstruct the relative partitioning of reservoir, seal and source rocks along shoreline to basin-floor profiles.

Here, we review clinoform research and propose a more systematic description and classification of clinoforms. This is a crucial step to improve predictions of facies and lithology distribution within shoreline to continental shelf and abyssal plain successions, together with the genesis, drivers and dynamics of their constituent sedimentary units.

Four basic clinoform types are here distinguished in delta/shorelines, lacustrine and marine environments, on the basis of their overall spatial and temporal scale, morphology, outbuilding dynamic and geodynamic and depositional setting: (1, 2) delta-scale clinoforms, which in turns are sub-divided into shoreline and delta-scale subaqueous clinoforms; (3) shelf-edge clinoforms; and (4) continental-margin clinoforms. Delta-scale clinoform sets are tens of metres high and typically represent $1–10^3$ kyr, with progradation rates ranging from 1,000–100,000 m/kyr for shorelines and "subaerial deltas" to 100–20,000 m/kyr for subaqueous deltas; shelf-edge clinoform sets are hundreds of metres high and are nucleated and accreted in 0.1–20 Myr (usual progradation rates of 1–100 m/kyr) by successive cross-shelf transits of delta-scale clinoforms; continental-margin clinoform sets are thousands of metres high, hallmark key geodynamic/crustal boundaries (e.g., continent/ocean transition) and slowly prograde basinwards in ca. 5–100 Myr, with typical rates of 0.1–10 m/kyr.

As a consequence of the very different progradation rates and of the difficulty of large-scale clinothems to backstep during transgressions, shorelines are the most dynamic clinoforms with regards to position, continental margins the least, and shelf-edges are intermediate. Shortly after a transgression, therefore, the four clinoform types may prograde synchronously along shoreline-to-abyssal plain transects, forming "compound clinoform" systems. During the subsequent regressive cycle, however, due to the dissimilarity in progradation rates, different clinoform types will normally merge progressively with each other, giving rise to "hybrid clinoforms" (e.g., shelf-edge deltas), and fewer depositional breaks-in-slope are distinguished along a single shoreline-to-abyssal plain transect. Overall, all clinoform systems are the result of the dynamic evolution of compound and hybrid clinoforms along a temporal and spatial continuum, regulated by the cyclical backstepping of the smaller-scale system within natural progradational-retrogradational cycles of larger-scale clinothem outbuilding.

All clinothem types may show either an accretionary/active or draping/passive style, depending on the proximity to the sediment source. Draping clinothems are nearly-always composed of condensed fine-grained sediments, while actively accreting clinothems can be composed of predominantly coarse-grained (i.e., reservoir-forming) or predominantly fine-grained (i.e., non-reservoir) lithotypes.

A novel hierarchical classification scheme for both Recent and Ancient clinoforms is here proposed, consisting of 12 classes. The four basic clinoform types (delta-scale shoreline, delta-scale subaqueous, shelf-edge and continental-margin) are sub-divided into eight accretionary/active and draping/passive sub-types (8-division). Each accretionary

sub-type is then sub-divided into a sandstone-prone and mudstone-prone variant (12-division), which can be at least tentatively predicted on the basis of the clinoform morphology, even in the absence of direct stratigraphic logs.
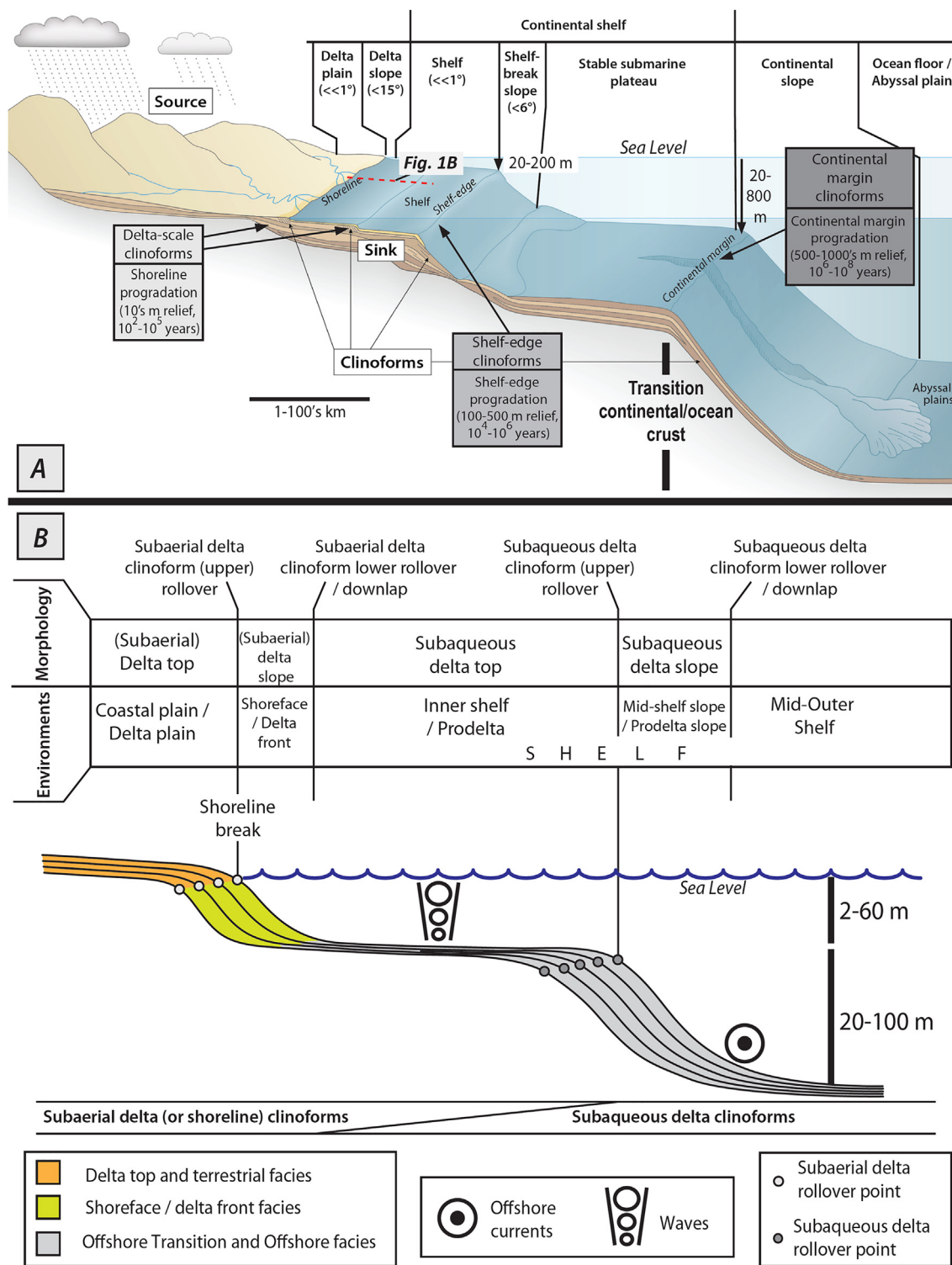

Fig. 1. Cross-sectional schemes parallel to the depositional dip, showing idealized compound clinoform systems at different scales. (A) Regional cross-section, highlighting three actively growing clinoforms systems: delta, shelf-edge and continental-margin scale clinoforms. (B) Cross-section through the nearshore to inner marine shelf area, showing a typical shoreline to delta-scale subaqueous clinoform compound system (located in Fig. 1A) (after Helland-Hansen and Hampson, 2009). The idealized line location of Fig. 1B is shown in Fig. 1A.

1. Introduction: clinoforms and clinothems

1.1. Definitions and historical perspective

Clinoforms are ubiquitous inclined stratal, chronostratigraphic and depositional surfaces corresponding to "frozen" palaeo-bathymetric profiles; clinothems are the clinoform-bounded sediment-body counterparts (Rich, 1951; Bates, 1953; Asquith, 1970; Pirmez et al., 1998; Adams and Schlager, 2000; Steel and Olsen, 2002; Patruno et al., 2015a).

Clinoforms have attracted the attention of researchers for more than one century. Gilbert (1885) identified topsets, foresets and bottomsets within the Pleistocene Lake Bonneville deltas. Joseph Barrell discussed the role of sloping bedding planes in deltas (Barrell, 1912). John Rich was the first to introduce the terms clinoform and clinothem, separating the depositional surface into undaform (topset equivalent), clinoform (foreset) and fondoform (bottomset) (Rich, 1951). Here we adapt to Steel and Olsen (2002), who redefined clinoforms and clinothems to include a steeper middle foreset segment and its topset and bottomset

extensions, respectively up-dip and down-dip.

Sloping depositional units occur at scales ranging from ripple- (centimetres), dune- and bar-foresets (decimetres to metres), delta and shoreface slopes (1–100 m) and up to sloping units formed by accretion of shelf edges (100's m) and continental margins (> 1000 m) (Larue and Martinez, 1989; Thorne, 1995; Henriksen et al., 2011) (Figs. 1, 2). Here we limit the use of clinoform and clinothem to larger sloping depositional surfaces and units (10's to 1000's m) generated by lateral accretion of sediment bodies in standing waters, or by passive sediment draping of existing slopes. Although both deep-water sediment drift "clinoforms" and smaller bedform foresets can have similar reliefs (e.g. tens of meter high aeolian dunes, tidal sand waves and sandy and muddy contourites Stow et al., 2002; Lancaster, 2004; Kubicki, 2008; Reeder et al., 2011; Pellegrini et al., 2016), they are beyond the scope of this review and are not further discussed. The same accounts for clinoformal drapes on tectonically generated structures such as intrabasinal highs and ridges and clinoformal drapes on erosional seascapes, such as drowned incised valleys and canyon walls (Fig. 3).
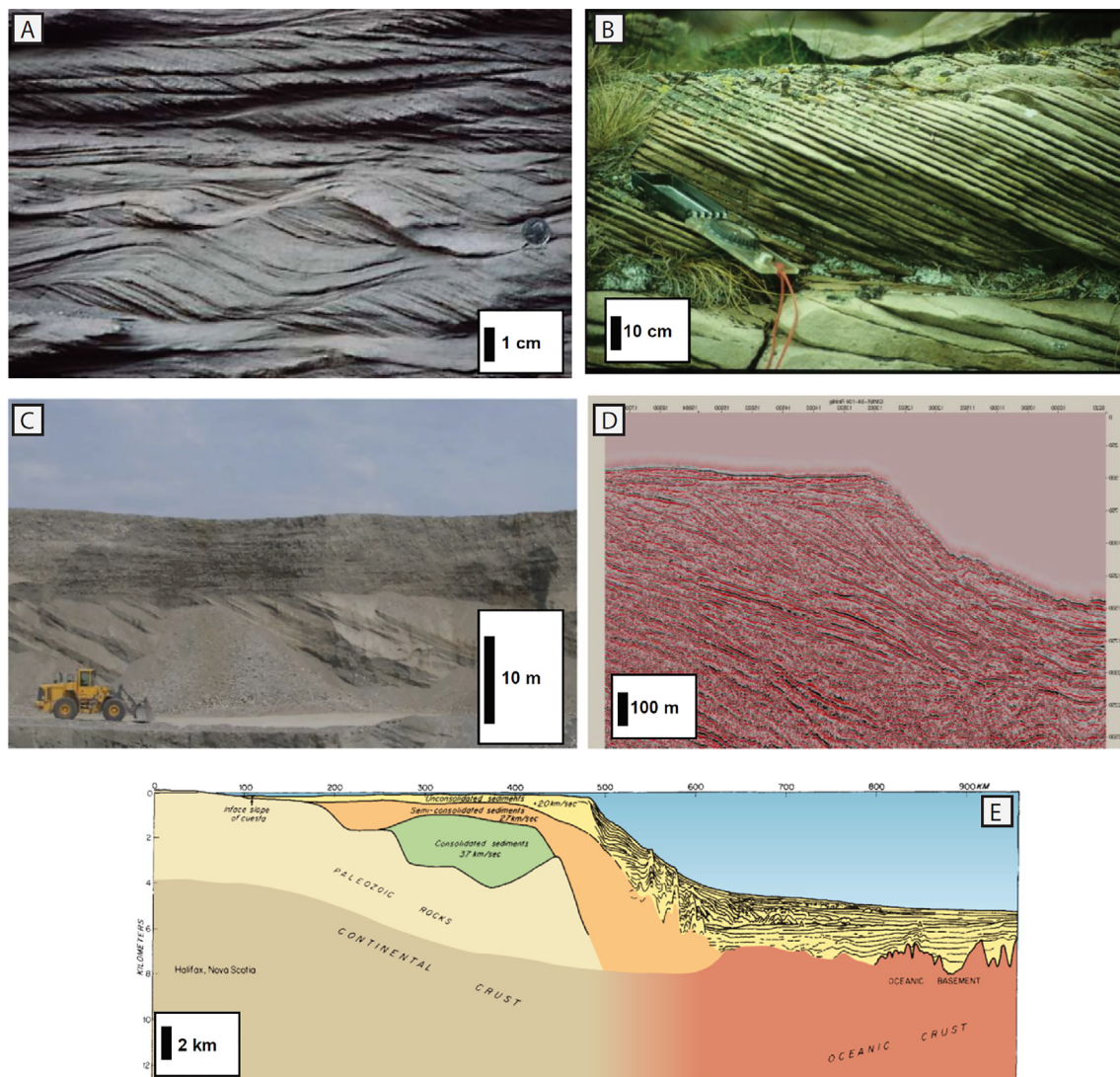

Fig. 2. Examples of inclined depositional palaeo-morphologies at different scale: (A) ripple-scale lamination (from Central Tertiary Basin, Svalbard); (B) dune-scale inclined bedding (from Late Proterozoic of the Varanger Peninsula, Norway); (C) delta-scale clinoforms (from Late Pleistocene terraces, Etne, Norway; photo by Ingrid Drange Enge); (D) shelf-edge scale clinoforms (from Neogene of the Mid Norwegian Shelf; courtesy of Norwegian Petroleum Directorate); (E) continental margin scale clinoforms (modified after Emery et al., 1970). The location of the continental margin clinoforms reflects the boundary between continental and oceanic crust (E).
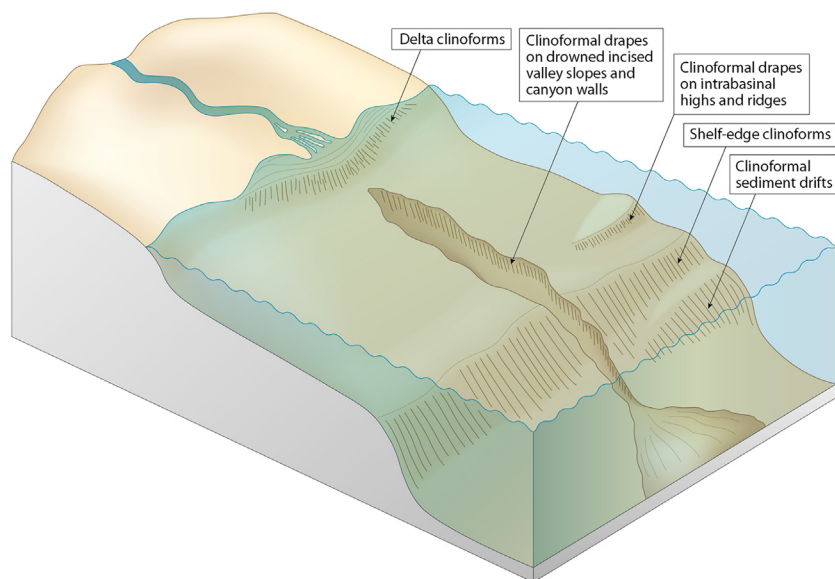
Fig. 3. Idealized sketch showing the distribution of accretional clinoforms and passive clinoforms, nucleating and propagating out from different types of depositional, structural or erosional reliefs. Clinoformal sediment drifts, clinoformal drapes on intrabasinal highs, ridges, as well as incised valley slopes and canyon slopes are beyond the scope of this paper.

1.2. Palaeoenvironmental significance

Only two basic types of slopes can be distinguished in deltaic, lacustrine and marine settings: erosional and progradational margins (Ross et al., 1994; Ryan et al., 2009a). Erosional margins are bathymetric escarpments characterized by widespread erosion, mass flows, slumping, incision and sediment bypass to the lower slope, with formation of onlapping fans. Progradational margins are comprised by sedimentary clinothems, with a depositional profile which represents the equilibrium between sediment supply, accommodation, basin physiography and oceanographic processes (Ross et al., 1994).

Clinoforms are ubiquitous both in carbonate (e.g., Mullins et al., 1988; Everts and Reijmer, 1995; Leeder, 1999; Bosence, 2002; Bosence and Wilson, 2002a, 2002b; Pomar et al., 2002; Eberli et al., 2004; Maurer et al., 2010; Lanfranchi et al., 2011; Betzler et al., 2015) and siliciclastic systems (e.g., Schlee et al., 1979; Steckler et al., 1999; Adams and Schlager, 2000; Tesson et al., 2000; Howell and Flint, 2002a, 2002b, 2002c; Cattaneo et al., 2003, 2007; Holgate et al., 2014, 2015; Pellegrini et al., 2018). Clinothems may be also formed by very shallow-water gypsum platform accretion (Tucker, 1991; Patruno et al., 2018, in press). Deltaic clinoforms have been even interpreted in ~3,600-3,200 Ma old sediments on Mars, suggesting that still-standing

shallow lakes existed on that planet (Grotzinger et al., 2015).

Clinoforms typically comprise basinward-accreting slopes, although landward-accreting exceptions are possible, as lagoons infilling by washover-fan progradation (Møller and Anthony, 2003; Garrison et al., 2010; Martínez-Carreño et al., 2017) and the progradation of flood-tidal bodies (e.g. Siringan and Anderson, 1993).

Clinoform cross-sectional shapes conform to three basic types of curve-fitting equations: a linear, an exponential (asymmetrical, concave-upward "oblique" clinoforms) and a Gaussian (symmetrical "sigmoidal" clinoforms). Clinoform equilibrium profiles and gradients have been shown to be a function of sediment grain-size, sediment supply, dispersal processes (e.g., wave climate) and physiography of the depositional foundation (Figs. 4–6). For example, increasingly large-scale clinoforms are deposited in progressively deeper-waters, over progressively larger time-spans (Pirmez et al., 1998; Driscoll and Karner, 1999; Adams and Schlager, 2000; Adams et al., 2001; Friedrichs and Wright, 2004; Patruno et al., 2015a) (cf. Figs. 7–9). As a general rule, the gradient of siliciclastic clinoforms of similar height is proportional to the average sediment grain-size, as coarser-grain sediments are characterized by steeper angles of repose (Orton and Reading, 1993; Patruno et al., 2015a). Carbonate clinoforms can be even steeper (even > 40°), owing to a rigid framework produced by carbonate secreting organisms
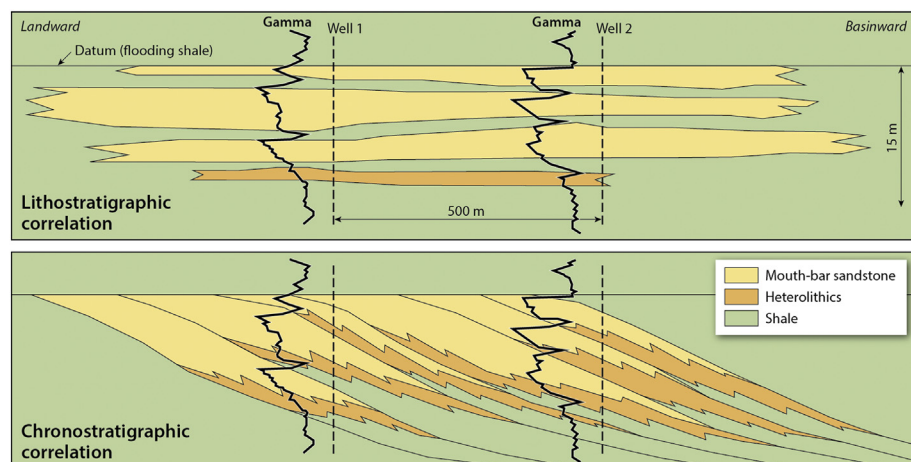

Fig. 4. Comparison between lithostratigraphic and chronostratigraphic correlations (modified after Ainsworth et al., 1999 and Gani and Bhattacharya, 2005). The chronostratigraphic correlation relies on clinoform-shaped time-lines that approximate the "real" depositional morphology and three-dimensional sedimentary architecture of clinothems.
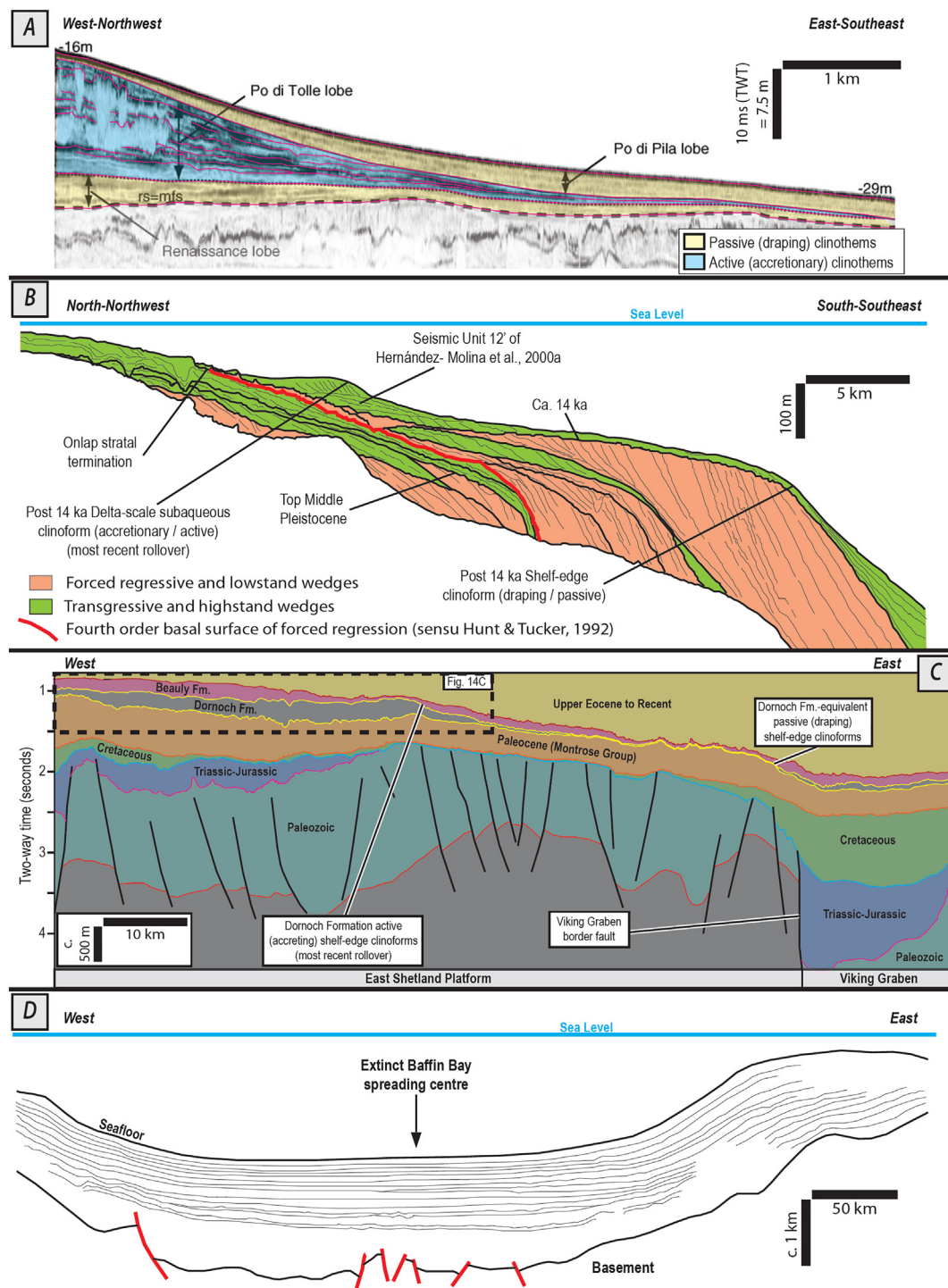
Fig. 5. Interpreted seismic cross-sections oriented parallel to the depositional dips, showing examples of passive (draping) clinoforms at various scale: (A) shoreline scale active and passive lobes of the Recent Po Delta, north-eastern Italy (after Correggiari et al., 2005); (B) transition between Quaternary active delta-scale subaqueous clinoforms and time-equivalent (compound) passive shelf-edge clinoforms (offshore Guadiana River mouth, southern Iberia, after Profile 1 of Hernández-Molina et al., 2000b); (C) transition between active uppermost Paleocene shelf-edge clinoforms (Dornoch Formation) and time-equivalent (compound) passive shelf-edge clinoforms draping over the palaeo-Viking Graben master-fault (East Shetland Platform and Viking Graben, U.K. northern North Sea, after Reid and Patruno, 2015; Patruno et al., in press; and Turner et al., in press); (D) passive continental margin scale clinoforms over the extinct Baffin Bay spreading centre, offshore Southern Greenland (after Rice and Shade, 1982).

and/or early slope cementation (Hubbard et al., 1986; Kenter, 1990).

Finally, caution should be made when making inferences about bathymetry and relief in ancient successions due to compaction which ultimately reduces relief and slope angles. Decompaction should therefore be carried out before estimation of these parameters is made (Steckler et al., 1999; Patruno et al., 2015c; Klausen and Helland-Hansen, 2018; Beelen et al., in review). For carbonate clinoforms, the compactional factor may be less important. Particularly, the reefal construction of a stiff skeleton by framework building organisms at the time of deposition in combination with early cementation indicate that reliefs and gradients in
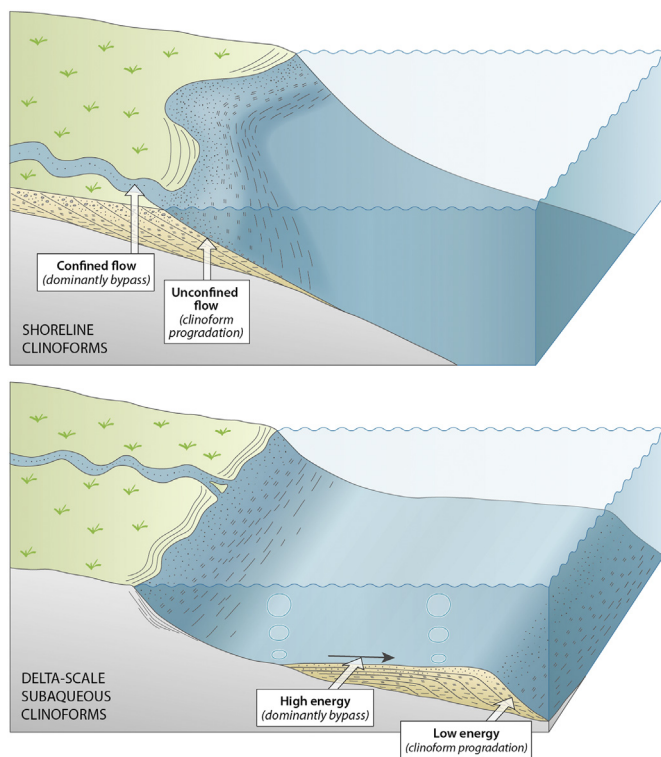
Fig. 6. Sketches illustrating the outbuilding of delta-scale clinoforms as a result of either: (A) the transition from confined to unconfined flow (shoreline clinoforms), or (B) from high-energy to low-energy marine transport (delta-scale subaqueous clinoforms).

the stratigraphic record may be closer to the original ones.

1.3. Sequence stratigraphic significance

Clinoforms may be difficult to identify. In outcrops, limited outcrop lateral extents combined with low slope angles limit clinoform visual recognition. In reflection seismic, for clinoforms to be imaged they need to be: (a) higher-relief than the vertical seismic resolution; (b) spaced wider than the tuning effect (c. 10 m); (c) associated to boundaries of facies with different acoustic properties or lined by thick carbonate-cemented layers (Holgate et al., 2014).

As a consequence, preserved or seismically-imaged clinoforms are often related to discharge variations in the feeder river, sediment condensation and/or diastem formation (i.e., short and transient interruptions in deposition with little or no erosion), operating at variable temporal scales. At these times, the deposition of carbonate cement, mudstone linings or organic matter enables the preservation of a paleo-bathymetric profile in the stratigraphic record, turning it into a clinoform that is visible in outcrops, detectable in cores and/or resolvable in seismic (Wood and Gorin, 1998; Saito et al., 2000; Savrda et al., 2001; Holgate et al., 2014). Major clinoforms represent more significant hiatuses or erosion, and are marked by reflector terminations and/or unconformities linked to key sequence stratigraphic boundaries (Mitchum et al., 1977; Neal and Abreu, 2009; Pellegrini et al., 2017).

Since a clinoform represents a "frozen" or "fossilized" palaeo-depositional interface preserved in the sedimentary record, its geometry gives direct information about past bathymetry and shoreface-shelf 3D morphology, as well as reflecting primary external forcing like accommodation, sediment supply and sediment-grade (Ross et al., 1994; Postma, 1995; Pirmez et al., 1998; Driscoll and Karner, 1999; Adams and Schlager, 2000; Steel and Olsen, 2002; Quiquerez and Dromart,

2006; Patruno et al., 2015a; Anell and Midtkandal, 2017).

The stratigraphic architecture of clinoforms sets, furthermore, provides a link in the understanding of how sediments are transported to deeper water settings (e.g., sediment partitioning between aggradational topset storage versus degradational topset bypass), as well as a physical record of the interplay between changes in sea-level, tectonics (uplift and subsidence), sediment supply, basin physiography, hydrodynamics, climate and other environmental forcing (e.g., Mitchum et al., 1977; McKee et al., 1983; Steel and Olsen, 2002; Porębski and Steel, 2003; Bullimore et al., 2005; Løseth et al., 2006; Ponce et al., 2008; Helland-Hansen and Hampson, 2009; Neal and Abreu, 2009; Charvin et al., 2010, 2011; Patruno et al., 2015c; Reeve et al., 2016; Pellegrini et al., 2017).

Clinoforms therefore represent key surfaces for sequence stratigraphy, and their stacking geometries and stratal terminations enable the very identification of system tracts and trajectory classes. Most clinoforms are formed during either highstands or lowstands, when sediment supply is expected to outpace the rate of relative sea-level rise (Neal and Abreu, 2009). Other clinoforms may be formed by regressive transits under overall transgressive conditions (e.g., Postma, 1995; Helland-Hansen and Martinsen, 1996; Plink-Björklund and Steel, 2002; Pellegrini et al., 2015), or when relative sea-level is falling (e.g. Plint and Nummedal, 2000).

1.4. Research avenues and economic value

Clinoform studies are essentially carried out along four different research avenues, including:

1. The study of ancient stratigraphy in outcrops, seismic, ground-penetrating radar and well-data (e.g., Mullins et al., 1988; Helland-Hansen, 1992, 2010; Hampson, 2000, 2010; Steel and Olsen, 2002; Porębski et al., 2003; Johannessen and Steel, 2005; Hampson and Howell, 2005; Gani and Bhattacharya, 2005; Patruno et al., 2015b, 2015c);
2. The analysis of modern sea-floor topography or sediments through echo-sounding, shallow seismic and cores (e.g., Field and Roy, 1984; DeMaster et al., 1985; Prior et al., 1986; Bellotti et al., 1994; Hernández-Molina et al., 2000a; Jol et al., 2002; Correggiari et al., 2005; Kuehl et al., 2005; Liu et al., 2006, 2007a, 2007b; Puig et al., 2007; Cattaneo et al., 2003, 2007; Bassetti et al., 2008; Palamenghi et al., 2011; Pellegrini et al., 2018);
3. Experimental studies in flumes and scaled physical models (e.g., McClay et al., 1998; Kostic et al., 2002; Muto and Steel, 2004; Gerber et al., 2008; Leva López et al., 2014);
4. Numerical modelling, focused on the controls on clinoform formation (e.g., Helland-Hansen et al., 1988; Ross et al., 1994; Pirmez et al., 1998; Driscoll and Karner, 1999; Adams et al., 2001, 2011; Friedrichs and Wright, 2004; Swenson et al., 2005; Friedrichs and Scully, 2007; Wolinsky and Pratson, 2007; Burgess et al., 2008; Charvin et al., 2011; Mitchell, 2012; Patruno et al., 2015c), clinoform imaging in reflection seismic (e.g., Holgate et al., 2014), and the impact of clinoforms on fluid flow (e.g., Enge and Howell, 2010; Graham et al., 2015a, 2015b; Howell et al., 2008; Jackson et al., 2009).

The realization that sediments building into standing water-bodies create sloping units gives far-reaching constraints on how stratigraphic units are correlated (cf. "shingled" versus "layer-cake" correlation in Gani and Bhattacharya, 2005) (Fig. 4). Clinothems have also significant storage potential for oil, gas, water and CO_2, and several hydrocarbon fields rely on intra-clinothem reservoirs units (e.g., Sydow et al., 2003; Cummings and Arnott, 2005; Holgate et al., 2013; Patruno et al., 2018, in press). Since most clinoforms are lined by low-permeability
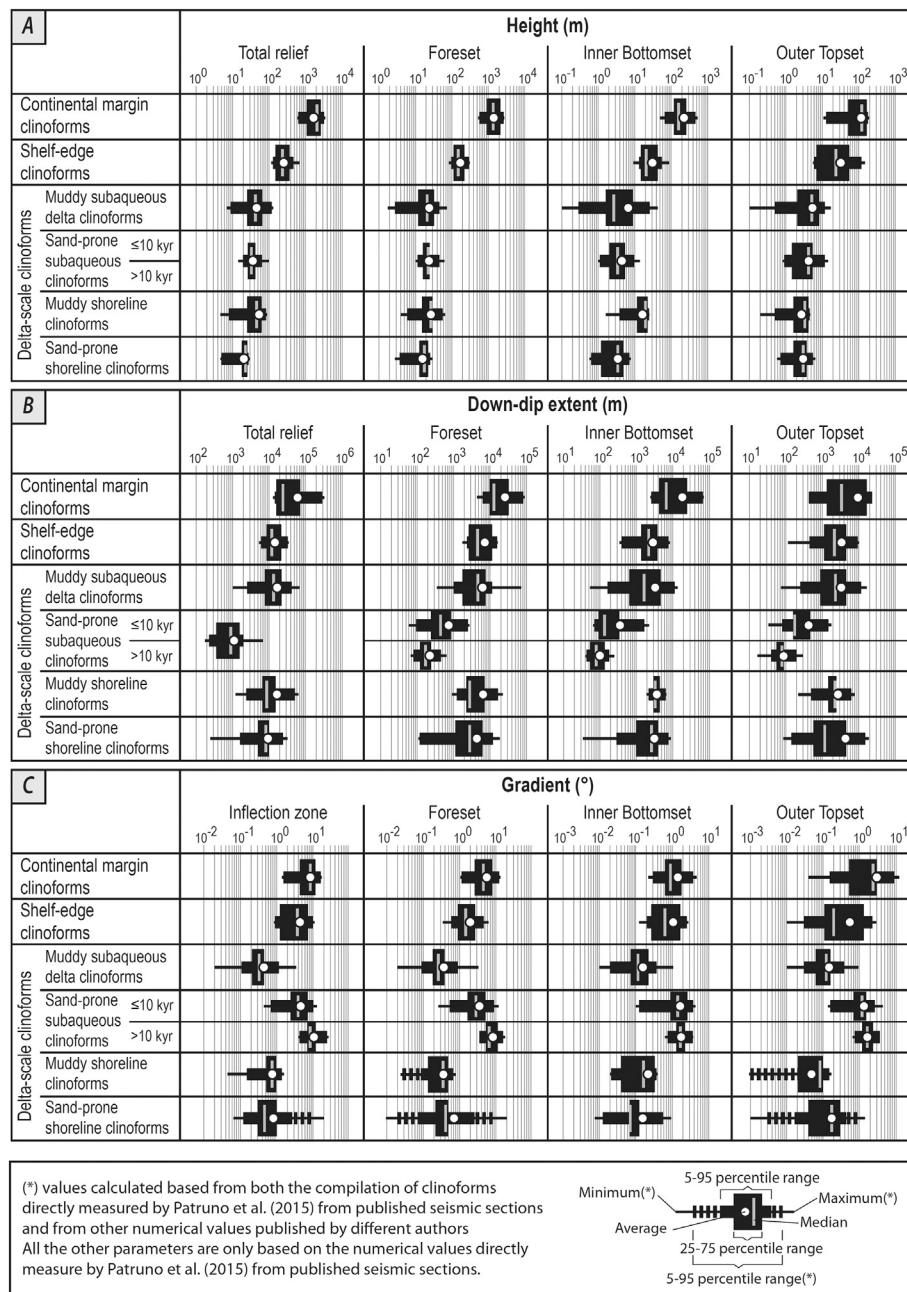
Fig. 7. Statistical distribution of clinoform heights, down-dip extents and gradients, based on the data compilation by Patruno et al. (2015a).

mudstones or cements (Holgate et al., 2014), they often act as baffles to hydrocarbon flow (Howell et al., 2008; Jackson et al., 2009; Graham et al., 2015a, 2015b). Therefore, only clinoform-based production models enable accurate prediction of hydrocarbon drainage patterns and recovery (Howell et al., 2008; Graham et al., 2015b).

2. A review of clinoform research

In this section, existing clinoform research has been reviewed through three logical patterns.

a) The scale-invariant clinoform genesis and dynamics, particularly the difference between actively accreting clinoforms and passive/draping clinoforms (sub-Section 2.1);
b) The distinction of three basic types of clinoform spatial and temporal scales: delta-, shelf-edge and continental-margin scale (sub-Section 2.2);
c) The spatial association of clinoforms formed at the same time: compound versus hybrid clinoforms (sub-Section 2.3).

These three aspects are utilized in Section 3 to devise a novel clinoform classification.

2.1. Clinoform genesis and dynamics: active versus passive clinoforms (scale invariant)

Clinoform deposition can be condensed into two main modes, present at every scale, ranging from tens to thousands of metres: (1) clinoforms plastered passively on existing slopes by distant sediment sources (draping or passive clinothems) (Fig. 5); or (2) clinoforms accretion by sediment supply from active, nearby sediment sources (constructional or active clinothems) (Figs. 5; 10-18). .
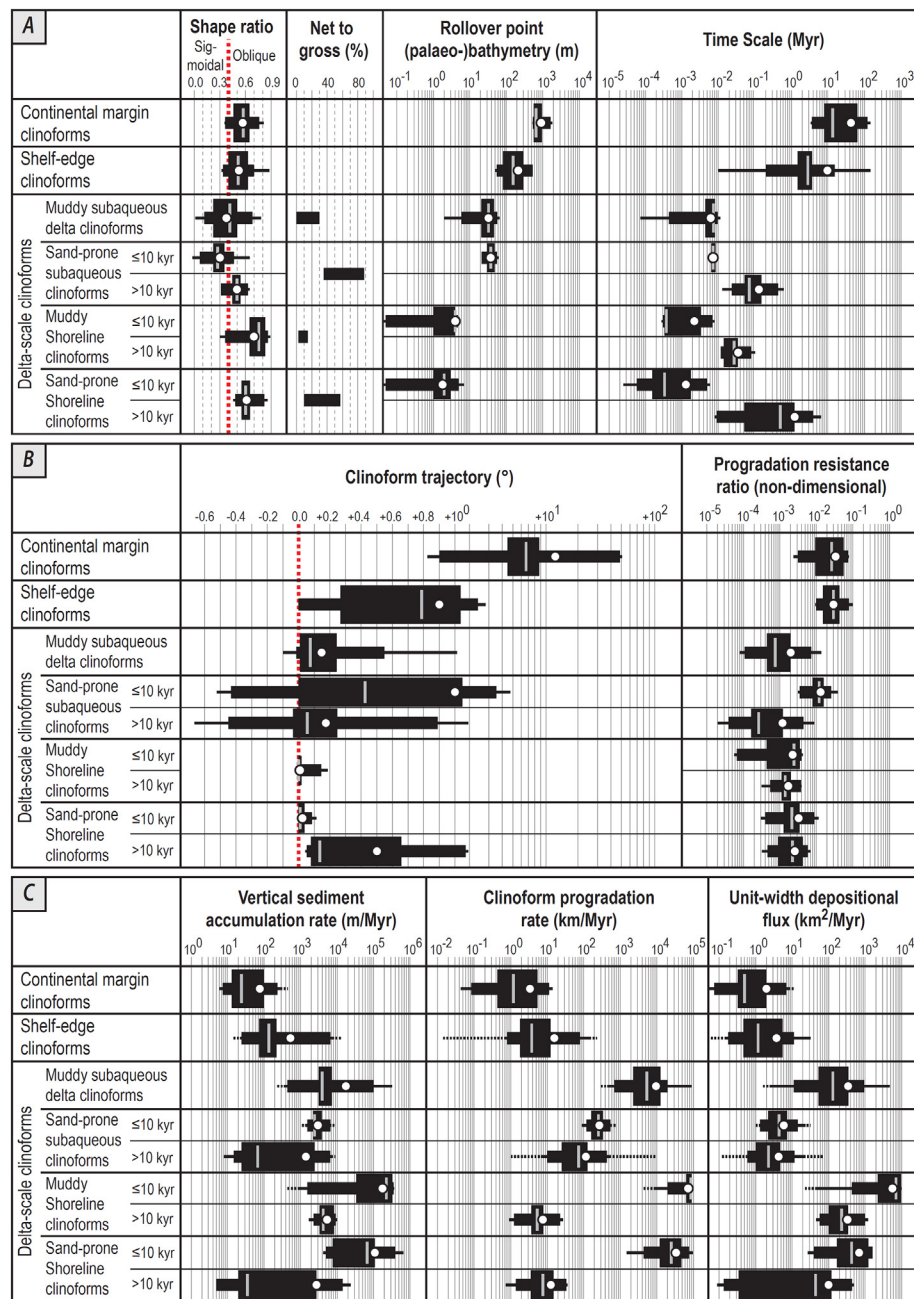
Fig. 8. Statistical distribution of various depostional and geometrical parameters of clinoforms, based on the data compilation by Patruno et al. (2015a). N.B. The case of lowstand shelf-edge deltas is not shown here, but is characterized by significantly faster "delta-like" rates (e.g. c. 10^4 m/kyr, see Pellegrini et al., 2017, 2018).

Constructional/active clinoforms imply active supply of sediments and sediment source proximity. Their nucleation and growth is associated to the change in sediment dispersion from confined to unconfined flow, or to the transitioning from high to lower energy levels (e.g., across the fairweather wave base) (Fig. 6; Driscoll and Karner, 1999; Puig et al., 2007). In either case, the loss of momentum and flow deceleration causes sediment load deposition. Much of it, and particularly all the coarsest-grained load is laid down in proximity of the sediment feeder (i.e., a river mouth or current head); the rest is transported further basinwards or alongshore (Kostic et al., 2002). Such basinward decline in sedimentation rate will lead to clinothem nucleation, propagation and amplification by continued deposition.

Passive/draping clinoforms imply nucleation or continued accretion by distant sediment sources, and more commonly have both aggradational clinoform trajectories and near-uniform thicknesses and

sediment accumulation rates throughout the topset, foreset and bottomset areas (e.g., Palinkas and Nittrouer, 2006) (Fig. 5). This contrasts with the accumulation rate and thickness profiles of constructional clinoforms, characterized by sedimentation rates greatest along the foreset portion and significantly lower towards both the topset and the bottomset (e.g., Alexander et al., 1991; Leithold, 1993; Michels et al., 1998; Pirmez et al., 1998; Walsh et al., 2004; Palinkas and Nittrouer, 2006; Cattaneo et al., 2007; Pellegrini et al., 2015) (Figs. 10–18).

Active phases of clinoform growth (often characterized by coarser-grained sediment supply) can alternate with or transition into long periods of passive fine-grained draping from distant sources. Accordingly, clinoform sets may lithologically diversify depending on what process contributed sediments (e.g., in shelf-edges – Porębski and Steel, 2003, see later).
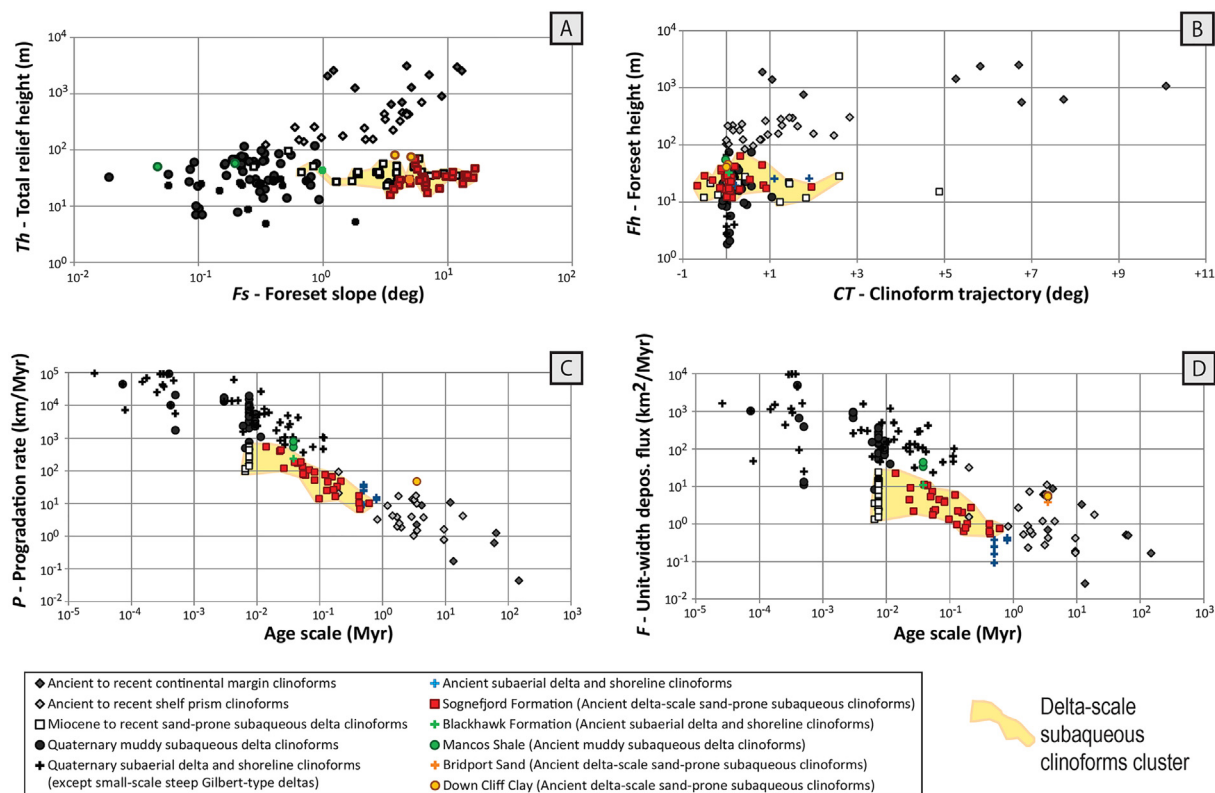
Fig. 9. Cross-plots of key architectural and depositional parameters, showing distinct statistical fields corresponding to the main clinoform types discussed here (after Patruno et al., 2015a).

2.2. Clinoform scales: shorelines/deltas, shelf-edges, continental margins

Clinoforms can be characterized based on their relief, gradient, position in a proximal-distal transect, (palaeo-)bathymetry, and their mode and time-scale of formation (Table 1; Figs. 7–9). Four clinoform types, termed shoreline, delta-scale subaqueous, shelf-edge and continental margin clinoforms, are here discussed (Figs. 7, 8, 10-18).

2.2.1. Delta scale clinoforms

Delta-scale clinoforms are characterized by reliefs of tens of metres (common foreset heights of 10–30 m – Table 1, Fig. 7A) and are formed over relatively short time spans (c. 1–10^3 kyr – Table 1, Fig. 8A; Clifton, 1981; Patruno et al., 2015a; Ainsworth et al., 2017) in association with the progradation of either shorelines and subaerial deltas ("shoreline clinoforms"), or underwater sediment slopes of similar scale ("delta-scale subaqueous clinoforms"). In particular, shoreline clinoforms are formed when transitioning from confined to unconfined water flow in neritic waters, either close to the river mouth (via delta front/shoreface migration) or alongshore (via redistribution and redeposition of the sediment load) (Fig. 6a). Delta-scale subaqueous clinoforms are accreted in shelfal waters when transitioning from high-energy to low-energy water flow (see later) (Fig. 6b).

While every bed-scale dipping surface in a delta-front or shoreface succession defines a clinoform, most individual delta-scale clinoforms that are visible in outcrops, detectable in cores and/or resolvable in seismic reflect stratigraphic discontinuities and/or variations in cementation or sandstone/shale content. These are driven by enhanced wave scour/erosion or sediment starvation/hiatus, which in turns reflect minor variations in river feeder discharge, relative sea-level, sediment supply and/or wave climate, with highly variable temporal scale significance (Hampson, 2000; Hampson and Storms, 2003; Roberts and Sydow, 2003; Gerber et al., 2008; Enge et al., 2010; Charvin et al., 2011; Zecchin and Catuneanu, 2013; Patruno et al.,

2015b, 2015c; Ainsworth et al., 2017). Regressive transits of delta-scale clinoforms generates the typical "parasequences" in marginal to shallow-marine successions (corresponding to a clinoform set), whereas repeated, high-frequency regressive-transgressive cross-shelf transits determines the stratigraphic architecture of shelves and shelf-edge clinothems (see later) (Van Wagoner et al., 1990; Burgess and Hovius, 1998; Johannessen and Steel, 2005; Olariu and Steel, 2009; Helland-Hansen et al., 2012).

Delta scale clinoform trajectory trends (Fig. 8) reflect regional or local fluctuations in sediment supply and relative sea-level. Local fluctuations are typically caused by autogenic processes such as delta-lobe shifting, differential compactional subsidence of shelfal muds in distal locations or sedimentary system self-organization linked to substrate physiography, such as autoretreat, autoincision and auto-accelleration (Clifton, 1981; Muto and Steel, 1992, 1997, 2004; Helland-Hansen and Martinsen, 1996; Hampson and Storms, 2003; Muto et al., 2007; Charvin et al., 2010; Leva López et al., 2014; Patruno et al., 2015c; Ainsworth et al., 2017). Regional fluctuations are caused by allogenic processes, such as eustatic sea-level changes or tectonically-generated regional changes in relative sea-level or sediment supply rates (e.g., variations in advance and retreat of Italian glaciers at the same centennial/millennial scale with the sediment supply fluctuations in the Adriatic basin, as reported by Pellegrini et al., 2018).

All the Recent delta-scale clinothems began prograding ca. 6–7 ka before present, with the waning of the rate of post-glacial eustatic rise (Summerhayes et al., 1978; Field and Roy, 1984; Stanley and Chen, 1996; Morales, 1997; Chen et al., 2000; Stouthamer and Berendsen, 2000; Goodbred and Kuehl, 2000a, 2000b; Hernández-Molina et al., 2000a; Ta et al., 2002a; Hori et al., 2002, 2004; Cattaneo et al., 2003, 2007; Palinkas and Nittrouer, 2006; Liu et al., 2006, 2007a, 2007b; Giosan et al., 2006b; Le Dantec et al., 2010; Qiu et al., 2014).

All delta-scale clinoforms, with the partial exception of smaller coarse-grained sub-types (see below), are characterized by fast cross-
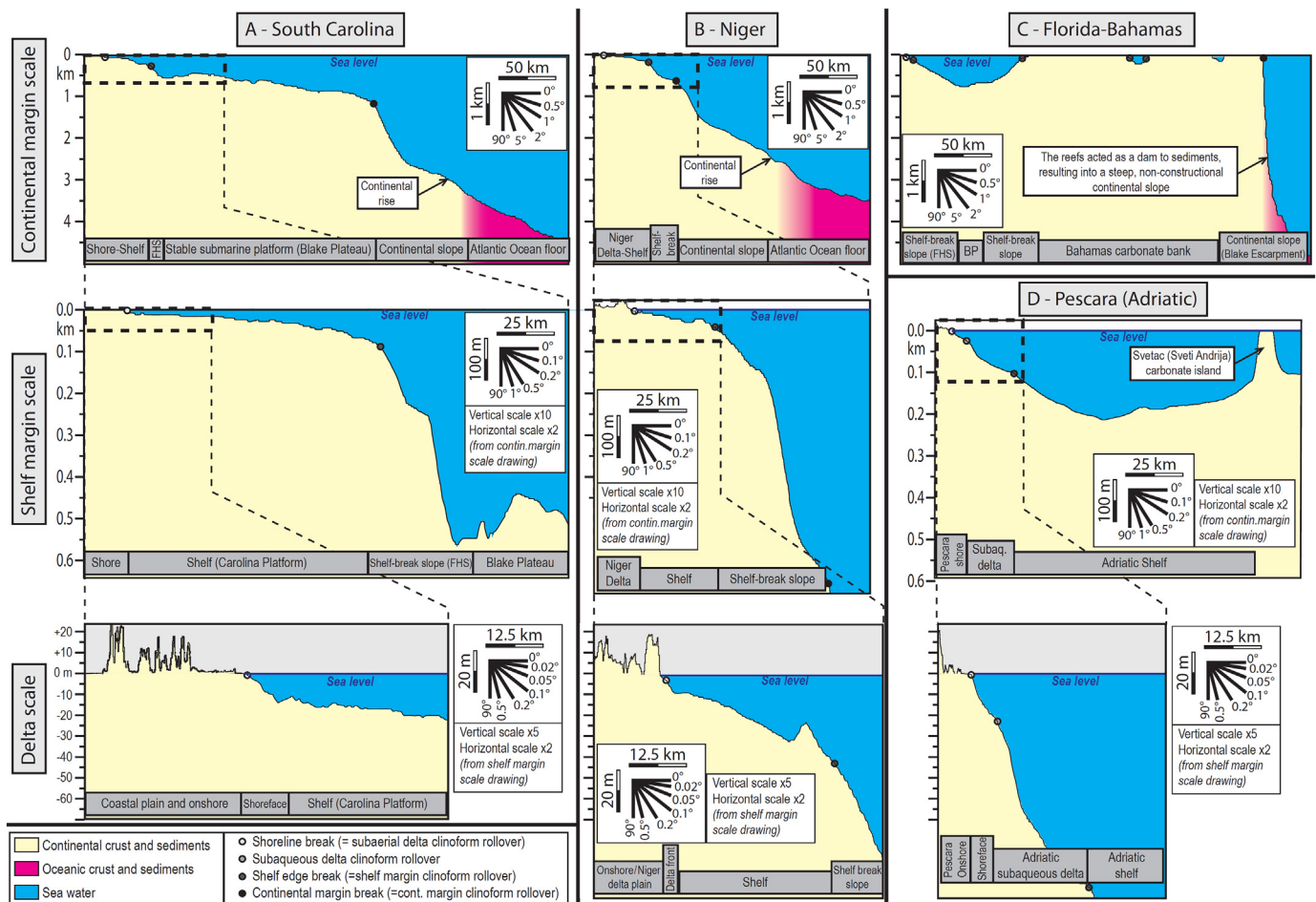
Fig. 10. Inclined present-day clinoforms at different scale: continental margin, shelf margin and delta scale. The bathymetric profiles off South Carolina (eastern United States continental margin, Atlantic Ocean) (A) and off the mouth of the Niger River (Central Atlantic Ocean) (B) contain the three scales of clinoforms, actively accreting at the same time (albeit at very different rates). (C) The profile between eastern Florida and the Bahamas (eastern United States continental margin, Atlantic Ocean) shows an inner carbonate shelf and a very steep continental margin slope. (D) The profile between the Pescara River mouth (central-eastern Italy) and Croatia (Central Adriatic Sea) shows present-day shoreline clinoforms, delta-scale subaqueous clinoforms and shelf-edge clinoforms. Each of the three sets of examples of continental margin, shelf margin and delta scale clinoforms are shown at the same horizontal and vertical scale. See Fig. 18A for a location map of the figures showing the U.S. Atlantic continental margin (Fig. 5A and C). FHS = Florida-Hatteras Slope; BP = Blake Plateau. The bathymetric information is after Ryan et al. (2009b).

shelf regressive cycles (progradation rates of c. 10^{-1}–10^2 km/kyr), very low progradation resistance ratios (*sensu*Patruno et al., 2015a) (10^{-4}–10^{-2}) and high progradation/aggradation ratios, highlighted by near-flat clinoform trajectories ($< 0.9°$) within each progradational clinoform set (Fig. 8). This is due to the relative proximity to sediment supply input points and with sediment accommodation which is vertically negligible (tens of metres) but laterally extensive (i.e., the whole marine shelf).

2.2.1.1. Shoreline clinoforms (Figs. 11–12). Shorelines correspond to the intersection between water and land surfaces, and their accurate recognition is critical for geologists and engineers (Dolan et al., 1991; Wessel and Smith, 1996; Stive et al., 2002; Boak and Turner, 2005). The topset-to-foreset rollover point of shoreline clinoforms, with typical median bathymetry of 0–5 m, is a key shoreline indicator (Fig. 8A).

Shoreline clinoforms are formed wherever river systems debouch into standing waterbodies (e.g., lakes, lagoons, bays, open sea), provided that the local rate of sediment input outpaces that of sediment erosion due to waves and currents. Depositional processes range from suspension fallout from buoyant plumes to tractional deposition by river currents, waves and tides, but gravitational depositional processes (e.g., turbidity currents) may also be important, particularly on the clinoform toe (e.g. Pattison, 2005).

Fluvial dominated "subaerial deltas" form clinoforms that are oriented radial or normal to the river-mouth point source (Barrell, 1912; Bhattacharya, 2006). In wave- or tide-dominated settings, sediments are reworked and redistributed by basinal processes away from the river mouth, both alongshore and across-shelf (e.g., Yang and Nio, 1989). Wave-dominated coastal environments, in particular, consists of alternations of erosional stretches and accretive shore-parallel clinothems in plan-view (e.g., wave-dominated deltas, shorelines/beaches, strandplains, spits, barrier islands and cheniers) (Augustinus, 1978; Morales, 1997; Heward, 1981; Jiménez et al., 1997; Jol et al., 1996, 2002; Bhattacharya and Giosan, 2003; Rasmussen, 2009). More generally, all shoreline clinoforms can be subject to a variable degree of wave, tide and riverine influence, with processes that may vary systematically in space and time during cross-shelf transits (e.g., increasing wave dominance as deltas prograde outwards on the shelf – Porębski and Steel, 2006; Steel et al., 2008; Patruno et al., 2015b, 2015c).

While on the short term (< 10 years), storms are the main agents responsible for the changes in shoreline morphologies by rapid redistribution of nearshore sediment (Morton et al., 1995), during longer timescales the shoreline geomorphology and the stratigraphic architecture of shoreline clinoform successions are sensitive to even the most subtle and high-frequency fluctuations in relative sea-level, sediment supply, climate, basin hydrodynamics, sediment compaction and
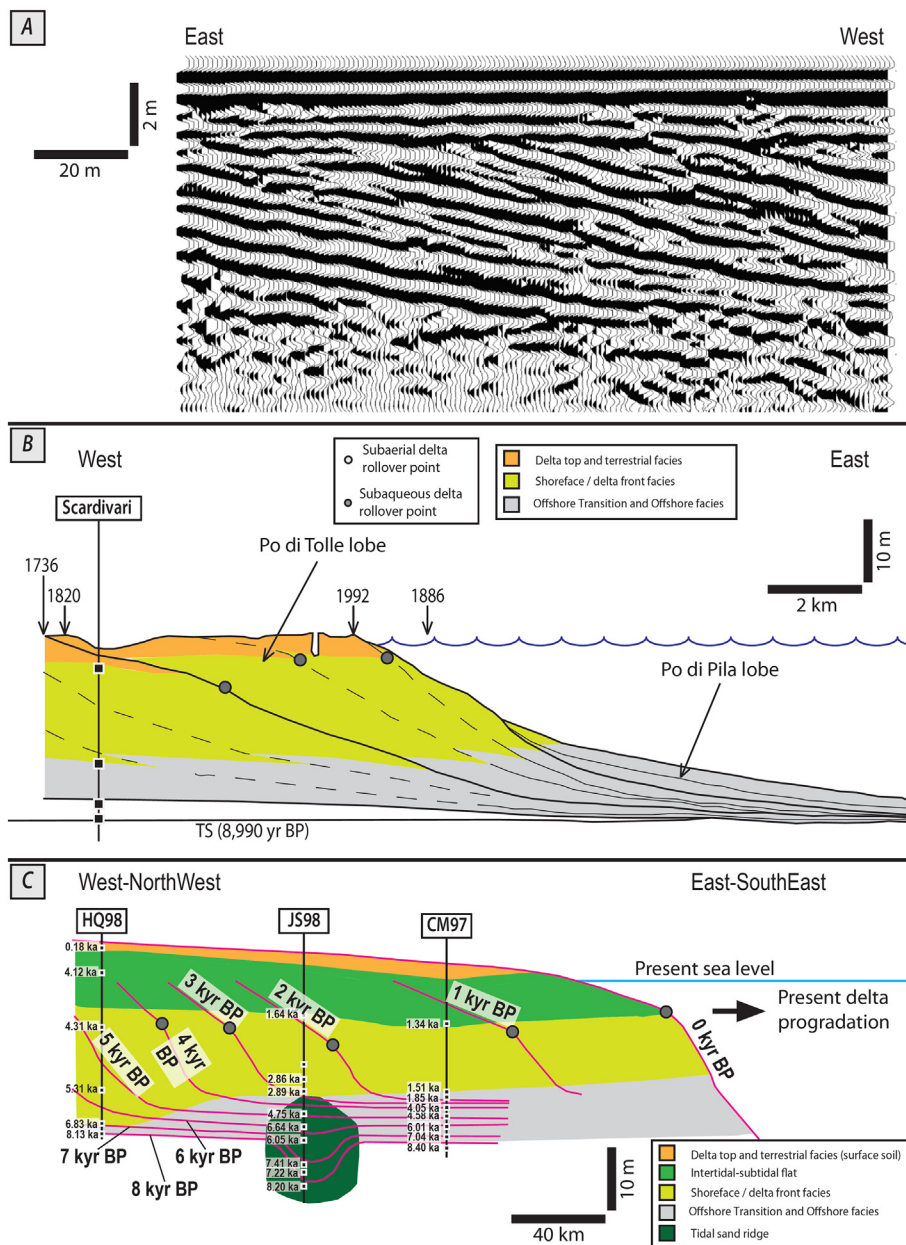
Fig. 11. Examples of cross-sections oriented approximately parallel the depositional dip of Recent shoreline (=subaerial delta) clinoform systems. These include: (A) coastal barrier spit, characterized by a vertical relief of < 10 m, from Long Beach (Willapa Bay, Washington State, U.S.A.), imaged with ground-penetrating radar technology (after Jol et al., 2002); (B) Po di Tolle lobe, characterized by a vertical relief of 20–30 m (Po River delta, northeastern Italy), with shoreline break position through the years annotated (after Correggiari et al., 2005); (C) Yangtze River delta (China), characterized by a vertical relief of 25–30 m, and isochron lines showing the position of the delta front clinoform through time (after Hori et al., 2001).

human influence (Morton and Suter, 1996; Foyle and Oertel, 1997; Morales, 1997; Sornoza et al., 1998; Hampson, 2000, 2010; Goodbred and Kuehl, 2000a, 2000b; Stive et al., 2002; Forbes et al., 2004; Mortimer et al., 2005; Bhattacharya, 2006; Charvin et al., 2011; Marriner et al., 2012; Ainsworth et al., 2017).

As a consequence of their genesis, the geomorphological components of shoreline clinoforms are associated with specific depositional facies. In particular: (1) topsets comprise subaerial delta top or coastal/alluvial plain deposits, including fluvial, lagoonal, floodplain and interdistributary bay facies; (2) the foresets consist of shoreface or delta front facies; and (3) the bottomset is composed of finer-grained prodelta or offshore shelfal sediments (Figs. 1B, 11, 12, Helland-Hansen and Hampson, 2009). Each progradational-aggradational shoreline clinoform set therefore typically corresponds to a typical deltaic/shoreface parasequence that is up to a few tens of metres thick (Clifton, 1981; Duke, 1990; Coutellier and Stanley, 1987; Sornoza et al., 1998; Hori et al., 2002; Ta et al., 2002a; Olariu and Bhattacharya, 2006; Charvin et al., 2010) (Figs. 11–12).

Shelf-edge delta clinoforms share many properties with shoreline clinoforms. Nevertheless, in this review, shelf-edge deltas are considered part of the shelf-edge clinoform types (see later), since they are both characterized by similar values of relief (100s m), slope gradient, laterally-extensive plan-view morphology and process sedimentology (e.g., they are the only type of "delta" with abundant slope-controlled soft-sediment deformation and growth faulting) (Suter and Berryhill Jr, 1985; Sydow and Roberts, 1994; Plink-Björklund et al., 2001; Plink-Björklund and Steel, 2002; Porębski and Steel, 2003, 2006). As a consequence, "true" shoreline clinoforms are characterized by typical foreset heights of c. 5–40 m, depending on the bathymetry of the receiving basin (Fig. 7A). These low relief values highlight the challenge of imaging "true" shoreline clinoform systems with seismic reflection techniques. However, they are often well-imaged by GPR data (Jol et al., 1996, 2002; Smith and Jol, 1997; Hampson et al., 2008) (Fig. 11a) or high-resolution shallow seismic (Tesson et al., 2000; Hansen and Rasmussen, 2008; Rasmussen, 2009). They are also demonstrated in outcrops (Gani and Bhattacharya, 2005; Hampson et al., 2008; Enge and Howell, 2010; Enge et al., 2010) (Fig. 12a and b) although slope gradients in many instances are too low to be seen.
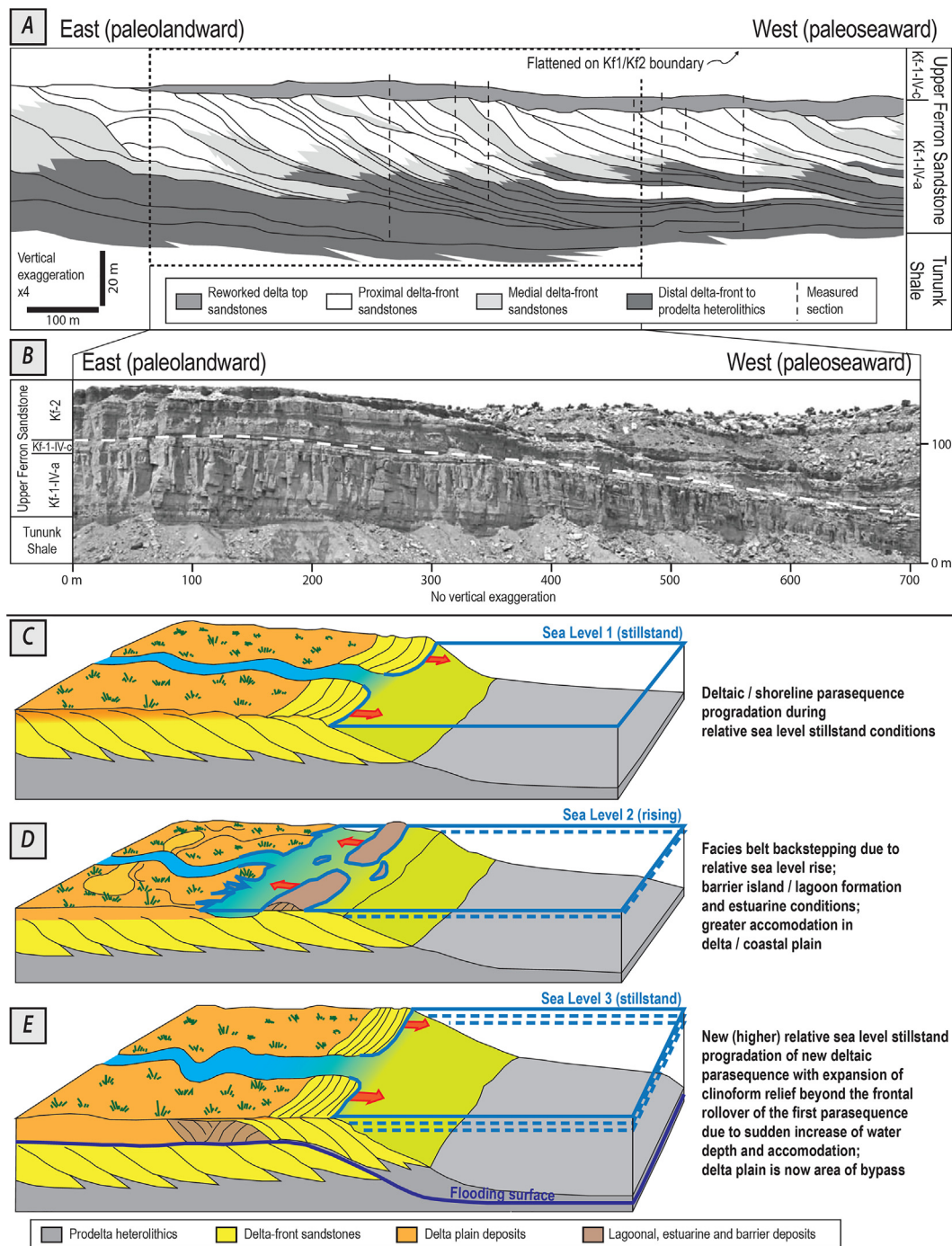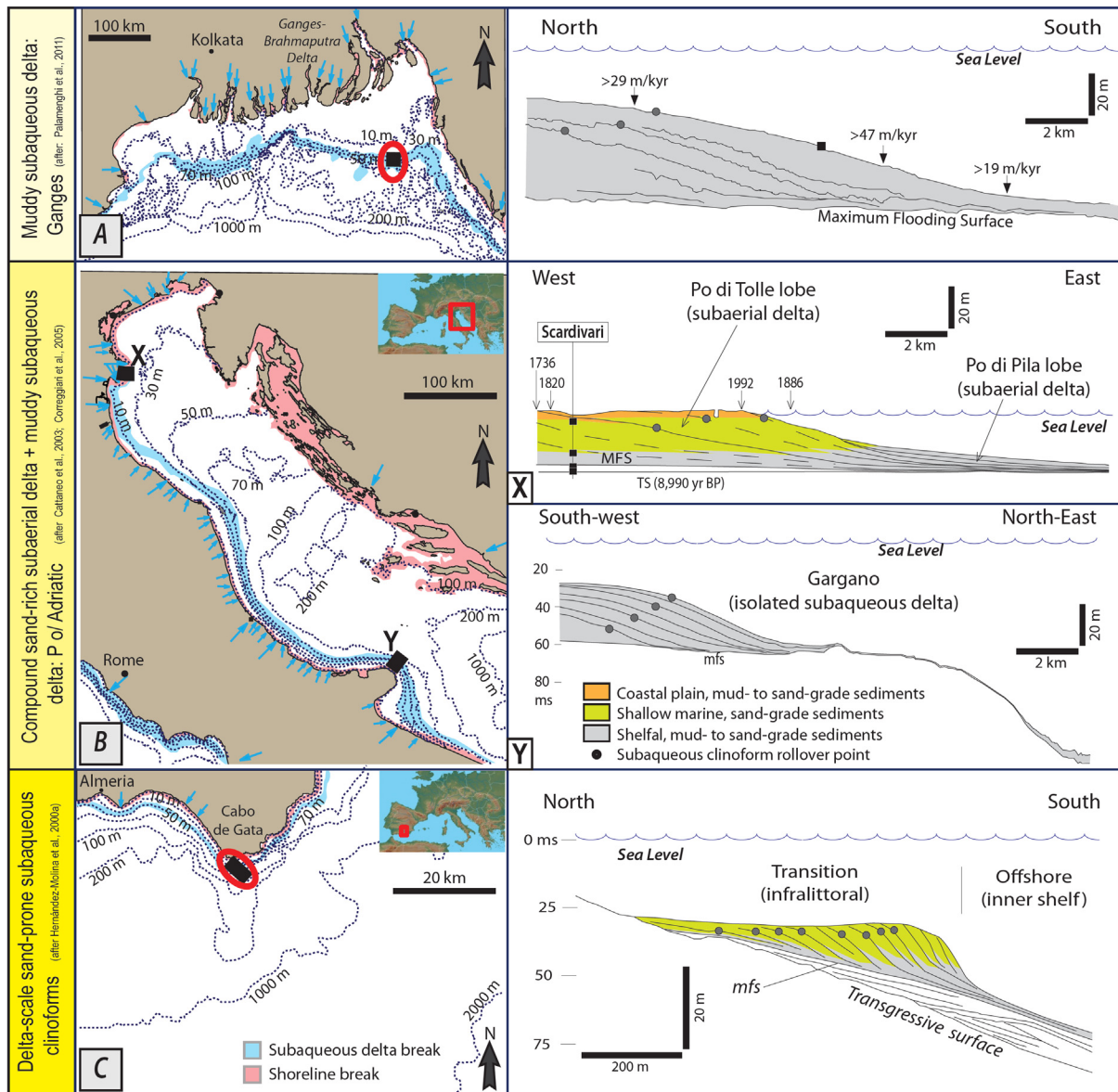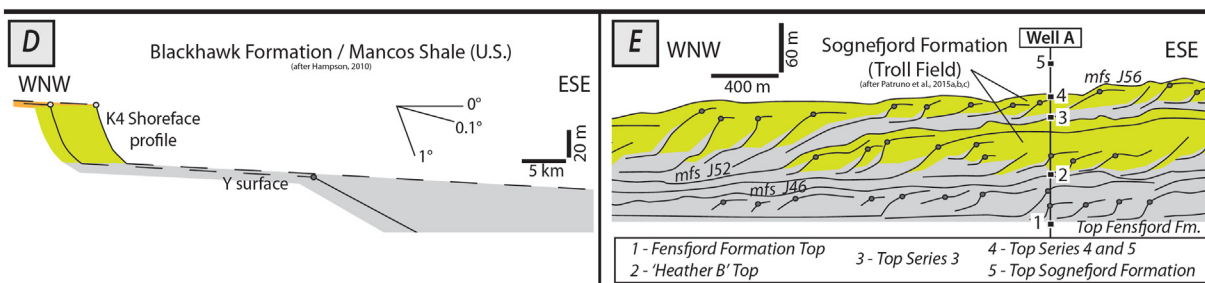
Fig. 12. (A-B) Examples of cross-sections oriented approximately parallel the depositional dip of Ancient shoreline (=subaerial delta) clinoform systems. (B) Photomosaic (no vertical exaggeration) and (A) facies interpretation (vertical exaggeration ×4) of a cliff face (along depositional dip) of the Cretaceous-age Ferron Sandstone ancient shoreline clinoform system (Ivie Creek amphitheatre, Utah, U.S.A.) (after Anderson et al., 2002 and Gani and Bhattacharya, 2005). (C–E) Sketches illustrating the evolution of an idealised wave-dominated shoreline through times, forming a succession of progradational clinoform sets, each deposited during phases of relative sea-level stillstand and stacked on top of each other due to the episodic transgressive backstepping of the coastal system (redrated after Howell and Flint, 2002b).

Grain size population is highly variable in shoreline clinoforms, ranging from muddy to sandy and pebbly (e.g., Gilbert-deltas and fan deltas – Postma, 1984; Nemec and Steel, 1988; Smith and Jol, 1997). Foreset heights tend to be noticeably lower in coarse-grained systems (c. 5–25 m) than in muddy shorelines (c. 6–60 m) (Fig. 7A). Variability of shoreline clinoform gradients is mainly a response to grain-size, although depositional processes are important additional drivers (Helland-Hansen, 2009). The usual inflection zone gradients of

shoreline clinoforms range from 0.1–1.5° (mud-dominated systems) to 0.1–2.7° (sand-dominated systems) (Fig. 7A), although coarser-grained Gilbert-type deltas can be as steep as the angle of repose of their dominant sediment (Smith and Jol, 1997). A diagnostic criterion of shoreline clinoforms is a highly oblique and asymmetric morphology, which is reflected by the highest values of shape ratios (i.e., the inflection point height divided by the clinoform total relief, *sensu* Patruno et al., 2015a) of all the clinoform types (Fig. 8A). These oblique profiles

Fig. 13. Examples of Recent (A–C) and Ancient (D–E) delta-scale clinoform systems, both in map-view and cross-sections oriented parallel to depositional dips (after Patruno et al., 2015a and references therein). These include: (A) Holocene Ganges muddy subaqueous delta (offshore India and Bangladesh) (modified after Palamenghi et al., 2011); (B, X and Y) –Holocene compound subaerial-subaqueous clinoform systems from the western Adriatic Sea (offshore eastern Italy) (modified after Cattaneo et al., 2003; Correggiari et al., 2005); (C) Holocene sand-prone delta-scale subaqueous clinoforms from offshore Cabo de Gata (southern Spain) (modified after Hernández-Molina et al., 2000a); (D) Cretaceous-age Blackhawk Formation-Mancos Shale subaerial-subaqueous compound clinoform system (modified after Hampson, 2010); (E) sand-prone delta-scale subaqueous clinoforms from the Upper Jurassic Sognefjord Formation (Norwegian Sea) (modified after Patruno et al., 2015a, 2015b, 2015c).

Fig. 14. Examples of cross-sections oriented approximately parallel the depositional dip of shelf-edge clinoform systems. These include: (A) New Jersey Atlantic passive margin, offshore U.S.A. (EW9009 line after Steckler et al., 1999); (B) Late Pliocene-Pleistocene Naust Formation on the Norwegian continental shelf (Line NVGTI-92-105 after Ottesen et al., 2009); (C) Shelf-edge delta lowstand wedge of the Late Pleistocene Po River, Adriatic Sea, offshore central Italy (after Pellegrini et al., 2017); (D) the Van Keulenfjorden outcrop transect from Spitsbergen, Svalbard Islands, showing a 30 km lateral accretion of shelf-edge clinoforms (after Steel and Olsen, 2002).

Fig. 15. Cycles of ascending and descending progradation during the outbuilding of the Dornoch Formation clinoform set (East Shetland Platform, north-eastern UK Continental Shelf) (modified after Reid and Patruno, 2015 and Patruno et al., in press). Likely basin floor fans are associated to cycles of forced regression (i.e., descending clinoform sets), with likely sequence boundaries between the two (*sensu* Neal and Abreu, 2009). Because of the overall increase in accommodation during the deposition of the clinoform set, clinoforms increase their overall vertical relief from the inner to the outer part of the progradational clinoform set. As a consequence, the clinoforms evolve from delta-scale to shelf-edge scale clinoforms.

are linked to river-driven processes and typical low-angle shoreline trajectories (< 0.10°) within each clinoform set (Driscoll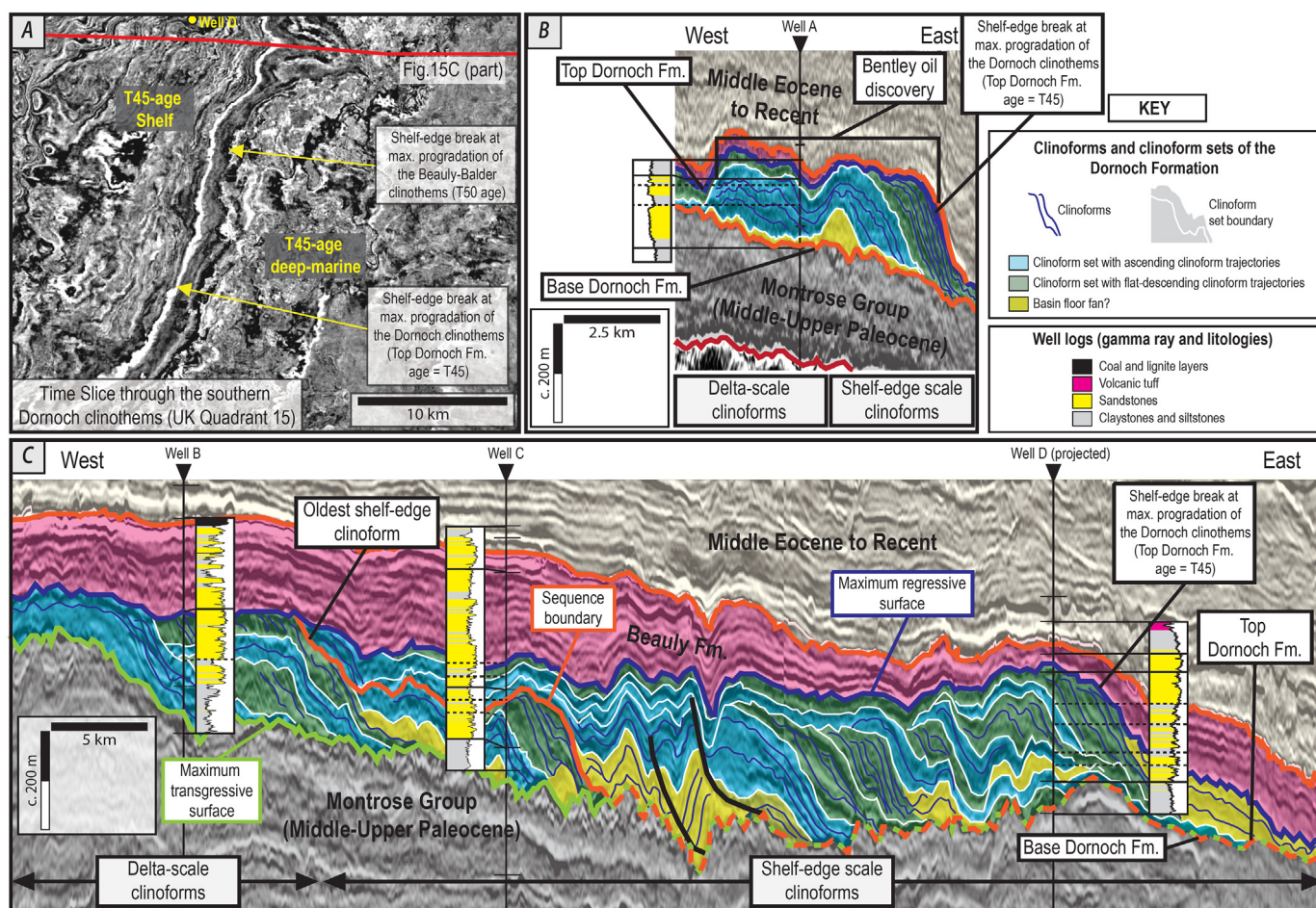 and Karner, 1999; Swenson et al., 2005; Patruno et al., 2015a). These features are in striking contrast with the typical sigmoidal profiles of delta-scale subaqueous clinoforms (see later).

As a consequence of the short time scales involved, the relative proximity of the deltaic source of sediment supply and the laterally-extensive accommodation distribution, shoreline clinoforms may very quickly prograde seaward over large distances. These clinoforms are therefore characterized by the highest values of progradation rates and depositional flux of all the clinoform types (respectively, 1–10^2 km/kyr, 10^{-2}–10^1 km^2/kyr, measured for sub-Milankovitch time spans) (Fig. 8C; Coutellier and Stanley, 1987; Patruno et al., 2015a). Examples of Recent systems include: (1) the Po Delta (Fig. 11b), that has prograded at a rate of 45 km/kyr in the last 360 years, partly because of anthropogenic forcing; (2) the Nile Delta, that has prograded seawards with an average rate of 10 km/kyr in the last 7,000 years; (3) the Ganges-Brahmaputra subaerial delta, that has accreted seaward at a rate of approximately 7 km^2/yr since 1792 (Bellotti et al., 1994; Coutellier and Stanley, 1987; Allison, 1997; Correggiari et al., 2005). More generally, analysis of landsat images show that progradation rates of modern deltaic systems range from 10^{-5} km^2/yr to 10 km^2/yr (Tore Aadland, pers.com. 2017).

In contrast with the uniformity of facies and stratigraphic architecture displayed by delta-scale subaqueous clinoforms, autigenic and high-frequency allogenic forcing in shoreline clinoforms result in episodes of very rapid progradation alternated with periods of abandonment, starvation, hiatuses, erosion and retreat (e.g., 91 episodes of Holocene avulsions in the Rhine-Meuse Delta) (Törnqvist, 1994; Allison, 1997; Saito et al., 2000; Stouthamer and Berendsen, 2000; Correggiari et al., 2005; Blum and Roberts, 2009; Dan et al., 2009). Avulsion periods are usually hallmarked by the deposition of draping clinoform and other diastemic geomorphological elements (e.g., Saito et al., 2000).

Progradational and retrogradational architectures may even be formed at the same time in different sections of the same shoreline/deltaic system (Martinsen and Helland-Hansen, 1995). Fast seaward progradation takes place in the sections of subaerial deltas that are closest to the current position of the main river outlets, while elsewhere the same delta front is sediment-starved and may be undergoing retreat. For example, in 1976–2000, due to fluvial course avulsions, two Yellow River abandoned delta lobes underwent landward retreat over 4.5–7.0 km while, over the same period, another delta lobe prograded quickly seaward over 20 km (Chu et al., 2006).

2.2.1.2. Delta-scale subaqueous clinoforms (Fig. 13). Shoreline-detached, fully subaqueous delta-scale clinoform wedges (or "delta-scale subaqueous clinoforms") build across high-energy shelves between fair-weather and storm wave bases during relative sea-level stillstands, and are arranged through time to form laterally-extensive
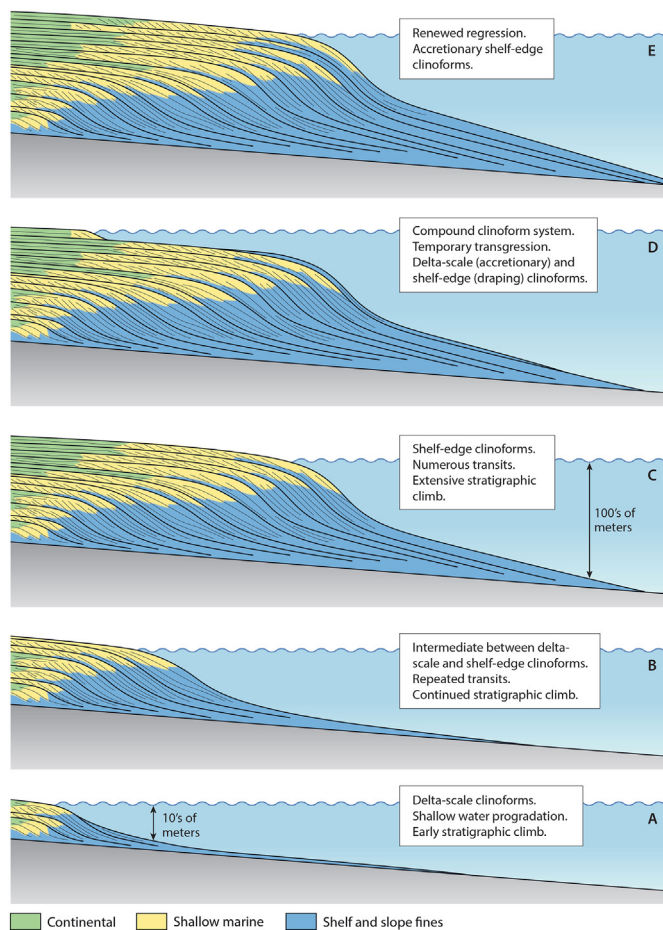
Continental   Shallow marine   Shelf and slope fines

Fig. 16. Sketches showing the nucleation and progressive outbuilding of a shelf-edge clinothem through the repeated regressive-transgressive cross-shelf transits of shoreline clinoforms (A–C). Following an episode of transgressive retreat of the shoreline, a compound shoreline/shelf-edge clinoform configuration is created (e.g., present-day Carolina margin) (D), until the quickly-prograding shoreline clinoforms reach again the shelf-edge, giving rise to a merged shelf-edge delta (E). One scale up, there is the same genetical dynamic relationship between shelf-edge clinoforms (which translate seawards but in cases of particularly high-magnitude relative sea-level rise might also translate landwards), and continental-margin clinoforms (which can only accrete seawards slowly).

clinoform sets (Patruno et al., 2015a).

In contrast with input-dominated subaerial deltas, sediment dispersal and deposition in delta-scale subaqueous clinoforms is driven by basin dynamics, including: (a) near-bed sediment resuspension and advection triggered by large wave-tide shear stresses; (b) advective coastal currents flowing parallel to the clinoform strike; (c) bottom-hugging shelf currents flowing parallel to the foreset-bottomset transition; (d) tidal, upwelling or geostrophic currents further offshore. Due to high near-bed shear stresses, the "subaqueous platform" topsets are regions of predominant bypass. Most river- and surf-derived sediment is transferred seawards, until reaching sufficiently deep bathymetries (typically 20–60 m) for the near-bed shear-stresses to decline below the sediment motion threshold, leading to the thick foreset deposition (Fig. 6b; Kuehl et al., 1986, 1997; Driscoll and Karner, 1999; Hernández-Molina et al., 2000a; Walsh et al., 2004; Swenson et al., 2005; Puig et al., 2007; Jaramillo et al., 2009; Sheremet et al., 2011; Mitchell, 2012; Mitchell et al., 2012; Qiu et al., 2014).

Delta-scale subaqueous clinoforms share many characteristics with shoreline clinoforms, including foreset heights (≤ 45 m) and time-scale of deposition (typically, c. 1–10 kyr) (Figs. 7A, 8A). Unlike shoreline clinoforms, however, delta-scale subaqueous clinoforms form shore-

detached offlap breaks, with typical rollover bathymetry of 20–60 m (Fig. 8). Diagnostic criteria are the presence of well-developed topsets hosting marine lithofacies and benthic fauna and lacking evidence of subaerial exposure, like palaeosols and coastal-plain facies (Cattaneo et al., 2003).

Because of the geometrical similarities between all delta-scale clinoforms, without direct coring it may be challenging to understand whether a mid-shelf delta-scale clinothem (e.g., in the Quaternary) is an actively accreting delta-scale subaqueous clinothem or an older lowstand shoreline abandoned in place following sea-level rise (e.g., Tesson et al., 1990; Hunt and Tucker, 1992; Casalbore et al., 2017). Nevertheless, the morphological classification of Patruno et al. (2015a) go some way to discriminate between these two clinothem types, as summarized below.

Unlike shoreline clinoforms, most delta-scale subaqueous clinoforms are sigmoidal, with the lowest shape ratios of all clinoform types (0.10–0.65), and their trajectories are typically higher-angle (0.1–2.0°) (Fig. 8; Patruno et al., 2015a). Delta-scale subaqueous clinoforms are subject to efficient basinal transport and sorting: therefore, their facies, grain-size, geomorphology and architecture are all more uniform than in shoreline clinoforms (e.g., near-linear plan-view morphology) (Driscoll and Karner, 1999; Goodbred and Kuehl, 2000a, 2000b; Chen et al., 2000; Hernández-Molina et al., 2000a; Cattaneo et al., 2003, 2007; Liu et al., 2004, 2006, 2007b; Lobo et al., 2005; Qiu et al., 2014; Patruno et al., 2015a, 2015b).

The high-angle clinoform trajectories coupled with high-energy shore-parallel advective transport belts create an oceanographic environment capable of trapping most river-fed sediments on the inner shelf and preferentially redistributing them alongshore. This leads to lower across-shelf progradation rates than in most shoreline clinoform sets (Fig. 8C), with a decreased likelihood of sediment transfer to the basin floor (c.f., Fly River and East China Sea sediment budget – Milliman et al., 1985; Walsh et al., 2004; Liu et al., 2006, 2007a). If the shelf and the subaqueous delta front become dissected by canyons, however, this closed system is breached, with shelf-bypass of river-fed sediment (e.g., the Ganges-Brahamaputra – Goodbred and Kuehl, 1999, 2000a, 2000b; Covault et al., 2007; Palamenghi et al., 2011).

Although the characteristics discussed thus far are shared by all delta-scale subaqueous clinoforms, sand-prone and mud-prone clinoform sub-types are characterized by further distinct geometric and genetic features (c.f., Patruno et al., 2015a), as detailed below.

2.2.1.2.1. Mud-prone versus sand-prone delta-scale subaqueous clinoforms. Modern muddy delta-scale subaqueous clinothems are characterized by shore-parallel, broad, low-angle cross-sectional profiles on wide (23–376 km) and gently-sloping (0.01–0.38°) shelves (Patruno et al., 2015a). Most of these clinoforms in the past were simply classified as "prodelta" (e.g., Roberts and Sydow, 2003), as they form muddy "subaqueous deltas" offshore major river outlets, usually developing a compound configuration (see later) with their subaerial delta counterparts (Driscoll and Karner, 1999; Swenson et al., 2005; Giosan et al., 2006a; Xue et al., 2010). Recent examples include the Ganges-Brahmaputra (Goodbred and Kuehl, 1999, 2000a, 2000b; Kuehl et al., 1997, 2005; Michels et al., 1998; Palamenghi et al., 2011, Fig. 13a); Yangtze and Yellow rivers (Chen et al., 2000; Hori et al., 2001; Liu et al., 2004, 2006, 2007a, 2007b; Qiu et al., 2014); Amazon (Kuehl et al., 1986; Nittrouer et al., 1986); Fly Delta (Walsh et al., 2004); Po-Adriatic Shelf (Cattaneo et al., 2003, 2007; Palinkas and Nittrouer, 2006; Puig et al., 2007; Palinkas, 2009, Fig. 13b); and Mahakam Delta (Roberts and Sydow, 2003). These systems are often found in cratonic or passive margin basins, with few exceptions (e.g., the Po-Adriatic – Calamita et al., 2007).

Recent sand-prone delta-scale subaqueous clinoforms, on the contrary, form actively-accreting shore-parallel clastic wedges on narrow (< 35 km) and steep (≥ 0.26°) high-energy shelves, between fair-weather and storm wave bases, and are commonly associated with non-deltaic shorelines and strandplains (Fernández-Salas et al., 2009;
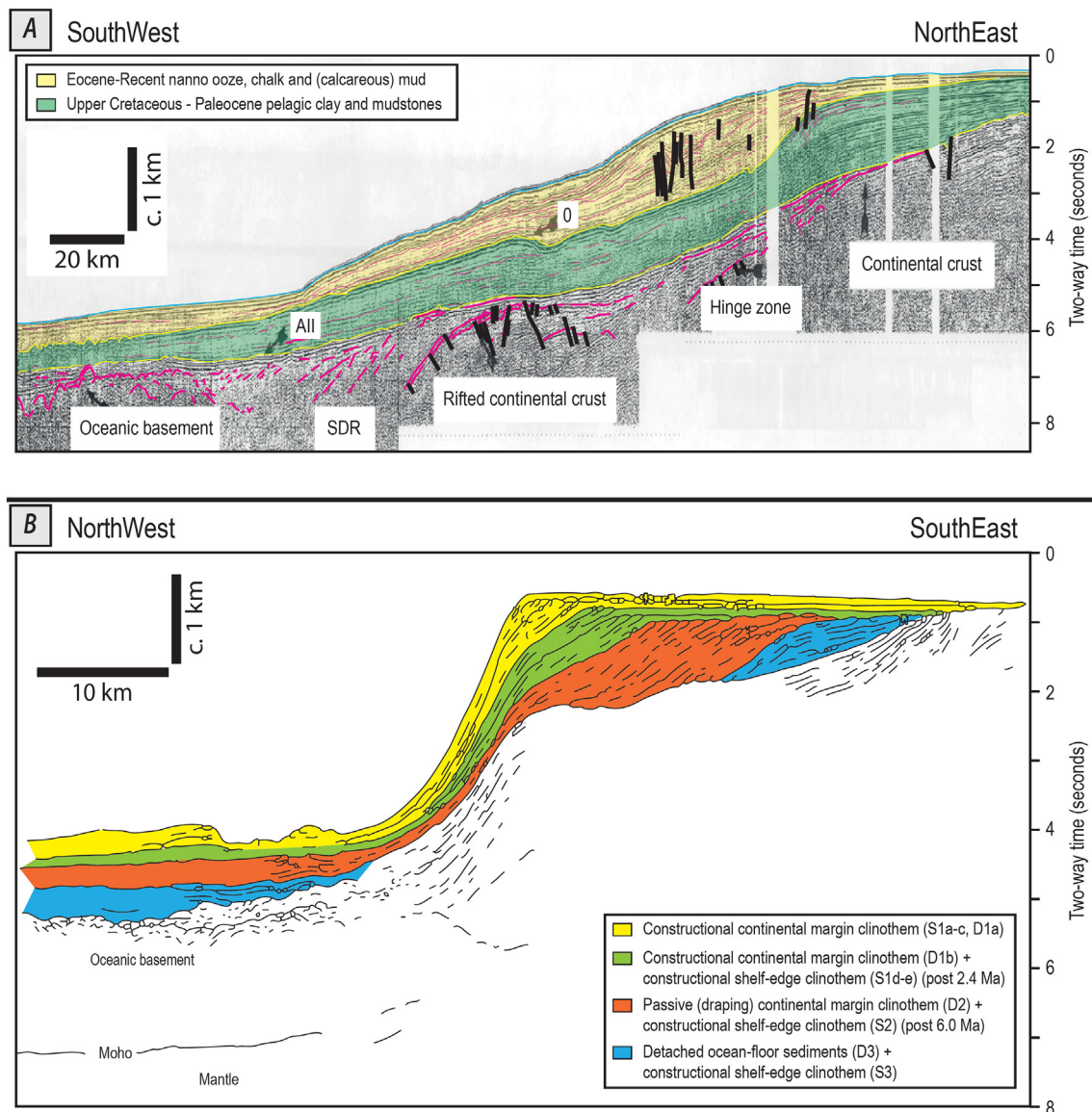
Fig. 17. Two cross-sections oriented approximately parallel to the depositional dip, showing examples of continental margin clinoforms, developed around the boundaries between continental and oceanic crust. (A) Continental margins off south-west Africa (after Profile AM56 of Austin and Uchupi, 1982); (B) Antarctic Pacific continental margins (after Line AMG845-08 of Larter and Barker, 1989).

Patruno et al., 2015a). Examples include the clinoforms offshore Australia and New Zealand (Field and Roy, 1984; Dunbar and Barrett, 2005); southern Spain-Portugal (Hernández-Molina et al., 2000a; Lobo et al., 2005; Fernández-Salas et al., 2009) (Fig. 13c), and California (Chin et al., 1988; Le Dantec et al., 2010). Most of these systems are in extensional or compressional tectonically active settings, which are effective in delivering a high coarse-grained sediment supply to a high-energy, steep and narrow shelf (Walsh and Nittrouer, 2003). The genesis and growth of these sandbodies is in fact linked to the seaward-transport of well-sorted surf-zone sand during storms. Due to wave and current interaction, sand is entrained during storms at sites even deeper than 60 m. Storm-related shore-parallel currents are generally predominant in strength and time-duration, sculpting shore-parallel and near-linear subaqueous clinoforms (Field and Roy, 1984; Hernández-Molina et al., 2000a; Mitchell, 2012; Mitchell et al., 2012). Since the topset-to-foreset rollover depths reflect the wave/current traction field base (Mitchell, 2012), the rollovers of this clinoform sub-type are typically 10–30 m deeper than in muddy subaqueous deltas (respectively, c. 20–60 m and 10–30 m, Fig. 8A).

With a few exceptions (e.g., Neill and Allison, 2005), muddy delta-scale subaqueous clinoform systems form significantly larger sedimentary bodies than sand-prone delta-scale subaqueous clinoforms. The along-strike extent of clinothems are of 10s of km for sand-prone subaqueous clinoforms, versus 100s–1000s of km for muddy subaqueous deltas (e.g. covering the whole East China Sea – Liu et al., 2006, 2007a). Along dip, rollovers of recent muddy subaqueous deltas are at much larger distance from the shorelines (7.5–125 km) than delta-scale sand-prone subaqueous clinoforms (0.6–7.2 km) (Patruno et al., 2015a). Because of the typical association between muddy subaqueous deltas with large river feeders, their values of sediment fluxes and progradation rates (10^{-1}–10^1 km/kyr) are high, and more similar to those of shoreline clinoforms than to those of sand-prone delta-scale subaqueous clinoforms. In contrast, because of the sporadic nature of depositional episodes, progradation rates and depositional flux of sand-prone subaqueous clinoforms are up to 3-4 and 2-3 orders of magnitude lower, respectively, than in subaerial deltas and muddy subaqueous deltas (Patruno et al., 2015a; Fig. 8C).

The down-dip extents of sand-prone delta-scale subaqueous clinoform foresets (≤ 2.6 km) are one order of magnitude smaller than in other delta-scale clinoform types. As a consequence, the gradients of

Fig. 18. Examples of continental margin clinoforms. (A) Regional structural-bathymetric map of the Atlantic margins of the south-eastern United States, showing the location of the continental margin scale sedimentary wedge in relation to the continent/ocean transition; (B) 3D cartoons showing the Meso-Cenozoic geological evolution of the eastern Carolina continental margin (south-eastern U.S. Atlantic margin), with the position of the Jurassic-Recent continental margin scale clinoform slopes reflecting the transition between continent and ocean crust (redrafted after Dillon et al., 1983); (C) Interpreted seismic cross-section off North Carolina, showing the progressive progradation of shelf-edge clinoforms towards the continental margin slope, forming an early shelf-edge to contieneral margin compound clinoform system and a late hybrid continental margin clinoform ("seismic image courtesy of the USGS https://walrus.wr.usgs.gov/namss/search/). BE = Blake Escarpment; FHS = Florida-Hatteras Slope. (Klitgord and Schouten, 1986)

their foresets (0.6–9.0° in modern examples, and up to 27° in ancient ones) and inner bottomsets (0.1–4.0°) are more similar to the gradients of continental-margin clinoforms (see later) than to other types of delta-scale clinoforms. In contrast, muddy subaqueous clinoforms are characterized by gentle slopes for both bottomsets/topsets (< 0.4°) and foresets (< 0.9°) (Fig. 7C). In Recent systems, a foreset gradient threshold of 0.3-0.5° between these two clinoform sub-types has been identified (Patruno et al., 2015a).

Table 1
Principal characteristics of clinoform types of different scale. Data after Patruno et al. (2015a).

			Delta-scale clinoforms				
	Continental margin clinoforms	Shelf-edge clinoforms	Muddy subaqueous delta clinoforms	Sand-prone subaqueous delta clinoforms		Shoreline clinoforms	
				≤ 20 kyr	> 20 kyr	≤ 20 kyr	> 20 kyr
Rollover water depth (m)	550–1770. It can be as shallow as 0 m in case of shelf-edge and continental margin deltas[a]	60–426	6–59	21–57		0–5	
Foreset — Heights (m)	590–2570	97–300	3–46	12–43		5–38	
Foreset — Down-dip extent (km)	6.5–82.3	2.4–17.2	1.0–11.8	0.1–2.6	0.05–1.8	0.1–19.6	
Foreset — Slope gradient (°)	1.1–12.5	0.6–4.8	0.1–0.9	0.6–9.0	0.7–27.0	0.05–6.1 (Coarse grained systems can be as steep as c.30°)	
Time scale (kyr)	10^3–10^5. Up to 10^1 kyr in case of shelf-edge deltas[a]	10^2–10^4	10^{-1}–10^1	10^1	10^1–10^2	10^{-2}–10^0	10^1–10^3
Progradation rate (m/kyr)	10^{-2}–10^1	10^{-1}–10^1. Up to 10^4 m/kyr in case of shelf–edge deltas[a]	10^2–10^4	10^1–10^2		10^3–10^4	
Clinoform trajectory (°)	+0.9 to +49	−0.4 to +2.4	0 to +0.5	−0.4 to +3.5	−0.5 to +2.0	0 to +0.13	0 to +0.90
Coarse-grained sediment dispersal	Gravity, large-scale deformation, canyons	Fluvio, wave, tide, gravity, sea-level control	Storm, tide, currents, gravity	Storm, gravity, currents		Fluvio, wave, tide, gravity	
Clinoform reservoir potential	Poor (distal drapes), less than for shelf-edge deltas	Poor (distal drapes)-excellent (shelf-edge delta)	Poor	Minor to Excellent		Poor-Excellent	
Basin floor reservoir potential	Thick, connected	Good potential, possibly disconnected	Minor	Minor, greater if close to the shelf-edge		Few, thin, disconnected	

[a] Values of water depth, progradation rates and time scale for shelf-edge deltas are based on 100s–1000s year cycles in the case-study of the Po shelf-edge delta during the Pleistocene lowstand (Pellegrini et al., 2017, 2018).

These and other anomalous values of geomorphological, sedimentological and stratigraphic features are helpful to identify ancient delta-scale subaqueous clinoforms (Patruno et al., 2015a). Examples include those described by Plint et al. (2009), Hampson (2010), Patruno et al. (2015a, 2015b, 2015c), Hampson et al. (2015) and Hampson and Premwichein (2017).

In the carbonate realm, there are also similar laterally-extensive, fully-subaqueous clinothems that strike parallel to the palaeo-shoreline. These contain coarse-grained cross-bedded grainstones, transported seaward by waves and currents and emplaced below wave base (c. 40–70 m), and are also associated to shore-parallel shelfal (topset) and bottom (toeset) currents (Cathro et al., 2003; Pomar and Tropeano, 2001; Pomar et al., 2002; Quiquerez and Dromart, 2006; Maurer et al., 2010). Both clastic and carbonate delta-scale coarse-grained subaqueous topsets and foresets comprise high-energy facies with good reservoir quality (Maurer et al., 2010; Patruno et al., 2015b).

2.2.2. Shelf-edge scale clinoforms (Figs. 14–16)

Shelf-edge clinoforms (in previous literature termed shelf-prism clinoforms – Helland-Hansen and Gjelberg, 2012; Patruno et al., 2015a) are surfaces of dynamic equilibrium that form at the margins of either marine or lacustrine basins characterized by minimum water depths of a few hundreds metres. In the case of non-erosional "progradational margins" (sensu Ross et al., 1994; Ryan et al., 2009a), the topsets and foresets of these clinoforms represent respectively the morphological shelf and slope, and the topset-to-foreset rollover point correspond to the shelf-slope break (Henriksen and Vorren, 1996; Steel et al., 2000; Steel and Olsen, 2002; Roberts and Sydow, 2003; Sztanó et al., 2013; Hodgson et al., 2018; Pellegrini et al., 2018). As a consequence, these clinoforms separate relatively shallow-water fluvio-deltaic to offshore transition and offshore facies (topsets) from deep-water bathyal, mass flow and turbiditic facies (bottomsets).

The above definition differentiates real "shelf-edge clinoforms" from thousands of metres high "continental margin clinoforms" (see next section). While the latter clinoform types represent the continental margin between the "continental shelf" and the abyssal plain, shelf-edge clinoforms are situated within the "continental shelf" itself, with their topset representing a bathymetric shelf *sensu stricto* and their bottomset corresponding to a deeper-water plateau, which is still part of the "continental shelf" (Gross and Gross, 1994) (Fig. 1). The distinction between bathymetric shelf and deeper-water plateau (with the "shelf edge" between them) is pragmatic as these two areas of the continental shelf are characterized by significantly different facies: fluvio-deltaic to offshore in the shelf *sensu stricto*, and bathyal facies (below storm wave base and photic zone) in the plateau. As a consequence, shelf-edge clinoform surfaces represent, as all the other clinoform types described here, a significant physiographic boundary in depositional processes and facies. It is also important to point out that there are very few recent examples of shelf-edge clinoforms on present-day continental shelves, which normally only host a large scale clinoform at the continental margin (i.e., a "hybrid" shelf-edge to continental-margin clinoform according to the nomenclature suggested here, see Section 2.3), and are devoid or real "plateaus" and "shelf edges" (c.f., Fig. 1). Exceptions to this rule are represented by for example the continental shelf off Carolina, eastern U.S. (Figs. 10A, 18) and by the Pleistocene lowstand mid-Adriatic shelf-edge delta (Pellegrini et al., 2017, 2018; Fig. 14C).

Shelf-edge clinoform sets typically represent c. 0.1–20 Myr; foreset heights are c. 100–300 m and slope gradients range from 0.9–10° (inflection zones) to 0.6–4.8° (average foreset) (Figs. 7–8; Vanney and Stanley, 1983; Steckler et al., 1999; Steel and Olsen, 2002; Patruno et al., 2015a). Because of the dominance of short-term progradation and long-term aggradation in cycles of continental shelf outbuilding (Bullimore et al., 2008; Carvajal et al., 2009), shelf-edge clinoforms show lower progradation/aggradation ratios (with clinoform trajectories as high as 2.4°) and higher progradation resistance ratios (10^{-2}–1) than delta-scale clinoforms (Patruno et al., 2015a) (Fig. 8). Because of the predominance of high-angle trajectories, basinal processes and fine-grained sizes, shelf-edge clinoforms often display sigmoidal profiles, albeit oblique geometries are present in case of shelf-

edge deltas and/or descending trajectories (Adams and Schlager, 2000; Pellegrini et al., 2017; Fig. 14B–C).

With the exception of draped structurally-controlled shelf-edge clinoforms (e.g., Fig. 5c), the repeated, regressive-transgressive, cross-shelf transit of delta-scale clinoforms is the key process that leads, through time, to the nucleation and evolution of most larger-scale shelf-edge clinoforms (Burgess and Hovius, 1998; Steel et al., 2000, 2003, 2008; Porębski and Steel, 2003, 2006; Johannessen and Steel, 2005; Olariu and Steel, 2009; Helland-Hansen et al., 2012) (Fig. 16). Initially, multiple superimposed delta-scale clinoform sets accrete by across-shelf delta progradation, repeatedly infilling the landward-tapering shelfal accommodation after each transgression (Fig. 16A–C). These repeated cross-shelf transits results in long-term "stratigraphic climb" and gradually steeper and higher frontal slopes, with an eventual transition of clinoforms from delta-scale to shelf-edge scale (Fig. 16); Sydow and Roberts, 1994; Deibert et al., 2003; Porębski and Steel, 2003; Anderson, 2005; Anderson et al., 2016; Sztanó et al., 2013).

Normally, both a proximal active delta-scale clinoform system and a distal shelf edge draping clinoform with rollover-point bathymetries of up to 500 m are present (Fig. 16D), forming a compound clinoform system (see later), and shelf-edge clinoforms prograde slowly (c. 1–20 m/kyr), via hemipelagic fallout (Steel et al., 2000, 2003, 2008; Steel and Olsen, 2002). Whenever the sediment-delivery deltaic systems reach the shelf break ("shelf-edge delta" stage, c.f. Johannessen and Steel, 2005), however, the shelf margin (i.e. the clinoform foreset) is subject to significant accretion, with much faster progradation rates (e.g., up to 10^4 m/kyr in the Pleistocene Po lowstand delta – Pellegrini et al., 2017, 2018) (Fig. 16E). As a consequence of this growth style, shelf-edge clinothems typically possess a bipartite lithology, reflecting alternate sourcing by starved hemipelagic-hyperpycnal mud-drapes and, during shelf-edge delta stages, by active mud- or sand-prone shoreline progradation (Porębski and Steel, 2003; Bhattacharya and MacEachern, 2009).

Several published case studies detail this relationship between shelf-edge clinoforms and superimposed delta-scale clinoform cycles (e.g., Oliveira et al., 2011). For example, the Eocene-age succession outcropping in Spitsbergen hosts both gently-dipping low-relief (tens of metres) shoreline clinoforms and more steeply-dipping (3–6°), high-relief (average 200 m) sandy shelf-edge clinoforms. Regressive-transgressive shoreline cycles across narrow (1–10 km) and shallow (< 50 m) shelves are reflected by the alternate deposition of actively accreting sand-prone shelf-edge delta clinothems and, after each transgression, mudstone-prone shelf-edge draping clinothems (Helland-Hansen, 1992, 2010; Helland-Hansen et al., 1994; Steel et al., 2000, 2003; Steel and Olsen, 2002; Mellere et al., 2002; Johannessen and Steel, 2005; Uroza and Steel, 2008; Johannessen et al., 2011; Grundvåg et al., 2014) (Fig. 14D). On the Shetland Platform (UK Continental Shelf), the Palaeogene Dornoch Formation forms sandstone-prone and laterally extensive clinoform sets that prograde over a largely Paleozoic substrate (Patruno and Reid, 2016, 2017; Patruno, 2017; Patruno et al., in press; Patruno and Lampart, 2018). These clinoforms gradually become higher-relief and more steeply-dipping basinward, due to both repeated stratigraphic climb and deeper palaeobathymetries linked to a gentle basinward tectonic titling of the substrate. On the outer platform, therefore, these clinoforms are interpretable as shelf-edge deltas (Fig. 15; Patruno and Reid, 2016, 2017; Scisciani et al., in press; Turner et al., in press). On the Norwegian Continental Shelf, the Jurassic-age Sognefjord Formation comprises transgressive-regressive delta-scale sand-prone clinoform cycles. When a new clinoform set progrades beyond the leading edge slope of the previous set, it expands its thickness (up to 70 m) and decreases its progradation rate, due to the sudden increase in accommodation controlled by antecedent palaeobathymetry (Patruno et al., 2015b, 2015c) (Fig. 13e). If this process had been repeated more times, a "true" shelf-edge scale clinothem (i.e. thicknesses > 100 m) would have been nucleated from delta-scale precursors.

As detailed in Section 2.3, shelf-edge clinoforms have been subject of intense active research, with the main focus to better predict the timing, amount and mode of emplacement of sand-transport from the shelf (topset) to the basin-floor (bottomset) (e.g., Steel and Olsen, 2002; Porębski and Steel, 2003, 2006; Løseth et al., 2006; Carvajal and Steel, 2009; Jones et al., 2013, 2015).

Shelf-edge clinoforms are identified on modern bathymetric profiles (Fig. 10 a,b,d) as well as in the ancient record (Steckler et al., 1999; Ryan et al., 2009a; Steel et al., 2000, 2003, 2008; Steel and Olsen, 2002; Johannessen and Steel, 2005; Glørstad-Clark et al., 2011; Klausen et al., 2016) (Figs. 14–15). Carbonatic shelf-edge scale clinoforms driven by both in-place carbonate production and off-shelf sediment transport have also been described (e.g., James and Von Der Borch, 1991; Puga-Bernabéu et al., 2010). As in siliciclastic systems, shelf-edge carbonate clinoforms are steeper and with a broader range of cross-sectional geometries than proximal delta-scale carbonate clinoforms, which typically show oblique/exponential profiles (Quiquerez and Dromart, 2006).

2.2.3. Continental margin scale clinoforms (Figs. 17-18)

Continental margin scale clinoforms are the largest clinoform types, with foreset heights of about 600–2600 m and slope gradients ranging from 1.6–16.2° (inflection zone) to 1.1–12.5° (average foresets) (Fig. 7; Patruno et al., 2015a). These large-scale clinoforms consist of topset-to-foreset rollover bathymetries of up to 1,770 m and develop over tens to hundreds of Myr (Fig. 8A) (e.g., Jurassic-Recent eastern United States continental margin – Figs. 10a, 18; Shipley et al., 1978; Schlee et al., 1979; Dillon et al., 1983; Klitgord and Hutchinson, 1988). Therefore, progradation rates and unit-width depositional flux of continental margin clinoforms are respectively up to 6 and 5 orders of magnitude lower than delta-scale clinoforms (Patruno et al., 2015a) (Fig. 8C). A relatively continuous and long-lasting but low-frequency stratigraphic record is thus revealed by continental margin clinoform trajectories (e.g., ice-sheet fluctuations – Larter and Barker, 1989).

Continental margin clinoform sets show the highest values of clinoform trajectories angles (0.9–49°) and progradation resistance ratios (up to 4×10^{-1}) of all the clinoform types (Fig. 8B). As a consequence of the low progradation/aggradation ratios, the predominance of basinal processes and fine-grained lithotypes, continental margin clinoforms are nearly universally characterized by sigmoidal, symmetrical cross-sectional profiles (Fig. 17; Pirmez et al., 1998; Adams and Schlager, 2000; Patruno et al., 2015a).

As previously pointed out, although both shelf-edge and continental-margin clinoforms are developed at the outer edge of a bathymetric "shelf" or "plateau", several authors differentiate these two categories on the basis that they correspond to statistically different clinoforms, associated to distinct structural styles and bathymetry (Carvajal et al., 2009; Henriksen et al., 2011; Patruno et al., 2015a). Diagnostic characteristics for continental-margin clinoforms over shelf-edge clinoforms include significantly slower progradation rate, lower progradation/aggradation ratios (Fig. 8C), and more common gravity-driven slope deformation (Wolinsky and Pratson, 2007; Carvajal et al., 2009; Patruno et al., 2015a). Only major structural elements (e.g., ocean/continent boundaries) can form slopes as high as thousands of metres. As a consequence, our definition of "continental-margin (scale) clinoform" comprises even clinoforms with heights as little as 500 m, as long as they are initially produced by the long-term sedimentary mantling of slopes associated with the transition from continental to oceanic crust, possibly followed by active "continental margin-delta" accretionary phases (see later) (Austin and Uchupi, 1982; Rice and Shade, 1982; Dillon et al., 1983; Larter and Barker, 1989; Hiscott, 2001; Walsh and Nittrouer, 2003; Lin et al., 2008; Houseknecht et al., 2009; Covault et al., 2009; Hubbard et al., 2010). This primary conditioning of continental-margin (scale) clinoform relief from geodynamics rather than sedimentary processes separates this clinoform class from the previous ones (including shelf-edge clinoforms), which are rarely

associated directly with continental margins, active tectonics or structural lineaments (Steel and Olsen, 2002).

Continental-margin clinothems are largely mudstone-prone (Porębski and Steel, 2003). Slopes and deep-water basins associated to continental margin clinoforms may nevertheless host a large amount of

reservoir-forming sandstones, particularly in supply-dominated shelf-margins, where delivery of sand beyond the shelf-edge is primarily a consequence of the high rate of sediment supply and/or relative sea-level falls (Carvajal et al., 2009). For example, Neogene slope-prone deposits accumulated on the Brazilian continental margin

Fig. 19. Interpreted seismic cross-sections oriented parallel to the depositional dip, showing examples of compound clinoform systems at various scale: (A) Jurassic to Recent shelf-edge (Florida-Hatteras Slope) to continental margin (Blake Escarpment) compound clinoforms from the Atlantic margins of the south-eastern U.S. (offshore Southern Carolina: Line FC8 after Schlee et al., 1979); (B) Quaternary-age delta-scale (accretionary) to shelf-edge (draping) compound clinoforms from southern Iberia (after Hernández-Molina et al., 2000b); (C) Holocene-age shoreline to delta-scale subaqueous clinoform compound clinoform system from the Tiber Delta, Tyrrhenian Sea, central Italy (after Amorosi and Milli, 2001).

clinoforms (Campos Basin area), with sand accumulations particularly concentrated on the upper slope and at the base of the continental slope, with a middle foreset area which is a predominant bypass zone (Viana et al., 1998). The processes responsible for the delivery of sand to the continental slope in this case study is a three-stage process, which involves: (a) waves, tides and surface currents with sufficient energy to form submarine sand-prone submarine dunes on the outer shelf; (b) export of this sand from the outer shelf to the slope via a combination of sand spillover, waves, eddies and gravity-driven turbidity currents; and (c) sand deposition on the slope, controlled by the interplay between slope physiography (e.g., presence of canyons), mass movements and deep-marine contour currents (Viana et al., 1998; Viana et al., 1998; Rodger et al., 2006; Carvajal et al., 2009). The episodic development of continental-margin deltas and gullied clinoform rollovers are the key processes responsible for the formation of sand-rich continental-margin clinothems, as detailed in the next section.

2.3. Spatial associations of coeval clinoforms: compound versus hybrid clinoforms

The clinoform types described thus far can occur in isolation or be dynamically linked down-depositional dip. The latter case corresponds to compound and hybrid clinoform systems.

Compound clinoform configurations comprise clinoforms in a more proximal position and genetically-linked and time-equivalent outer clinoforms situated down depositional dip, such that the bottomset of a clinoform located in an up-dip location corresponds to the topset of a larger-scale clinoform set further down-dip (Figs. 19 and 20; Patruno et al., 2015a). In an extreme case, the four types of clinoforms (shoreline clinoforms, delta-scale subaqueous clinoforms, shelf edge clinoforms and continental margin clinoforms) may prograde simultaneously along shoreline-to-abyssal plain transects, although at significantly different rates (e.g., the U.S. Atlantic margin – Fig. 18). In other cases, progradation, erosion and retrogradation may take place at the same time in different sectors of a shoreline to abyssal plain transect (e.g., Madof et al., 2016).

Although delta-scale compound clinoform progradation during overall transgressive conditions have been recently reported (Pellegrini et al., 2015), compound clinoforms are typically developed during early highstands, after a prior transgression lead to the physical separation of shorelines and shelf-edge. During many subsequent episodes of cross-shelf shoreline transits, however, due to the exponential differences in progradation rates between clinoforms at the shoreline (c. 1,000–100,000 m/kyr), subaqueous delta (c. 100–20,000 m/kyr), shelf-edge (c. 1–100 m/kyr) and continental margin (c. 0.1–10 m/kyr) (Fig. 8C), these clinoforms types will gradually merge together through the establishment of shelf-edge deltas and continental-margin deltas, leading to a progressive reduction of the depositional breaks-in-slope along a shoreline-to-abyssal plain transect (e.g., only one, in the extreme case of continental-margin deltas). These "hybrid clinoforms" are simultaneously characterized by reliefs typical of the largest-scale clinoform type and by intermediate facies, progradation rates,

Fig. 20. (A) 3D cartoon illustrating the architectural and facies relationships in a mixed sandstone/mudstone subaerial to subaqueous delta-scale compound clinoform system associated to its time-equivalent shelf-edge clinoform (based on the Mahakam Delta system from the Makassar Strait, eastern Borneo, Indonesia - redrafted after Gerard & Oesterle, 1973); (B) 3D cartoon illustrating the architectural and facies relationships in a sand-prone delta-scale compound clinoform system (based on the offshore southern Iberia "infralittoral prograding wedge" – redrafted after Hernández-Molina et al., 2000a); (C) 2D cartoon oriented parallel to the depositional dip, illustrating the main differences in architecture, facies and depositional regime between mudstone-prone and sandstone-prone delta-scale compound clinoform systems (after Patruno et al., 2015a).

morphologies and architectures (e.g., anomalously fast "shoreline-like" progradation rates of shelf-edge deltas).

The cycle of hybrid clinoform formation begins with the shoreline clinoforms merging with the normally slower delta-scale subaqueous clinoforms, giving rise, during the middle part of a highstand cross-shelf regression, to a single delta-scale clinoform system within the shelf ("hybrid shorelines"). For example, over the past 500 years, the Nile discharge has been confined to two main distributaries (Rosetta and Damietta), leading to their extensive progradation and a change of the Nile Delta from a precedent arcuate and wave-dominated delta-front with associated mid-shelf muddy subaqueous delta fed by high-energy longshore currents (c. 5,000–500 years ago) to a more river-dominated and strongly prograding hybrid subaerial delta since 500 years ago, focused on the Rosetta and Damietta lobes and devoid of subaqueous delta counterparts (Summerhayes et al., 1978). This process of hybrid shoreline formation might not take place, however, in basins persistently dominated by high hydrodynamic energy (compared to river-driven sediment supply). In these cases, most of the river-driven sediment is supplied to the subaqueous delta, which is therefore characterized by a higher progradation rate than its «subaerial» counterpart (e.g., Liu et al., 2006; Liu et al., 2007a, 2007b; Hampson, 2010).

After its initial formation, the hybrid shoreline system reaches the shelf-edge, giving rise to a "shelf-edge delta", that is a unique shoreline/shelf-break slope at the shelf-edge (0–5 m rollover bathymetry). In this context, Pellegrini et al. (2018) shows that, as shorelines approach the shelf-edge in the final stages of the formation of a shelf-edge delta "hybrid clinoform", the distance between shorelines and shelf-edge can give rise to different clinoform geometry and distinctive basinal deposits. Finally, if the shelf-edge delta reaches the continental margin (i.e. the edge of a whole continental shelf), a hybrid "continental margin delta" is created (e.g., present-day Niger, Congo, Mississippi and Amazon deltas – Fisk et al., 1954; Short and Stauble, 1967; Damuth, 1994; Hiscott, 2001; Rodger et al., 2006; Peltier and Fairbanks, 2006) (see Section 2.3.2).

This whole cycle of cross-shelf delta transit and progressively higher-relief hybrid clinoform formation (c.f., Porębski and Steel, 2006) usually lasts less than 100 kyr (Burgess and Hovius, 1998; Steel et al., 2008), and could be significantly faster in cases of sea-level fluctuations characterized by higher-than-normal amplitude and frequency (e.g., Pleistocene glacio-eustatic changes). Cross-shelf delta transits are controlled by the interplay between: (a) relative sea level changes; (b) rates of river-fed sediment supply and calibre of sediment input; (c) alongshore and shore-perpendicular marine transport rates and the dominant depositional processes; (d) initial volume, length, gradient and physiography of shelf and slope. These factors determine: (1) the possibility for a shoreline to reach the shelf edge during any particular transit; (2) the time needed for that to happen; and (3) the sand/mud budget partitioning along the different segments of the shoreline-shelf-slope-basin delivery systems (Burgess and Hovius, 1998; Steel and Olsen, 2002; Muto and Steel, 2002; Johannessen and Steel, 2005; Porębski and Steel, 2003; Steel et al., 2008).

Cycles of alternate compound and hybrid clinoform development take place because regressive cross-shelf delta transits can be interrupted at any point by ensuing transgressions or auto-retreats (Muto et al., 2007). For a typical relative sea-level rise of < 100 m, delta-scale clinoforms retreat landward, while shelf-edge clinoforms are left in place, giving rise to a new compound system with an accretional delta-scale clinoform and a shelf-edge passive clinoform. Subsequently, if delta-scale clinoforms prograde across the shelf at a sufficiently fast rate, they will reach the shelf-edge before the onset of the next transgression, and the compound-hybrid clinoform cycle continues.

A similar evolutionary cycle occurs for shelf-edge to continental margin compound clinoform systems, but involving low-frequency and high-magnitude relative sea-level cycles over timescales of millions of years, and rare instances of shelf-edge landward retreats. For example, in the Mesozoic, a single hybrid shelf-edge to continental-margin

clinoform system existed offshore Carolina (U.S.) (Fig. 19a). Following the onset of the "middle Cretaceous" climate warming and global oceanic anoxia (e.g., Patruno et al., 2015d; Unida and Patruno, 2016), a major Late Cretaceous eustatic rise (c. 100–200 m) caused the shelf-edge to be shifted up to 300 km landward, giving rise to a detached shelf-edge clinoform (Florida-Hatteras Slope) and a compound passive/draping continental margin clinoform (Blake Escarpment), separated by the wide submarine Blake Plateau (Figs. 10A, C, 18A–B, 19A; Uchupi, 1968; Shipley et al., 1978; Schlee et al., 1979; Dillon et al., 1983).

The best-known compound and hybrid clinoforms are delta-scale compound clinoforms and shelf-edge delta or continental-margin delta hybrid clinoforms, as further discussed below.

2.3.1. Delta-scale compound clinoforms (Figs. 19c, 20)

Delta-scale compound clinoforms consist of genetically-related paired subaerial and subaqueous delta-scale clinoforms, separated by a "subaqueous platform" bypass region (i.e., the subaqueous clinoform topset) (Fig. 19) (Allison, 1997; Pirmez et al., 1998; Driscoll and Karner, 1999; Goodbred et al., 2003; Swenson et al., 2005; Kuehl et al., 2005; Giosan et al., 2006a; Pellegrini et al., 2015). Examples of Recent delta-scale compound clinoforms were formed at the onset of the Late Holocene highstand, and include the Western Adriatic (Fig. 13b), the Ganges-Brahmaputra, the Yellow Sea and the Mahakam River Delta (Fig. 20a) (Nittrouer et al., 1986; Michels et al., 1998; Cattaneo et al., 2003, 2007; Kuehl et al., 2005; Liu et al., 2004, 2007a, 2007b).

Generally, the partitioning of river-fed sediment between subaerial and subaqueous delta clinoform components is determined by the interplay between fluvial input and basin hydrodynamics. The portion of sediments reaching the subaqueous delta increases with: (1) greater magnitude and frequency of storm events; (2) decreasing river-flood discharge; and (3) decreasing sediment grain-size (Pirmez et al., 1998; Driscoll and Karner, 1999; Goodbred et al., 2003; Cattaneo et al., 2003, 2007; Swenson et al., 2005; Palinkas and Nittrouer, 2006; Puig et al., 2007; Palinkas, 2009; Mitchell, 2012).

As a consequence of the above, the relative growth and development of subaqueous and subaerial delta-scale clinoforms are inversely related to each other, as suggested by negative correlations between the width of shelfal mudstone and coastal plain belts (Swenson et al., 2005; Hampson, 2010). For example, the Late Holocene Nile Delta evolved from a wave-dominated compound system (ca. 5–0.5 ka B.P.) into a strongly progradational river-dominated subaerial delta (i.e., a "hybrid shoreline", since 0.5 ka B.P.) due to an increase in sediment input (Summerhayes et al., 1978; Frihy, 1988; Goodfriend and Stanley, 1999). The case study of the Atchafalaya Delta (U.S.), similarly, revealed a slightly diachronous development of a delta-scale compound clinoform system, with a 22 year difference between the onset of subaqueous and subaerial deltas (Roberts et al., 1980).

In cases where subaqueous deltas are well-developed, these will receive larger amounts of river-fed sediments than subaerial deltas, and will therefore form larger sedimentary bodies with faster progradation rates, resulting in a progressive lengthening of the subaqueous platform during regression (Liu et al., 2006, Liu et al., 2007a, 2007b; Hampson, 2010).

2.3.2. Shelf-edge delta and continental-margin delta hybrid clinoforms

Shelf-edge and continental-margin deltas are a common component of Quaternary shelves (Fig. 19a), and are the only instances when «deltaic clinothems» can be as thick as 100s–1000s m (Suter and Berryhill Jr., 1985; Mayall et al., 1992; Sydow and Roberts, 1994; Morton and Suter, 1996; Steel et al., 2000, 2003, 2008; Steel and Olsen, 2002; Porębski and Steel, 2003; Sydow et al., 2003; Johannessen and Steel, 2005; Covault et al., 2009; Hubbard et al., 2010; Pellegrini et al., 2018). In particular, example of Quaternary continental-margin deltas include the Niger, Congo, Mississippi and Amazon deltas (Fisk et al., 1954; Short and Stauble, 1967; Damuth, 1994; Hiscott, 2001; Rodger et al., 2006; Peltier and Fairbanks, 2006).

Accretional shelf-edge and continental-margin delta clinothems are separated by hemipelagic clinothems plastered on the shelf- or continental-margin after each delta retreat. Accretional shelf-edge clinothems might host highly continuous and laterally extensive reservoir intervals, forming some of the most prolific hydrocarbon fields in the World (e.g., Sydow et al., 2003). Furthermore, as detailed below, they might be associated with significant deep-water coarse-grained sediment transfer, depending on four factors: (1) clinoform trajectories; (2) sediment supply; (3) depositional processes; (4) presence of gullied shelf-edges.

Lowstand stages or phases of highly progradational, flat or descending clinoform trajectories (i.e., forced regressions) favour the establishment of the factors for the accelerated growth of sand-rich basin-floor fans, with efficient and rapid (<0.1 Myr) sand transport beyond river-dominated shelf-edge or continental-margin deltas through focused and long-lived channelized shelf-slope pathways. During normal regression (i.e., ascending clinoform trajectories), in contrast, continental-margin and shelf-edge deltas are normally associated with aggradational wave-dominated clinoforms that are near-linear in plan-view, lack focused sediment dispersal and, in the absence of gullied shelf-edges, are characterised by slopes that are either mudstone-prone or host only minor tempestite sheet sandstones, and by negligible or

muddy submarine fan development (Kolla et al., 2000; Steel and Olsen, 2002; Plink-Björklund and Steel, 2002, 2006; Deibert et al., 2003; Ritchie et al., 2004a, 2004b; Bullimore et al., 2005; Johannessen and Steel, 2005; Porębski and Steel, 2006; Carvajal and Steel, 2009; Uroza and Steel, 2008; Gong et al., 2015; Gong et al., 2015; c.f. also the c2 clinothem of the upper Pleistocene Po-Adriatic succession, as detailed in Pellegrini et al., 2018).

In cases of very high sediment supply, however, deep-water sand transport may take place even during normal regressions and/or highstands, through un-channellized slumping, mass transport complexes and low-density turbidites (Carvajal and Steel, 2006, 2009; Steel et al., 2008; Carvajal et al., 2009; Kertznus and Kneller, 2009; Henriksen et al., 2011; Dixon et al., 2012a, 2012b). A key example in this respect is the Neogene lacustrine shelf-edge scale clinoform succession in the Pannonian shelf-edge lacustrine basins (Magyar et al., 2013; Sztanó et al., 2013), where each phase of rising base-level corresponded to a time of climate-driven high sediment supply, when large volumes of sediments bypassed the aggrading topsets onto the slope and basin-floor. During times of base-level stagnation or minor fall, however, sediment supply was not enough to bypass the slope, and no deep-water fan was formed.

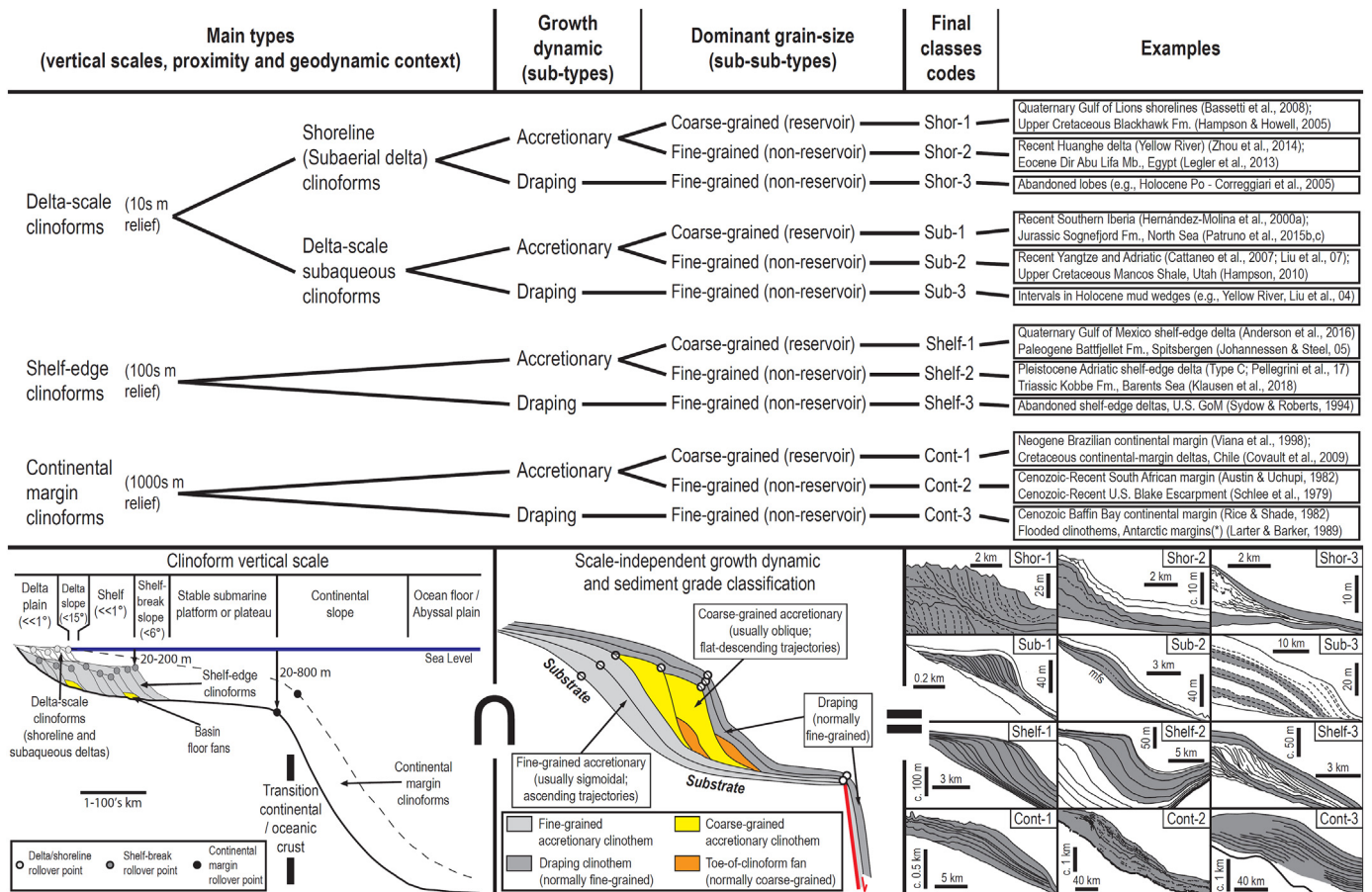Deep-water sediment transfer in wave-dominated shelf-edge and

Fig. 21. Logical scheme of the new classification scheme for clinoforms proposed here. The main clinoform-types are sub-divided into sub-types based on the growth dynamic (accretionary versus draping). Each sub-type is further divided into smaller classes based on the dominant grain-size (reservoir-forming versus non-reservoir forming). Existing examples of each of the 12 final classes are also proposed here. The examples shown for each of 12 classes have been modified after: Shor-1: Quaternary Gulf of Lions shorelines (Bassetti et al., 2008); Shor-2: Recent Huanghe Delta (Zhou et al., 2014); Shor-3: Holocene Po Delta (Correggiari et al., 2005); Sub-1: Recent Southern Iberia (Hernández-Molina et al., 2000a); Sub-2: Recent Adriatic shelf (Cattaneo et al., 2007); Sub-3: Intervals in Holocene mud wedges (Huanghe subaqueous delta: Liu et al., 2004); Shelf-1: Quaternary Gulf of Mexico shelf-edge delta (Anderson et al., 2016); Shelf-2: Type C clinothems from the Pleistocene mid-Adriatic shelf-edge Po Delta (Pellegrini et al., 2017); Shelf-3: abandoned shelf-edge deltas from the Quaternary United States Gulf of Mexico (Sydow and Roberts, 1994); Cont-1: Neogene Brazilian continental margin (Viana et al., 1998); Cont-2: Cenozoic-Recent South African margin (Austin and Uchupi, 1982); Cont-3: Cenozoic Baffin Bay continental margin (Rice and Shade, 1982). In each of these images, the clinothems highlighted with grey shading correspond to each given clinothem class. (Legler et al., 2013)

continental-margin deltas only takes place if they are associated to high sediment supply, low shelf accomodation and/or gullied shelf-edges. In contrast, regardless of other conditions, whenever incised valleys and submarine canyons are developed, river-dominated shelf-edge deltas are the most efficient agents of coarse-grained sediment delivery to the slope and basin-floor, with significant basin-floor fan development (Short and Stauble, 1967; Suter and Berryhill Jr, 1985; Mayall et al., 1992; Sydow and Roberts, 1994; Steel et al., 2000, 2003, 2008; Plink-Björklund et al., 2001; Mellere et al., 2002; Porębski et al., 2003; Deibert et al., 2003; Porębski and Steel, 2003, 2006; Roberts and Sydow, 2003; Sydow et al., 2003; Crabaugh and Steel, 2004; Anderson, 2005; Anderson et al., 2016; Johannessen and Steel, 2005; Plink-Björklund and Steel, 2006; Burgess et al., 2008; Carvajal et al., 2009; Jones et al., 2013; Pellegrini et al., 2018). This includes large-scale sediment transfer to the basin-floor of continental-margin clinoforms (e.g., oceanic abyssal plains), as in the Niger Delta and the Cretaceous Tres Pasos-Dorotea formations, Chile (Uchupi, 1968; Damuth, 1994; Hiscott, 2001; Covault et al., 2009; Hubbard et al., 2010). More generally, in continental-margin clinoforms, only negligible river-derived sediment transport towards the abyssal plain takes place, particularly during highstands (e.g., < 5% in the Recent Gulf of Papua), but the presence of submarine canyons extending in proximity of river mouths changes dramatically this sediment balance (e.g., about 90% of Recent sediment off the Sepik River) (Walsh and Nittrouer, 2003; Sweet and Blum, 2016).

In overpressured continental margin delta and larger shelf-edge delta clinoforms, the high relief, steep slopes and long run-out distances affect loading intensity and therefore slope stability, particularly during the fastest phases of delta progradation ("unstable shelf-margin deltas" *sensu* Porębski and Steel, 2003; e.g., Short and Stauble, 1967; Damuth, 1994), aided by reduction of shear strength due to overpressuring (Wolinsky and Pratson, 2007). These slope instability features include possible attractive targets for hydrocarbon exploration, such as listric growth faults and rollover anticlines, mud or salt diapirs, large-scale slope collapse, major slumps and mass-transport complexes and gravity-sliding tectonics (Porębski and Steel, 2003; Sydow et al., 2003).

There are practical identification criteria for shelf-edge and continental-margin deltas. These are clinothems thicker than 100 m, laterally-extensive in plan-view and hosting widespread delta-slope and toe-of-slope deformation, including slumps and sand-laden hyperpycnal tubidites with abundant land-derived organic matter (Suter and Berryhill Jr, 1985; Mayall et al., 1992; Sydow and Roberts, 1994; Tesson et al., 1990; Mellere et al., 2002; Porębski et al., 2003; Porębski and Steel, 2003, 2006; Sydow et al., 2003; Covault et al., 2009; Hubbard et al., 2010). The upper part of these clinothems is often eroded due to late-regressive and/or forced regressive extensive fluvial scours (Sydow and Roberts, 1994). The largest part of a shelf-edge delta beneath this sequence boundary therefore lies within a "highstand system tract" (*sensu* Van Wagoner et al., 1990 and Neal and Abreu, 2009).

3. Towards a hierarchical classification of deltaic and subaqueous siliciclastic clinoforms

The correct palaeoenvironmental interpretation of ancient clinoform sets tied to modern examples is crucial to envisage a realistic architectural and depositional model, including estimates of rates of progradation and depositional flux (e.g., Patruno et al., 2015c).

The theoretical quantitative framework of diagnostic architectural, sedimentological and stratigraphic features provided by both this work and Patruno et al. (2015a) can assist in the identification of ancient clinoform types and their dominant grain-size. These features can be directly measured or inferred from subsurface data (seismic, cores, logs, biostratigraphic and chronostratigraphic data). In particular, a statistically significant mathematical correlation has been pointed out between morphometric (e.g., foreset heights, gradients etc.),

palaeoenvironmental (e.g., palaeobathymetry at the rollover) and chronostratigraphically-constrained parameters (e.g., progradation rate, aggradation rate, sediment flux) (cf. Figs. 7–9). From these data it is possible to calculate clinoform palaeobathymetries once clinoform heights, age spans or progradation rates have been measured, and vice versa. Chronostratigraphically-constrained relationships are indirect consequences of the accumulation of hiatuses of different scales over increasingly longer time spans (Sadler, 1981; Patruno et al., 2015a, 2015b, 2015c, 2015d), which makes depositional rates measured for ancient and recent units not directly relatable to each other. As a consequence, most statistical correlations shown in Figs. 7–8 for delta-scale clinoforms have been subdivided into longer-term (> 10 kyr duration) and shorter term (sub-Milankovitch) (< 10 kyr duration) sub-groups. For larger-scale, longer timescale clinoforms, the "Sadler effect" is less important (Fig. 8A).

3.1. Four division

The classification scheme that we propose here is primarily based on the four main clinoform types that have been discussed above: (1) shoreline clinoforms; (2) delta-scale subaqueous clinoforms; (3) shelf-edge clinoforms; (4) continental margin clinoforms (Fig. 21). The differentiation of these four main types is based on vertical relief, sedimentary facies and facies associations within each segment of these different clinothem types, degree of proximity along an idealized shoreline-to-abyssal plain transect, oceanographic setting and geodynamic context.

Autogenic and high-frequency allogenic drivers exert increasingly less influence on the geometry and architecture of clinoform sets developed at increasingly larger spatial and temporal scales. As such, continental margin and shelf- edge clinoforms are characterized by simpler clinoform trajectories than delta-scale clinoforms, and form units that normally can only translate seawards (Helland-Hansen and Hampson, 2009). This is an expression of the increasing discrepancy between clinoform relief and amplitude of relative sea level changes as clinoforms grow larger. Sea-level change amplitudes will normally be in the same order of magnitude as the relief of delta-scale clinoforms (i.e., tens of metres): hence, landward-stepping of clinoform successions will nearly-exclusively take place for this clinoform class (i.e., shorelines and delta-scale subaqueous clinoforms).

Some aspects of clinoform outbuilding, nevertheless, are scale-invariant. For example, all clinoforms record maximum vertical sediment accumulation rate in their upper foreset (e.g., Pratson et al., 1994; Michels et al., 1998; Cattaneo et al., 2007). In all clinoform types, laterally-extensive, linear to gently curvilinear plan-view morphologies are indicative of times and areas dominated by basinal processes over fluvial input (Palinkas and Nittrouer, 2006; Palinkas, 2009; Johannessen and Steel, 2005; Olariu and Steel, 2009).

3.2. 8-division

Each of the four main clinoform types can be sub-divided into two sub-types based on growth dynamic. This can be summarized as a binary subdivision between actively accretionary (or "active") and passively draping (or "passive") clinoforms (Fig. 21). The former sub-types are characterized by a continuous sediment supply which drives a basinward facies belt migration through time, resulting in clinothem cross-sectional morphologies characterized by thin topsets and bottomsets and significantly thicker foreset sections. The latter clinoform sub-types are instead characterized by relative sediment starvation and condensation, which results into the deposition of passive drapes over an underlying inherited clinoformal morphology, with less pronounced contrast in thicknesses between topsets, foresets and bottomsets. Nucleation of draping clinoforms occurs due to many possible reasons. Examples include: in all deltaic and subaqueous settings, sedimentary starvation and condensation due to relative base-level rises or changes

in the oceanographic transport belts or wave climate; in subaerial deltas, sedimentary starvation and condensation due to lobe avulsion.

Actively accreting and passively draping clinothems often occur in alternation through the same clinoform set. In shelf-edge and continental margin clinoforms, this alternation reflects the repeated separation and merging between shelf-margin and deltaic sediment inputs. In subaerial deltas, processes of lateral lobe switching mean that parallel cross-sections through the same clinoform set will show different combinations of accretional/draping clinothem alternations (Correggiari et al., 2005).

3.3. 12-division

Draping clinothems are nearly always composed of condensed fine-grained sediments. Actively accreting clinothems, on the contrary, either comprise predominantly coarse-grained (i.e., reservoir-forming) or predominantly fine-grained (i.e., non-reservoir) lithotypes. This is a practical sub-division, driven by the necessity to devise a classification scheme through which clinoform geometries are associated to reservoir presence and quality (Fig. 21).

The key geometrical diagnostic features of coarse-grained and fine-grained clinothems are likely scale invariant and include: (1) higher-angle slope gradients associated to steeper angles of repose for coarse-grained systems; (2) predominance of sigmoidal profiles for finer lithologies and oblique to top-truncated morphologies in coarse-grained systems; (3) descending clinoform trajectories are preferentially associated to coarser-grained systems (e.g. Tesson et al., 2000; Breda et al., 2007; Tamura et al., 2008; Pellegrini et al., 2017, 2018).

As a consequence of this final sub-division, 12 classes of clinoforms are here proposed, as outlined below and in Fig. 21.

1. Delta-1 = Delta scale, shoreline/subaerial delta, accretionary, coarse-grained clinoforms
2. Delta-2 = Delta scale, shoreline/subaerial delta, accretionary, fine-grained clinoforms
3. Delta-3 = Delta scale, shoreline/subaerial delta, draping/passive, fine-grained clinoforms
4. Sub-1 = Delta scale, subaqueous, accretionary, coarse-grained clinoforms
5. Sub-2 = Delta scale, subaqueous, accretionary, fine-grained clinoforms
6. Sub-3 = Delta scale, subaqueous, draping/passive, fine-grained clinoforms
7. Shelf-1 = Shelf-edge, accretionary, coarse-grained clinoforms
8. Shelf-2 = Shelf-edge, accretionary, fine-grained clinoforms
9. Shelf-3 = Shelf-edge, draping/passive, fine-grained clinoforms
10. Cont-1 = Continental margin, accretionary, coarse-grained clinoforms
11. Cont-2 = Continental margin, accretionary, fine-grained clinoforms
12. Cont-3 = Continental margin, draping/passive, fine-grained clinoforms

4. Conclusions

Clinoforms are "frozen" bathymetric profiles that give information about depositional processes, environments, bathymetry and gradients, as well as aiding the correlation of sedimentary units laid down in standing water bodies. Clinoform sets record the interplay between sediment supply and relative sea-level changes and enable us to understand the partition of land-derived sediment along non-marine to abyssal plain transects. The systematic description of relief, slope angle, and clinoform set trajectory and the clinoform classification itself all give premises to better assess these parameters.

Where rivers debouch into standing waters, (delta-scale) shoreline clinoforms are formed as a response to the current-deceleration and the

increased accommodation. For delta-scale subaqueous clinoforms it is the deceleration associated with the transitioning from a high energy into deeper and less agitated waters (e.g., fairweather wave base) that causes clinoform nucleation and growth. Both delta-scale subaqueous and shoreline clinoforms have reliefs of few tens of metres, but the clinoform rollover bathymetries are c. 20–60 m for the formed and very shallow (0–5 m) for the latter. Shelf-edge scale clinoforms are usually formed by the stratigraphic climb associated with repeated cross-shelf transits of delta-scale clinoform through extended time-periods, forming clinoforms hundreds of meters high. Finally, the kilometer-scale high continental margin clinoforms are the result of sedimentary accretion of the continental margin slope.

Increasingly larger-scale clinoforms types, from delta-scale to shelf-edge and continental margin scale, reflect increasing distance from the source-area, increasing time spans of formation, decreasing progradation rates, increasingly ascending clinoform trajectories and reduced ability to step landwards. The latter factor is an effect of the increasing mismatch between relative sea-level rise amplitudes and clinoform reliefs, as sea-level amplitudes are typically of the same order of magnitude as delta-scale clinoform heights.

Different clinoform types can be clearly separated along the same non-marine to abyssal plain (palaeo-)bathymetric profiles ("compound clinoforms"), or they may for periods of time have coincided and moved together as "hybrid clinoforms" (e.g., hybrid shorelines, shelf-edge deltas, continental-margin deltas).

Clinoforms record the lateral accretion of depositional slopes either through active deposition from nearby sources ("accretionary/active clinoforms"), or by passive hemipelagic draping from distant sources ("draping/passive clinoforms"). All clinoform types discussed above may show an accretionary or draping style, depending on sediment source proximity.

In this article, a hierarchical classification of siliciclastic clinoforms has been proposed that can be applicable to both Recent and Ancient clinoforms. This consists of the four main types: delta-scale shoreline clinoforms, delta-scale subaqueous clinoforms, shelf-edge clinoforms and continental margin clinoforms. Each of these type is subdivided into accretionary and draping components; for the accretionary clinoforms a further breakdown into fine-grained and coarse-grained types is proposed, resulting in a final sub-division of clinoforms into 12 classes.

Naturally, finer-scale details are not fully captured by this classification (e.g., mixed lithology); on the other side, simplicity and pragmatism are key virtues for all effective classification schemes. The proposed classification, furthermore, has the merit to bring together all the dynamic stratigraphy elements reviewed here, to honour both modern and ancient clinoform data and to be relatively flexible (e.g., delta-scale clinoforms can turn into shelf-edge clinoforms along the same clinoform set).

Acknowledgements

References

Adams, E.W., Schlager, W., 2000. Basic types of submarine slope curvature. J. Sediment. Res. 70, 814–828.

Adams, E.W., Schlager, W., Anselmetti, F.S., 2001. Morphology and curvature of delta slopes in Swiss lakes: lessons for the interpretation of clinoforms in seismic data. Sedimentology 48 (3), 661–679.

Adams, E.W., Grélaud, C., Pal, M., Csoma, A.É., Al Ja'aidi, O.S., Al Hinai, R., 2011. Improving reservoir models of Cretaceous carbonates with digital outcrop modelling (Jabal Madmar, Oman): static modelling and simulating clinoforms. Pet. Geosci. 17 (3), 309–332.

Ainsworth, B.R., Sanlung, M., Duivenvoorden, S.T.C., 1999. Correlation techniques, perforation strategies, and recovery factors: an integrated 3-D reservoir modeling study. Sirikit Field Thailand 83, 1535–1551.

Ainsworth, R.B., Vakarelov, B.K., MacEachern, J.A., Rarity, F., Lane, T.I., Nanson, R.A., 2017. Anatomy of a shoreline regression: Implications for the high-resolution stratigraphic architecture of deltas. J. Sediment. Res. 87 (5), 425–459.

Alexander, C.R., DeMaster, D.J., Nittrouer, C.A., 1991. Sediment accumulation in a modern epicontinental-shelf setting: the Yellow Sea. Mar. Geol. 998, 51–72.

Allison, M.A., 1997. Historical changes in the Ganges-Brahmaputra delta front. J. Coast. Res. 1269–1275.

Amorosi, A., Milli, S., 2001. Late Quaternary depositional architecture of Po and Tevere river deltas (Italy) and worldwide comparison with deltaic successions. Sediment. Geol. 144, 357–375.

Anderson, J.B., 2005. Diachronous Development of Late Quaternary Shelf-Margin Deltas in the Northwestern Gulf of Mexico: Implications for Sequence Stratigraphy and Deep-Water Reservoir Occurrence.

Anderson, P.B., Chidsey Jr., T.C., McClure, K., Mattson, A., Snelgrove, S.H., 2002. Ferron Sandstone Stratigraphic Cross-Sections, Ivie Creek Area, Emery County. Utah Geological Survey, Utah Open File Report 390 (CD).

Anderson, J.B., Wallace, D.J., Simms, A.R., Rodriguez, A.B., Weight, R.W., Taha, Z.P., 2016. Recycling sediments between source and sink during a eustatic cycle: Systems of late Quaternary northwestern Gulf of Mexico Basin. Earth Sci. Rev. 153, 111–138.

Anell, I., Midtkandal, I., 2017. The quantifiable clinothem – types, shapes and geometric relationships in the Plio-Pleistocene Giant Foresets Formation, Taranaki Basin, New Zealand. Basin Res. 29 (S1), 277–297.

Asquith, D.O., 1970. Depositional topography and major marine environments, Late Cretaceous, Wyoming. AAPG Bull. 54, 1184–1224.

Augustinus, P.G.E.F., 1978. The changing Shoreline of Suriname (South America). Doctoral dissertation. University Utrecht.

Austin, J.A., Uchupi, E., 1982. Continental-oceanic crustal transition off Southwest Africa. Am. Assoc. Pet. Geol. Bull. 66, 1328–1347.

Barrell, J., 1912. Criteria for the recognition of ancient delta deposits. Geol. Soc. Am. Bull. 23, 377–446.

Bassetti, M.A., Berne, S., Jouet, G., Taviani, M., Dennielou, B., Flores, J.A., Gaillot, A., Gelfort, R., Lafuerza, S., Sultan, N., 2008. The 100-ka and rapid sea level changes recorded by prograding shelf sand bodies in the Gulf of Lions (western Mediterranean Sea). Geochem. Geophys. Geosyst. 9 (11).

Bates, C.C., 1953. Rational theory of delta formation. Am. Assoc. Pet. Geol. Bull. 37, 2119–2162.

Beelen, D., Jackson, C.A.L., Patruno, S., Hodgson, D.M., Trabucho Alexandre, J.P., Rising not falling? Differential compaction of shelf-edge trajectories and clinothem geometries. Geology.

Bellotti, P., Chiocci, F.L., Milli, S., Tortora, P., Valeri, P., 1994. Sequence stratigraphy and depositional setting of the Tiber delta: integration of high-resolution seismics, well logs, and archeological data. J. Sediment. Res 64 (3).

Betzler, C.G., Eberli, G.P., Alvarez Zarikian, C.A., 2015. Expedition 359 Preliminary Report: Maldives Monsoon and Sea Level. International Ocean Discovery Program, pp. 53. http://dx.doi.org/10.14379/iodp.pr.359.2016.

Bhattacharya, J.P., 2006. Deltas. In: Walker, R.G., Posamentier, H. (Eds.), Facies Models Revisited. vol. 84. SEPM (Society for Sedimentary Geology) Special Publications, Tulsa, Oklahoma, pp. 237–292.

Bhattacharya, J.P., Giosan, L., 2003. Wave-influenced deltas: geomorphological implications for facies reconstruction. Sedimentology 50, 187–210.

Bhattacharya, J.P., MacEachern, J.A., 2009. Hyperpycnal rivers and prodeltaic shelves in the Cretaceous seaway of North America. J. Sediment. Res. 79 (4), 184–209.

Blum, M.D., Roberts, H.H., 2009. Drowning of the Mississippi Delta due to insufficient sediment supply and global sea-level rise. Nat. Geosci. 2 (7), 488.

Boak, E.H., Turner, I.L., 2005. Shoreline definition and detection: a review. J. Coast. Res. 688–703.

Bosence, D.W.J., 2002. Part 4 carbonates: 13 application of sequence stratigraphical analysis to ancient carbonate platforms. In: Coe, A.L. (Ed.), The Sedimentary Record of Sea-Level Change. The Open University, Cambridge University Press, New York, U.S.A, pp. 234–256.

Bosence, D.W.J., Wilson, R.C.L., 2002a. Part 4 carbonates: 11 carbonate depositional systems. In: Coe, A.L. (Ed.), The Sedimentary Record of Sea-Level Change. The Open University, Cambridge University Press, New York, U.S.A, pp. 209–233.

Bosence, D.W.J., Wilson, R.C.L., 2002b. Part 4 carbonates: 12 sequence stratigraphy of carbonate depositional systems. In: Coe, A.L. (Ed.), The Sedimentary Record of Sea-Level Change. The Open University, Cambridge University Press, New York, U.S.A, pp. 234–256.

Breda, A., Mellere, D., Massari, F., 2007. Facies and processes in a Gilbert-delta-filled incised valley (Pliocene of Ventimiglia, NW Italy). Sediment. Geol 200 (1-2), 31–55.

Bullimore, S., Henriksen, S., Liestøl, F.M., Helland-Hansen, W., 2005. Clinoform stacking patterns, shelf-edge trajectories and facies associations in Tertiary coastal deltas, offshore Norway: Implications for the prediction of lithology in prograding systems. Norwegian J. Geol. 85.

Bullimore, S.A., Helland-Hansen, W., Henriksen, S., Steel, R.J., 2008. Shoreline trajectory and its impact on coastal depositional environments: an example from the Upper Cretaceous Mesaverde Group, NW Colorado. In: Hampson, G.J., Steel, R.J., Burgess, P.M., Dalrymple, R.W. (Eds.), Recent Advances in Models of Siliciclastic Shallow-Marine Stratigraphy. vol. 90. SEPM Special Publication, pp. 209–236.

Burgess, P.M., Hovius, N., 1998. Rates of delta progradation during highstands; consequences for timing of deposition in deep-marine systems. J. Geol. Soc. 155, 217–222.

Burgess, P.M., Steel, R.J., Granjeon, D.I., 2008. Stratigraphic forward modeling of basin-margin clinoform systems: Implications for controls on topset and shelf width and timing of formation of shelf-edge deltas. In: Recent Advances in Models of Siliciclastic Shallow-Marine Stratigraphy. vol. 90. pp. 35–45.

Calamita, F., Patruno, S., Pomposo, G., Tavarnelli, E., 2007. Geometry and kinematics of the thrust-related anticlines from the central outer Apennines: the role of the Jurassic normal faults ('Geometria e cinematica delle anticlinali dell'Appenino centrale esterno: il ruolo delle faglie dirette giurassiche'). Rend. Soc. Geol. Ital. 4, 167–192.

Carvajal, C., Steel, R.S., 2006. Thick turbidite successions from supply-dominated shelves during sea-level highstand. Geology 34, 665–668.

Carvajal, C., Steel, R.S., 2009. Shelf-edge architecture and bypass of sand to deep water: influence of shelf-edge processes, sea level and sediment supply. J. Sediment. Res. 79, 652–672.

Carvajal, C., Steel, R., Petter, A., 2009. Sediment supply: the main driver of shelf-margin growth. Earth Sci. Rev. 96 (4), 221–248.

Casalbore, D., Falese, F., Martorelli, E., Romagnoli, C., Chiocci, F.L., 2017. Submarine depositional terraces in the Tyrrhenian Sea as a proxy for paleo-sea level reconstruction: problems and perspective. Quat. Int. 439, 169–180.

Cathro, D.L., Austin Jr., J.A., Moss, G.D., 2003. Progradation along a deeply submerged OligoceneMiocene heterozoan carbonate shelf: How sensitive are clinoforms to sea level variations? AAPG Bull. 87 (10), 1547–1574.

Cattaneo, A., Correggiari, A., Langone, L., Trincardi, F., 2003. The late-Holocene Gargano subaqueous delta, Adriatic shelf: Sediment pathways and supply fluctuations. Mar. Geol. 193, 61–91.

Cattaneo, A., Trincardi, F., Asioli, A., Correggiari, A., 2007. The Western Adriatic shelf clinoform: energy-limited bottomset. Cont. Shelf Res. 27 (3), 506–525.

Charvin, K., Hampson, G.J., Gallagher, K.L., Labourdette, R., 2010. Intra-parasequence architecture of an interpreted asymmetrical wave-dominated delta. Sedimentology 57, 760–785. http://dx.doi.org/10.1111/j.1365-3091.2009.01118.x.

Charvin, K., Hampson, G.J., Gallagher, K.L., Storms, J.E.A., Labourdette, R., 2011. Characterization of controls on highresolution stratigraphic architecture in wave-dominated shoreface-shelf parasequences using inverse numerical modeling. J. Sediment. Res. 81, 562–578. http://dx.doi.org/10.2110/jsr.2011.48.

Chen, Z., Song, B., Wang, Z., Cai, Y., 2000. Late quaternary evolution of the sub-aqueous Yangtze Delta, China: sedimentation, stratigraphy, palynology, and deformation. Mar. Geol. 162 (2), 423–441.

Chin, J.L., Clifton, H.E., Mullins, H.T., 1988. Seismic stratigraphy and late Quaternary shelf history, south-central Monterey Bay, California. Mar. Geol. 181, 137–157.

Chu, Z.X., Sun, X.G., Zhai, S.K., Xu, K.H., 2006. Changing pattern of accretion/erosion of the modern Yellow River (Huanghe) subaerial delta, China: Based on remote sensing images. Mar. Geol. 227 (1), 13–30.

Clifton, H.E., 1981. Progradational sequences in Miocene shoreline deposits, southeastern Caliente Range. California: J. Sedimen. Res. 51, 1.

Correggiari, A., Cattaneo, A., Trincardi, F., 2005. The modern Po Delta system: lobe switching and asymmetric prodelta growth. Mar. Geol. 222-223, 49–74.

Coutellier, V., Stanley, D.J., 1987. Late quaternary stratigraphy and paleogeography of the eastern Nile Delta, Egypt. Mar. Geol. 77 (3-4), 257–275.

Covault, J.A., Normark, W.R., Romans, B.W., Graham, S.A., 2007. Highstand fans in the California borderland: The overlooked deep-water depositional systems. Geology 35, 783–786.

Covault, J.A., Romans, B.W., Graham, S.A., 2009. Outcrop expression of a continental-margin-scale shelf-edge delta from the Cretaceous Magallanes Basin, Chile. J. Sediment. Res. 79 (7), 523–539.

Crabaugh, J.P., Steel, R.J., 2004. Basin-floor fans of the Central Tertiary Basin, Spitsbergen: relationship of basin-floor sand-bodies to prograding clinoforms in a structurally active basin. Geol. Soc. Lond., Spec. Publ. 222 (1), 187–208.

Cummings, D.I., Arnott, R.W.C., 2005. Growth-faulted shelf-margin deltas: a new (but old) play type, offshore Nova Scotia. Bull. Can. Petrol. Geol. 53 (3), 211–236.

Damuth, J.E., 1994. Neogene gravity tectonics and depositional processes on the deep Niger Delta continental margin. Mar. Pet. Geol. 11 (3), 320–346.

Dan, S., Stive, M.J., Walstra, D.J.R., Panin, N., 2009. Wave climate, coastal sediment budget and shoreline changes for the Danube Delta. Mar. Geol. 262 (1), 39–49.

Deibert, J.E., Benda, T., Løseth, T., Schellpeper, M., Steel, R.J., 2003. Eocene clinoform growth in front of a storm-wave-dominated shelf, Central Basin, Spitsbergen: no significant sand delivery to deepwater areas. J. Sediment. Res. 73 (4), 546–558.

DeMaster, D.J., McKee, B.A., Nittrouer, C.A., Jiangchu, Q., Guodong, C., 1985. Rates of sediment accumulation and particle reworking based on radiochemical measurements from continental shelf deposits in the East China Sea. Cont. Shelf Res. 4 (1), 143–158.

Dillon, W.P., Klitgord, K.D., Paull, C.K., 1983. Mesozoic development and structure of the continental margin off South Carolina. US Department of the Interior, Geological Survey, pp. N1–N16.

Dixon, J.F., Steel, R.J., Olariu, C., 2012a. Shelf-edge delta regime as a predictor of deep-water deposition. J. Sediment. Res. 82 (9), 681–687.

Dixon, J.F., Steel, R.J., Olariu, C., 2012b. River-dominated, shelf-edge deltas: delivery of sand across the shelf break in the absence of slope incision. Sedimentology 59 (4), 1133–1157.

Dolan, R., Fenster, M.S., Holme, S.J., 1991. Temporal analysis of shoreline recession and accretion. J. Coast. Res. 723–744.

Driscoll, N.W., Karner, G.D., 1999. Three-dimensional quantitative modeling of clinoform development. Mar. Geol. 154 (1), 383–398.

Duke, W.L., 1990. Geostrophic circulation or shallow marine turbidity currents? The dilemma of paleoflow patterns in storm-influenced prograding shoreline systems. J. Sediment. Res. 60 (6).

Dunbar, G.B., Barrett, P.J., 2005. Estimating palaeobathymetry of wave-graded continental shelves from sediment texture. Sedimentology 52, 253–269.

Eberli, G.P., Anselmetti, F.S., Betzler, C., Van Konijnenburg, J.-H., Bernoulli, D., 2004. Carbonate platform to basin transitions on seismic data and in outcrops: Great Bahama Bank and the Maiella Platform margin, Italy. In: Seismic Imaging of Carbonate Reservoirs and Systems: AAPG Memoir. vol. 81. pp. 207–250.

Emery, K.O., Uchupi, E., Phillips, J.D., Bowin, C.O., Bunce, E.T., Knott, S.T., 1970.

Continental Rise Off Eastern North-America. Am. Assoc. Pet. Geol. Bull. 54 (1), 44–108.

Enge, H.D., Howell, J.A., 2010. Impact of deltaic clinothems on reservoir performance: Dynamic studies of reservoir analogs from the Ferron Sandstone Member and Panther Tongue, Utah. AAPG Bull. 94 (2), 139–161.

Enge, H.D., Howell, J.A., Buckley, S.J., 2010. Quantifying Clinothem Geometry in a Forced-Regressive River-Dominated Delta. vol. 57. Sedimentology, Panther Tongue, Utah, USA, pp. 1750–1770. http://dx.doi.org/10.1111/sed.2010.57.issue-7.

Everts, A.J., Reijmer, J.J., 1995. Clinoform composition and margin geometries of a Lower Cretaceous carbonate platform (Vercors, SE France). Palaeogeogr. Palaeoclimatol. Palaeoecol. 119 (1-2), 19–33.

Fernández-Salas, L.M., Dabrio, C.J., Goy, J.L., Díaz Del Río, V., Zazo, C., Lobo, F.J., Sanz, J.L., Lario, J., 2009. Land-sea correlation between Late Holocene coastal and infra-littoral deposits in the SE Iberian Peninsula (Western Mediterranean). Geomorphology 104, 4–11.

Field, M.E., Roy, P.S., 1984. Offshore transport and sand-body formation: evidence from a steep, high-energy shoreface, southeastern Australia. J. Sediment. Petrol. 54, 1292–1302.

Fisk, H.N., McFarlan, E., Kolb, C.R., Wilbert, L.J., 1954. Sedimentary framework of the modern Mississippi delta. J. Sediment. Res. 24 (2).

Forbes, D.L., Parkes, G.S., Manson, G.K., Ketch, L.A., 2004. Storms and shoreline retreat in the southern Gulf of St. Lawrence. Mar. Geol. 210 (1), 169–204.

Foyle, A.M., Oertel, G.F., 1997. Transgressive systems tract development and incised-valley fills within a Quaternary estuary-shelf system: Virginia inner shelf, USA. Mar. Geol. 137 (3-4), 227–249.

Friedrichs, C.T., Scully, M.E., 2007. Modeling deposition by wave-supported gravity flows on the Po River prodelta: from seasonal floods to prograding clinoforms. Cont. Shelf Res. 27 (3), 322–337.

Friedrichs, C.T., Wright, L.D., 2004. Gravity-driven sediment transport on the continental shelf: implications for equilibrium profiles near river mouths. Coast. Eng. 51 (8), 795–811.

Frihy, O.E., 1988. Nile Delta shoreline changes: aerial photographic study of a 28-year period. J. Coast. Res. 597–606.

Gani, M.R., Bhattacharya, J.P., 2005. Lithostratigraphy versus chronostratigraphy in facies correlations of Quaternary deltas: Application for bedding correlation. In: Giosan, L., Bhattacharya, J.P. (Eds.), River Deltas: Concepts, Models and Examples. vol. 83. SEPM Special Publication, pp. 31–48.

Garrison, J.R., Williams, J., Miller, S.P., Weber, E.T., McMechan, G., Zeng, X., 2010. Ground-penetrating radar study of North Padre Island: implications for barrier island internal architecture, model for growth of progradational microtidal barrier islands, and Gulf of Mexico sea-level cyclicity. J. Sediment. Res. 80 (4), 303–319.

Gerard, J., Oesterle, H., 1973. Facies study of the offshore Mahakam area. In: Proceedings Indonesian Petroleum Association, 2nd Annual Convention Proceedings, pp. 187–194.

Gerber, T.P., Pratson, L.F., Wolinsky, M.A., Steel, R., Mohr, J., Swenson, J.B., Paola, C., 2008. Clinoform progradation by turbidity currents: modeling and experiments. J. Sediment. Res. 78 (3), 220–238.

Gilbert, G.K., 1885. The Topographic Feature of Lake Shores. vol. 5. U.S. Geological Survey, pp. 104–108 Annual Report.

Giosan, L., Constantinescu, S., Clift, P.D., Tabrez, A.R., Danish, M., Inam, A., 2006a. Recent morphodynamics of the Indus delta shore and shelf. Cont. Shelf Res. 26 (14), 1668–1684.

Giosan, L., Donnelly, J.P., Constantinescu, S., Filip, F., Ovejanu, I., Vespremeanu-Stroe, A., Vespremeanu, E., Duller, G.A., 2006b. Young Danube delta documents stable Black Sea level since the middle Holocene: morphodynamic, paleogeographic, and archaeological implications. Geology 34 (9), 757–760.

Glørstad-Clark, E., Birkeland, E.P., Nystuen, J.P., Faleide, J.I., Midtkandal, I., 2011. Triassic platform-margin deltas in the western Barents Sea. Mar. Pet. Geol. 28 (7), 1294–1314.

Gong, C., Wang, Y., Steel, R.J., Olariu, C., Xu, Q., Liu, X., Zhao, Q., 2015. Growth styles of shelf-margin clinoforms: prediction of sand-and-sediment-budget partitioning into and across the shelf. J. Sediment. Res. 85 (3), 209–229.

Goodbred, S.L., Kuehl, S.A., 1999. Holocene and modern sediment budgets for the Ganges-Brahmaputra river system: Evidence for highstand dispersal to flood-plain, shelf, and deep-sea depocenters. Geology 27 (6), 559–562.

Goodbred, S.L., Kuehl, S.A., 2000a. The significance of large sediment supply, active tectonism, and eustasy on margin sequence development: Late Quaternary stratigraphy and evolution of the Ganges–Brahmaputra delta. Sediment. Geol. 133 (3), 227–248.

Goodbred, S.L., Kuehl, S.A., 2000b. Enormous Ganges-Brahmaputra sediment discharge during strengthened early Holocene monsoon. Geology 28 (12), 1083–1086.

Goodbred, S.L., Kuehl, S.A., Steckler, M.S., Sarker, M.H., 2003. Controls on facies distribution and stratigraphic preservation in the Ganges–Brahmaputra delta sequence. Sediment. Geol. 155 (3), 301–316.

Goodfriend, G.A., Stanley, D.J., 1999. Rapid strand-plain accretion in the northeastern Nile Delta in the 9th century AD and the demise of the port of Pelusium. Geology 27 (2), 147–150.

Graham, G.H., Jackson, M.D., Hampson, G.J., 2015a. Three-dimensional modeling of clinoforms in shallow-marine reservoirs: Part 1 Concepts and application. AAPG Bull. 99 (6), 1013–1047.

Graham, G.H., Jackson, M.D., Hampson, G.J., 2015b. Three-dimensional modeling of clinoforms in shallow-marine reservoirs: Part 2. Impact on fluid flow and hydrocarbon recovery in fluvial-dominated deltaic reservoirs. AAPG Bull. 99 (6), 1049–1080.

Gross, M.G., Gross, E., 1994. Oceanography, A View of Earth, 7th edn. Prentice-Hall, Englewood Cliffs, NJ, pp. 472.

Grotzinger, J.P., Gupta, S., Malin, M.C., Rubin, D.M., Schieber, J., Siebach, K., Sumner, D.Y., Stack, K.M., Vasavada, A.R., Arvidson, R.E., Calef, F., 2015. Deposition, exhumation, and paleoclimate of an ancient lake deposit, Gale crater, Mars. Science 350 (6257), aac7575.

Grundvåg, S.-A., Helland-Hansen, W., Johannessen, E.P., Olsen, A.H., Stene, S.A.K., 2014. The depositional architecture and facies variability of shelf deltas in the Eocene Battfjellet Formation, Nathorst Land, Spitsbergen. Sedimentology 61 (7), 2172–2204.

Hampson, G.J., 2000. Discontinuity surfaces, clinoforms, and facies architecture in a wave-dominated, shoreface-shelf parasequence. J. Sediment. Res. 70 (2).

Hampson, G.J., 2010. Sediment dispersal and quantitative stratigraphic architecture across an ancient shelf. Sedimentology 57, 96–141.

Hampson, G.J., Howell, J.A., 2005. Sedimentologic and geomorphic characterization of ancient wave-dominated deltaic shorelines: upper Cretaceous Blackhawk Formation. In: Giosan, Bhattacharya (Ed.), River Deltas – Concepts, Models and Examples. SEPM, Book Cliffs, Utah, USA, pp. 133–154. ISBN: 9781565761131. https://doi.org/10.2110/pec.05.83.0131.

Hampson, G.J., Premwichein, K., 2017. Sedimentologic Character of Ancient Muddy Subaqueous-Deltaic Clinoforms: Down Cliff Clay Member, Bridport Sand Formation, Wessex Basin, UK. J. Sediment. Res. 87 (9), 951–966.

Hampson, G.J., Storms, J.E., 2003. Geomorphological and sequence stratigraphic variability in wave-dominated, shoreface-shelf parasequences. Sedimentology 50 (4), 667–701.

Hampson, G.J., Rodriguez, A.B., Storms, J.E., Johnson, H.D., Meyer, C.T., 2008. Geomorphology and high-resolution stratigraphy of progradational wave-dominated shoreline deposits: Impact on reservoir-scale facies architecture. In: Recent Advances in Models of Siliciclastic Shallow-Marine Stratigraphy. vol. 90. SEPM Special Publication, pp. 117–142.

Hampson, G.J., Morris, J.E., Johnson, H.D., 2015. Synthesis of time-stratigraphic relationships and their impact on hydrocarbon reservoir distribution and performance, Bridport Sand Formation, Wessex Basin, UK. In: Smith, D.G., Bailey, R.J., Burgess, P.M., Fraser, A.J. (Eds.), Strata and Time Probing the Gaps in our Understanding. Geological Society of London, Special Publications, London, pp. 404. http://dx.doi.org/10.1144/SP404.2.

Hansen, J.P.V., Rasmussen, E.S., 2008. Structural, sedimentologic, and sea-level controls on sand distribution in a steep-clinoform asymmetric wave-influenced delta: Miocene Billund sand, eastern Danish North Sea and Jylland. J. Sediment. Res. 78 (2), 130–146.

Helland-Hansen, W., 1992. Geometry and facies of Tertiary clinothems, Spitsbergen. Sedimentology 39 (6), 1013–1029.

Helland-Hansen, W., 2009. Clinoforms and clinothems: concepts, cases and challenges (abs.). In: Exploration Revived, Norwegian Petroleum Society Conference, Bergen.

Helland-Hansen, W., 2010. Facies and stacking patterns of shelf-deltas within the Palaeogene Battfjellet Formation, Nordenskiöld Land, Svalbard: implications for subsurface reservoir prediction. Sedimentology 57 (1), 190–208.

Helland-Hansen, W., Gjelberg, H., 2012. Towards a Hierarchical Classification of Clinoforms. American Association of Petroleum Geologists, Annual Convention and Exhibition Search and discovery article, 90142.

Helland-Hansen, W., Hampson, G.J., 2009. Trajectory analysis: concepts and applications. Basin Res. 21, 454–483.

Helland-Hansen, W., Martinsen, O.J., 1996. Shoreline trajectories and sequences: description of variable depositional-dip scenarios. J. Sediment. Res. 66 (4).

Helland-Hansen, W., Kendall, C.G., Lerche, I., Nakayama, K., 1988. A simulation of continental basin margin sedimentation in response to crustal movements, Eustatic Sea level change, and sediment accumulation rates. Math. Geol. 20 (7), 777–802.

Helland-Hansen, W., Helle, H., Sunde, J., 1994. Seismic modeling of Tertiary sandstone clinothems, Spitsbergen. Basin Res. 6 (4), 181–191.

Helland-Hansen, W., Steel, R.J., Sømme, T.O., 2012. Shelf genesis revisited. J. Sediment. Res. 82, 133–148.

Henriksen, S., Vorren, T.O., 1996. Late Cenozoic sedimentation and uplift history on the mid-Norwegian continental shelf. Glob. Planet. Chang. 12 (1-4), 171–199.

Henriksen, S., Helland-Hansen, W., Bullimore, S., 2011. Relationships between shelf-edge trajectories and sediment dispersal along depositional dip and strike: a different approach to sequence stratigraphy. Basin Res. 23 (1), 3–21.

Hernández-Molina, F.J., Fernández-Salas, L.M., Lobo, F., Somoza, L., Díaz-del-Río, V., Alveirinho Dias, J.M., 2000a. The infralittoral prograding wedge. a new large-scale progradational sedimentary body in shallow marine environments. Geo-Mar. Lett. 20, 109–117.

Hernández-Molina, F.J., Somoza, L., Lobo, F., 2000b. Seismic stratigraphy of the Gulf of Cadiz Continental Shelf: a model for Late Quaternary very high-resolution sequence stratigraphy and response to sea-level fall. In: Hunt, D., Gawthorpe, R.L. (Eds.), Sedimentary Responses to Forced Regression. vol. 172. Geological Society of London, Special Publications, London, pp. 329–362.

Heward, A.P., 1981. A review of wave-dominated clastic shoreline deposits. Earth Sci. Rev. 17 (3), 223–276.

Hiscott, R.N., 2001. Depositional sequences controlled by high rates of sediment supply, sea-level variations, and growth faulting: the Quaternary Baram Delta of northwestern Borneo. Mar. Geol. 175 (1), 67–102.

Hodgson, D.M., Browning, J.V., Miller, K.G., Hesselbo, S.P., Poyatos-More, M., Mountain, G.S., Proust, J.N., 2018. Sedimentology, stratigraphic context, and implications of Miocene intrashelf bottomset deposits, offshore New Jersey. Geosphere 14 (1), 95–114.

Holgate, N.E., Jackson, C.A.L., Hampson, G.J., Dreyer, T., 2013. Sedimentology and sequence stratigraphy of the Middle–Upper Jurassic Krossfjord and Fensfjord formations, Troll Field, northern North Sea. Pet. Geosci. 19 (3), 237–258.

Holgate, N.E., Hampson, G.J., Jackson, C.A.L., Petersen, S.A., 2014. Constraining uncertainty in interpretation of seismically imaged clinoforms in deltaic reservoirs, Troll

field, Norwegian North Sea: Insights from forward seismic models of outcrop analogs. AAPG Bull. 98 (12), 2629–2663.

Holgate, N.E., Jackson, C.A., Hampson, G.J., Dreyer, T., 2015. Seismic stratigraphic analysis of the Middle Jurassic Krossfjord and Fensfjord formations, Troll oil and gas field, northern North Sea. Mar. Pet. Geol. 68, 352–380.

Hori, K., Saito, Y., Zhao, Q., Cheng, X., Wang, P., Sato, Y., Li, C., 2001. Sedimentary facies and Holocene progradation rates of the Cahngjiang (Yangtze) delta, China. Geomorphology 41, 233–248.

Hori, K., Saito, Y., Zhao, Q., Wang, P., 2002. Architecture and evolution of the tide-dominated Changjiang (Yangtze) River delta, China. Sediment. Geol. 146 (3), 249–264.

Hori, K., Tanabe, S., Saito, Y., Haruyama, S., Nguyen, V., Kitamura, A., 2004. Delta initiation and Holocene sea-level change: example from the Song Hong (Red River) delta, Vietnam. Sediment. Geol. 164 (3), 237–249.

Houseknecht, D.W., Bird, K.J., Schenk, C.J., 2009. Seismic analysis of clinoform depositional sequences and shelf-margin trajectories in Lower Cretaceous (Albian) strata, Alaska North Slope. Basin Res. 21 (5), 644–654.

Howell, J.A., Flint, S.S., 2002a. Part 3 Siliciclastics case study: the Book Cliffs. 7 Tectonic setting, stratigraphy and sedimentology of the Book Cliffs. In: Coe, A.L. (Ed.), The Sedimentary Record of Sea-Level Change. The Open University, Cambridge University Press, New York, U.S.A, pp. 135–157.

Howell, J.A., Flint, S.S., 2002b. Part 3 Siliciclastics case study: the Book Cliffs. 8 The parasequences of the the Book Cliffs. In: Coe, A.L. (Ed.), The Sedimentary Record of Sea-Level Change. The Open University, Cambridge University Press, New York, U.S.A, pp. 158–178.

Howell, J.A., Flint, S.S., 2002c. Part 3 Siliciclastics case study: the Book Cliffs. 9 Sequences and system tracts in the Book Cliffs. In: Coe, A.L. (Ed.), The Sedimentary Record of Sea-Level Change. The Open University, Cambridge University Press, New York, U.S.A, pp. 179–197.

Howell, J., Vassel, Å., Aune, T., 2008. Modelling of dipping clinoform barriers within deltaic outcrop analogues from the Cretaceous Western Interior Basin, USA. Geol. Soc. Lond., Spec. Publ. 309 (1), 99–121.

Hubbard, S.M., et al., 1986. Styles of Reef Accretion Along a Steep, Shelf-Edge Reef. St. Croix, U.S. Virgin Islands.

Hubbard, S.M., Fildani, A., Romans, B.W., Covault, J.A., McHargue, T.R., 2010. High-relief slope clinoform development: insights from outcrop, Magallanes Basin, Chile. J. Sediment. Res. 80 (5), 357–375.

Hunt, D., Tucker, M.E., 1992. Stranded parasequences and the forced regressive wedge systems tract: deposition during base-level fall. Sediment. Geol. 81, 1–9.

Jackson, M.D., Hampson, G.J., Sech, R.P., 2009. Three-dimensional modeling of a shoreface-shelf parasequence reservoir analog: Part 2. Geological controls on fluid flow and hydrocarbon production. AAPG Bull. (93), 1183–1208.

James, N.P., Von Der Borch, C.C., 1991. Carbonate shelf edge off southern Australia: A prograding open-platform margin. Geology 19, 1005–1008.

Jaramillo, S., Sheremet, A., Allison, M.A., Reed, A.H., Holland, K.T., 2009. Wave-mud interactions over the muddy Atchafalaya subaqueous clinoform, Louisiana, United States: Wave-supported sediment transport. J. Geophys. Res. (C4), 114.

Jiménez, J., Sánchez-Arcilla, A., Valdemoro, H.I., Gracia, V., Nieto, F., 1997. Processes reshaping the Ebro delta. Mar. Geol. 144 (1-3), 59–79.

Johannessen, E.P., Steel, R.J., 2005. Shelf-margin clinoforms and prediction of deepwater sands. Basin Res. 17 (4), 521–550.

Johannessen, E.P., Henningsen, T., Bakke, N.E., Johansen, T.A., Ruud, B.E., Riste, P., Elvebakk, H., Jochmann, M., Elvebakk, G., Woldengen, M.S., 2011. Palaeogene clinoform succession on Svalbard expressed in outcrops, seismic data logs and cores. First Break 29 (2), 35–44.

Jol, H.M., Smith, D.G., Meyers, R.A., 1996. Digital ground penetrating radar (GPR): a new geophysical tool for coastal barrier research examples from the Atlantic, Gulf and Pacific Coasts, USA. J. Coastal Res. 12 (4), 960–968.

Jol, H.M., Lawton, D.C., Smith, D.G., 2002. Ground penetrating radar: 2-D and 3-D subsurface imaging of a coastal barrier spit, Long Beach, WA, USA. Geomorphology 53, 165–181.

Jones, G.E., Hodgson, D.M., Flint, S.S., 2013. Contrast in the process response of stacked clinothems to the shelf-slope rollover. Geosphere 9 (2), 299–316.

Jones, G.E., Hodgson, D.M., Flint, S.S., 2015. Lateral variability in clinoform trajectory, process regime, and sediment dispersal patterns beyond the shelf-edge rollover in exhumed basin margin-scale clinothems. Basin Res. 27 (6), 657–680.

Kenter, J.A.M., 1990. Carbonate platform flanks: slope angle and sediment fabric. Sedimentology 37, 777–794.

Kertznus, V., Kneller, B., 2009. Clinoform quantification for assessing the effects of external forcing on continental margin development. Basin Res. 21 (5), 738–758.

Klausen, T.G., Helland-Hansen, W., 2018. Methods for restoring and describing ancient clinoform surfaces. J. Sediment. Res. 88 (2), 241–259.

Klausen, T.G., Ryseth, A.E., Helland-Hansen, W., Gjelberg, H.K., 2016. Progradational and backstepping shoreface deposits in the Ladinian to Early Norian Snadd Formation of the Barents Sea. Sedimentology 63 (4), 893–916.

Klitgord, K.D., Hutchinson, D.R., Schouten, H., 1988. U.S. Atlantic continental margin; Structural and tectonic framework. In: Sheridan, R.E., Grow, J.A. (Eds.), The Geology of North America. Vol. 1. The Atlantic Continental Margin, pp. 19–56.

Klitgord, K.D., Schouten, H., 1986. Plate kinematics of the Central Atlantic. In: Vogt, P.R., Tucholke, B.E. (Eds.), The Western North Atlantic Region. Geological Society of America, The Geology of North America, Boulder, Colorado, pp. 351–378.

Kolla, V., Biondi, P., Long, B., Fillon, R., 2000. Sequence stratigraphy and architecture of the late Pleistocene Lagniappe delta complex, northeast Gulf of Mexico. Geol. Soc. Lond., Spec. Publ. 172 (1), 291–327.

Kostic, S., Parker, G., Marr, J.G., 2002. Role of turbidity currents in setting the foreset slope of clinoforms prograding into standing fresh water. J. Sediment. Res. 72 (3), 353–362.

Kubicki, A., 2008. Large and very large subaqueous dunes on the continental shelf off southern Vietnam, South China Sea. Geo-Mar. Lett. 28 (4), 229.

Kuehl, S.A., Nittrouer, C.A., DeMaster, D.J., 1986. Nature of sediment accumulation on the Amazon continental shelf. Cont. Shelf Res. 6, 209–225.

Kuehl, S.A., Levy, B.M., Moore, W.S., Allison, M.A., 1997. Subaqueous delta of the Ganges-Brahmaputra river system. Mar. Geol. 144, 81–96.

Kuehl, S.A., Allison, M.A., Goodbred, S.L., Kudrass, H., 2005. The Ganges-Brahmaputra Delta. In: Giosan, L., Bhattacharya, J.P. (Eds.), River Deltas: Concepts Models and Examples. vol. 83. SEPM Special Publications, pp. 413–434.

Lancaster, N., 2004. Geomorphology of Desert Dunes. Taylor & Francis e-Library, London, UK, pp. 244.

Lanfranchi, A., Berra, F., Jadoul, F., 2011. Compositional changes in sigmoidal carbonate clinoforms (Late Tithonian, eastern Sardinia, Italy): insights from quantitative microfacies analyses. Sedimentology 2011.

Larter, R.D., Barker, P.F., 1989. Seismic stratigraphy of the Antarctic Peninsula Pacific margin: A record of Pliocene–Pleistocene ice volume and paleoclimate. Geology 17, 731–734.

Larue, D.K., Martinez, P.A., 1989. Use of bed-form models to analyze geometry and preservation potential of clastic facies and erosional surfaces. AAPG Bull. 73 (1), 40–53.

Le Dantec, N., Hogarth, L.J., Driscoll, N.W., Babcock, J.M., Barnhardt, W.A., Schwab, W.C., 2010. Tectonic controls on nearshore sediment accumulation and submarine canyon morphology offshore La Jolla, Southern California. Mar. Geol. 268, 115–128.

Leeder, M.R., 1999. Carbonate-evaporite shorelines, shelves and basins. In: Leeder, M.R. (Ed.), Sedimentology and Sedimentary Basins: From Turbulence to Tectonics. Blackwell Science Publishing, Malaysia, pp. 414–443.

Legler, B., Johnson, H.D., Hampson, G.J., Massart, B.Y., Jackson, C.A.L., Jackson, M.D., El-Barkooky, A., Ravnas, R., 2013. Facies model of a fine-grained, tide-dominated delta: Lower Dir Abu Lifa Member (Eocene), Western Desert, Egypt. Sedimentology 60 (5), 1313–1356.

Leithold, E.L., 1993. Preservation of laminated shale in ancient clinoforms; comparison to modern subaqueous deltas. Geology 21 (4), 359–362.

Leva López, J., Kim, W., Steel, R.J., 2014. Autoacceleration of clinoform progradation in foreland basins: theory and experiments. Basin Res. 26 (4), 489–504.

Lin, A.T., Liu, C.S., Lin, C.C., Schnurle, P., Chen, G.Y., Liao, W.Z., Teng, L.S., Chuang, H.J., Wu, M.S., 2008. Tectonic features associated with the overriding of an accretionary wedge on top of a rifted continental margin: an example from Taiwan. Mar. Geol. 255 (3), 186–203.

Liu, J.P., Milliman, J.D., Gao, S., Cheng, P., 2004. Holocene development of the Yellow River's subaqueous delta, North Yellow Sea. Mar. Geol. 209, 45–67.

Liu, J.P., Li, A.C., Xu, K.H., Velozzi, D.M., Yang, Z.S., Milliman, J.D., DeMaster, D.J., 2006. Sedimentary features of the Yangtze River-derived along-shelf clinoform deposit in the East China Sea. Cont. Shelf Res. 26 (17), 2141–2156.

Liu, J.P., Xu, K.H., Li, A.C., Milliman, J.D., Velozzi, D.M., Xiao, S.B., Yang, Z.S., 2007a. Flux and fate of Yangtze River sediment delivered to the East China Sea. Geomorphology 85 (2007), 208–224.

Liu, J., Saito, Y., Wang, H., Yang, Z., Nakashima, R., 2007b. Sedimentary evolution of the Holocene subaqueous clinoform off the Shandong Peninsula in the Yellow Sea. Mar. Geol. 236 (3), 165–187.

Lobo, F.J., Fernández-Salas, L.M., Hernández-Molina, F.J., González, R., Dias, J.M.A., Díaz Del Río, G., Somoza, L., 2005. Holocene highstand deposits in the Gulf of Cadiz, SW Iberian Peninsula: a high-resolution record of hierarchical environmental changes. Mar. Geol. 219, 109–131.

Løseth, T.M., Steel, R.J., Crabaugh, J.P., Schellpeper, M., 2006. Interplay between shoreline migration paths, architecture and pinchout distance for siliciclastic shoreline tongues: evidence from the rock record. Sedimentology 53, 735–767.

Madof, A.S., Harris, A.D., Connell, S.D., 2016. Nearshore along-strike variability: is the concept of the systems tract unhinged? Geology 44 (4), 315–318.

Magyar, I., Radivojević, D., Sztanó, O., Synak, R., Ujszászi, K., Pócsik, M., 2013. Progradation of the paleo-Danube shelf margin across the Pannonian Basin during the Late Miocene and Early Pliocene. Glob. Planet. Chang. 103, 168–173.

Marriner, N., Flaux, C., Morhange, C., Kaniewski, D., 2012. Nile Delta's sinking past: Quantifiable links with Holocene compaction and climate-driven changes in sediment supply? Geology 40 (12), 1083–1086.

Martínez-Carreño, N., García-Gil, S., Cartelle, V., 2017. An unusual Holocene fan-shaped subaqueous prograding body at the back of the Cíes Islands ridge (Ría de Vigo, NW Spain): Geomorphology, facies and stratigraphic architecture. Mar. Geol. 385, 13–26.

Martinsen, O.J., Helland-Hansen, W., 1995. Strike variability of clastic depositional systems: Does it matter for sequence-stratigraphic analysis? Geology 23 (5), 439–442.

Maurer, F., Al-Mehsin, K., Pierson, B.J., Eberli, G.P., Warrlich, G., Drysdale, D., Droste, H.J., 2010. Facies characteristics and architecture of Upper Aptian Shu'aiba clinoforms in Abu Dhabi. Barremian–Aptian Stratigraphy and Hydrocarbon Habitat of the Eastern Arabian Plate. GeoArabia Special Publ. 4 (2), 445–468.

Mayall, M.J., Yeilding, C.A., Oldroyd, J.D., Pulham, A.J., Sakurai, S., 1992. Facies in a shelf-edge delta—an example from the subsurface of the Gulf of Mexico, Middle Pliocene, Mississippi Canyon, Block 109 (1). AAPG Bull. 76 (4), 435–448.

McClay, K.R., Dooley, T., Lewis, G., 1998. Analog modeling of progradational delta systems. Geology 26 (9), 771–774.

McKee, B.A., Nittrouer, C.A., DeMaster, D.J., 1983. Concepts of sediment deposition and accumulation applied to the continental shelf near the mouth of the Yangtze River. Geology 11 (11), 631–633.

Mellere, D., Plink-Björklund, P., Steel, R., 2002. Anatomy of shelf deltas at the edge of a prograding Eocene shelf margin, Spitsbergen. Sedimentology 49 (6), 1181–1206.

Michels, K.H., Kudrass, H.R., Hübscher, C., Suckow, A., Wiedicke, M., 1998. The submarine delta of the Ganges-Brahmaputra: cyclone-dominated sedimentation patterns.

Mar. Geol. 149, 133–154.

Milliman, J.D., Huang-Ting, S., Zuo-Sheng, Y., Mead, R.H., 1985. Transport and deposition of river sediment in the Changjiang estuary and adjacent continental shelf. Cont. Shelf Res. 4 (1-2), 37–45.

Mitchell, N.C., 2012. Modeling the rollovers of sandy clinoforms from the gravity effect on wave-agitated sand. J. Sediment. Res. 82 (7), 464–468.

Mitchell, N.C., Masselink, G., Huthnance, J.M., Fernández-Salas, L.M., Lobo, F.J., 2012. Depths of modern coastal sand clinoforms. J. Sediment. Res. 82 (7), 469–481.

Mitchum, R.M., Vail, P.R., Sangree, J.B., 1977. Seismic Stratigraphy and Global Changes of Sea Level: Part 6. Stratigraphic Interpretation of Seismic Reflection Patterns in Depositional Sequences: Section 2. Application of Seismic Reflection Configuration to Stratigraphic Interpretation.

Møller, I., Anthony, D., 2003. A GPR study of sedimentary structures within a transgressive coastal barrier along the Danish North Sea coast. Geol. Soc. Lond., Spec. Publ. 211 (1), 55–65.

Morales, J.A., 1997. Evolution and facies architecture of the mesotidal Guadiana River delta (SW Spain-Portugal). Mar. Geol. 138 (1-2), 127–148.

Mortimer, E., Gupta, S., Cowie, P., 2005. Clinoform nucleation and growth in coarse-grained deltas, Loreto basin, Baja California Sur, Mexico: a response to episodic accelerations in fault displacement. Basin Res. 17 (3), 337–359.

Morton, R.A., Suter, J.R., 1996. Sequence stratigraphy and composition of late Quaternary shelf-margin deltas, northern Gulf of Mexico. AAPG Bull. 80, 505–530.

Morton, R.A., Gibeaut, J.C., Paine, J.G., 1995. Meso-scale transfer of sand during and after storms: implications for prediction of shoreline movement. Mar. Geol. 126 (1-4), 161–179.

Mullins, H.T., Gardulski, A.F., Hine, A.C., Melillo, A.J., Wise, S.W., Applegate, J., 1988. Three-dimensional framework of the carbonate ramp slope of central west Florida: a sequential seismic stratigraphic perspective. Geol. Soc. Am. Bull. 100, 514–533.

Muto, T., Steel, R.J., 1992. Retreat of the front in a prograding delta. Geology 20, 967–970.

Muto, T., Steel, R.J., 1997. Principles of regression and transgression: the nature of the interplay between accommodation and sediment supply: perspectives. J. Sediment. Res. (6), 67.

Muto, T., Steel, R.J., 2002. In defence of shelf- edge delta development during falling and lowstand of relative sea level. J. Geol. 110, 421–436.

Muto, T., Steel, R.J., 2004. Autogenic response of fluvial deltas to steady sea-level fall: Implications from flume-tank experiments. Geology 32 (5), 401–404.

Muto, T., Steel, R.J., Swenson, J.B., 2007. Autostratigraphy: a framework norm for genetic stratigraphy. J. Sediment. Res. 77, 2–12.

Neal, J., Abreu, V., 2009. Sequence stratigraphy hierarchy and the accommodation succession method. Geology 37 (9), 779–782.

Neill, C.F., Allison, M.A., 2005. Subaqueous deltaic formation on the Atchafalaya Shelf, Louisiana. Mar. Geol. 214, 411–430.

Nemec, W., Steel, R.J., 1988. What is a Fan Delta and How Do We Recognize It. Fan Deltas: Sedimentology and Tectonic Settings. pp. 3–13.

Nittrouer, C.A., Kuehl, S.A., DeMaster, D.J., Kowsmann, R.O., 1986. The deltaic nature of Amazon shelf sedimentation. Geol. Soc. Am. Bull. 97 (4), 444–458.

Olariu, C., Bhattacharya, J.P., 2006. Terminal distributary channels and delta front architecture of river-dominated delta systems. J. Sediment. Res. 76 (2), 212–233.

Olariu, C., Steel, R.J., 2009. Influence of point- source sediment- supply on modern shelf-break morphology: implications for interpretation of ancient shelf margins. Basin Res. 21, 484–501.

Oliveira, C.M., Hodgson, D.M., Flint, S.S., 2011. Distribution of soft-sediment deformation structures in clinoform successions of the Permian Ecca Group, Karoo Basin South Africa. Sediment. Geol. 235 (3), 314–330.

Orton, G.J., Reading, H.G., 1993. Variability of deltaic processes in terms of sediment supply, with particular emphasis on grain size. Sedimentology 40, 475–512.

Ottesen, D., Rise, L., Sletten Andersen, E., Bugge, T., Eidvin, T., 2009. Geological evolution of the Norwegian continental shelf between 61° N and 68° N during the last 3 million years. Norwegian J. Geol. 89 (4).

Palamenghi, L., Schwenk, T., Spiess, V., Kudrass, H.R., 2011. Seismostratigraphic analysis with centennial to decadal time resolution of the sediment sink in the Ganges-Brahmaputra subaqueous delta. Cont. Shelf Res. 31, 712–739.

Palinkas, C.M., 2009. The timing of floods and storms as a controlling mechanism for shelf deposit morphology. J. Coast. Res. 1122–1129.

Palinkas, C.M., Nittrouer, C.A., 2006. Clinoform sedimentation along the Apennine shelf, Adriatic Sea. Mar. Geol. 234 (1), 245–260.

Patruno, S., 2017. A new look at the geology and prospectivity of a North Sea frontier area with modern seismic: the East Shetland Platform. In: 79th EAGE Conference and Exhibition 2017, Paris, France (Expo Porte de Versailles), Volume: Oral Presentation Session: Exploration Plays, Prospects and Prospects Evaluation II, Abstract Th C2 09. Extended abstract and oral presentation. Extended abstract available online at. http://www.earthdoc.org/publication/publicationdetails/?publication=88346 (June 15).

Patruno, S., Lampart, V., 2018. Newly-observed post-Variscan extensional mini-basins: the key to the prospectivity of the under-explored platform areas. In: Extended Abstract and Oral Presentation, 80th EAGE Conference and Exhibition, Copenaghen, Denmark, June 13.

Patruno, S., Reid, W., 2016. New plays on the Greater East Shetland Platform (UKCS Quadrants 3, 8–9, 14–16) – part 1: Regional setting and a working petroleum system. First Break 34, 33–45.

Patruno, S., Reid, W., 2017. New plays on the Greater East Shetland Platform (UKCS Quadrants 3, 8–9, 14–16) – part 2: Newly reported Permo-Triassic intra-platform basins and their influence on the Devonian-Paleogene prospectivity of the area. First Break (35), 59–69.

Patruno, S., Hampson, G.J., Jackson, C.A., 2015a. Quantitative characterisation of deltaic and subaqueous clinoforms. Earth Sci. Rev. 142, 79–119.

Patruno, S., Hampson, G.J., Jackson, C.A.L., Dreyer, T., 2015b. Clinoform geometry, geomorphology, facies character and stratigraphic architecture of a sand-rich subaqueous delta: Jurassic Sognefjord Formation, offshore Norway. Sedimentology 62 (1), 350–388.

Patruno, S., Hampson, G.J., Jackson, C.A.L., Whipp, P.S., 2015c. Quantitative progradation dynamics and stratigraphic architecture of ancient shallow-marine clinoform sets: a new method and its application to the Upper Jurassic Sognefjord Formation, Troll Field, offshore Norway. Basin Res. 27 (4), 412–452.

Patruno, S., Triantaphyllou, M.V., Erba, E., Dimiza, M.D., Bottini, C., Kaminski, M.A., 2015d. The Barremian and Aptian stepwise development of the 'Oceanic Anoxic Event 1a' (OAE 1a) crisis: integrated benthic and planktic high-resolution palaeoecology along the Gorgo a Cerbara stratotype section (Umbria-Marche Basin, Italy). Palaeogeogr. Palaeoecol. Palaeoecol. 424, 147–182.

Patruno, S., Reid, W., Jackson, C.A., Davies, C., Bowman, M., Levell, B., 2018. New insights into the unexploited reservoir potential of the Mid North Sea High (UKCS Quadrants 35–38, 41–43): a newly-described intra Zechstein sulphate-carbonate platform complex. In: Petroleum Geology of Northwest Europe: 50 Years of Learning – Proceedings of the 8th Petroleum Geology Conference. Geological Society, London, pp. 87–124. http://dx.doi.org/10.1144/PGC8.9. http://pgc.lyellcollection.org/content/early/2017/06/07/PGC8.9.full.pdf+html.

Patruno, S., Reid, W., Berndt, C., Feuilleaubois, L., 2018;al., in press. Polyphase tectonic inversion and its role in controlling hydrocarbon prospectivity in the Greater East Shetland Platform and Mid North Sea High, offshore UK. In: Monaghan, A.A., Underhill, J.R., Hewett, A.J., Marshall, J.E.A. (Eds.), Palaeozoic Plays of NW Europe. vol. 471 The Geological Society, Special Publications, London, United Kingdom (May 4). https://doi.org/10.1144/SP471.9. http://sp.lyellcollection.org/content/early/2018/05/03/SP471.9 (in press).

Pattison, S.A.J., 2005. Storm-influenced prodelta turbidite complex in the lower Kenilworth Member at Hatch Mesa, Book Cliffs, Utah, U.S.A.: implications for shallow marine facies models. J. Sediment. Res. 75 (3), 420–439.

Pellegrini, C., Maselli, V., Cattaneo, A., Piva, A., Ceregato, A., Trincardi, F., 2015. Anatomy of a compound delta from the post-glacial transgressive record in the Adriatic Sea. Mar. Geol. 362, 43–59.

Pellegrini, C., Maselli, V., Trincardi, F., 2016. Pliocene-Quaternary countourite depositional system along the south-western Adriatic margin: changes in sedimentary stacking pattern and associated bottom currents. Geo-Marine Letters 36 (1), 67–79.

Pellegrini, C., Maselli, V., Gamberi, F., Asioli, A., Bohacs, K.M., Drexler, T.M., Trincardi, F., 2017. How to make a 350-m-thick lowstand systems tract in 17,000 years: The Late Pleistocene Po River (Italy) lowstand wedge. Geology 45 (4), 327–330.

Pellegrini, C., Asioli, A., Bohacs, K.M., Drexler, T.M., Feldman, H.R., Sweet, M.L., Maselli, V., Rovere, M., Gamberi, F., Dalla Valle, G., Trincardi, F., 2018. The late Pleistocene Po River lowstand wedge in the Adriatic Sea: Controls on architecture variability and sediment partitioning. Mar. Pet. Geol. 93. http://dx.doi.org/10.1016/j.marpetgeo.2018.03.002.

Peltier, W.R., Fairbanks, R.G., 2006. Global glacial ice volume and Last Glacial Maximum duration from an extended Barbados sea level record. Quat. Sci. Rev. 25 (23), 3322–3337.

Pirmez, C., Pratson, L.F., Steckler, M.S., 1998. Clinoform development by advection-diffusion of suspended sediment: modeling and comparison to natural systems. J. Geophys. Res. Solid Earth 103 (B10), 24141–24157.

Plink-Björklund, P., Steel, R., 2002. Sea-level fall below the shelf edge, without basin-floor fans. Geology 30 (2), 115–118.

Plink-Björklund, P., Steel, R., 2006. Incised Valleys on an Eocene Coastal Plain and Shelf, Spitsbergen—Part of a Linked Shelf–Slope System.

Plink-Björklund, P., Mellere, D., Steel, R.J., 2001. Turbidite variability and architecture of sand-prone, deep-water slopes: eocene clinoforms in the Central Basin, Spitsbergen. J. Sediment. Res. 71 (6), 895–912.

Plint, A.G., Tyagi, A., Hay, M.J., Varban, B.L., Zhang, H., Roca, X., 2009. Clinoforms, paleobathymetry, and mud dispersal across the Western Canada Cretaceous foreland basin: evidence from the Cenomanian Dunvegan Formation and contiguous strata. J. Sediment. Res. 79 (3), 144–161.

Plint, A.G., Nummedal, D., 2000. The falling stage systems tract: recognition and importance in sequence stratigraphic analysis. In: Hunt, D., Gawthorpe, R.L. (Eds.), Sedimentary Responses to Forced Regressions, Geological Society. 172. Special Publications, London, pp. 1–17.

Pomar, L., Tropeano, M., 2001. The Calcarenite di Gravina Formation in Matera (southern Italy): new insights for coarse-grained, large-scale, cross-bedded bodies encased in offshore deposits. AAPG Bull. 85, 661–689.

Pomar, L., Obrador, A., Westphal, H., 2002. Sub-wave base cross-bedded grainstones on a distally steepened carbonate ramp, Upper Miocene, Menorca, Spain. Sedimentology 49, 139–169.

Ponce, J.J., Olivero, E.B., Martinioni, D.R., 2008. Upper Oligocene–Miocene clinoforms of the foreland Austral Basin of Tierra del Fuego, Argentina: Stratigraphy, depositional sequences and architecture of the foredeep deposits. J. S. Am. Earth Sci. 26 (1), 36–54.

Porębski, S.J., Steel, R.J., 2003. Shelf-margin deltas: their stratigraphic significance and relation to deepwater sands. Earth-Sci. Rev. 62, 283–326.

Porębski, S.J., Steel, R.J., 2006. Deltas and sea-level change. J. Sediment. Res. 76, 390–403.

Porębski, S.J., Pietsch, K., Hodiak, R., Steel, R.J., 2003. Origin and sequential development of Badenian-Sarmatian clinoforms in the Carpathian foreland basin (SE Poland). Geol. Carpath. 54, 119–136.

Postma, G., 1984. Slumps and their deposits in fan delta front and slope. Geology 12 (1), 27–30.

Postma, G., 1995. Sea-level-related architectural trends in coarse-grained delta

complexes. Sediment. Geol. 98 (1-4), 3–12.

Pratson, L.F., Ryan, W.B.F., Mountain, G.S., Twichell, D.C., 1994. Submarine canyon initiation by downslope eroding sediment flows: evidence in Late Cenozoic strata on the New Jersey continental slope. Geol. Soc. Am. Bull. 106, 395–412.

Prior, D.B., Yang, Z.S., Bornhold, B.D., Keller, G.H., Lin, Z.H., Wiseman, W.J., Wright, L.D., Lin, T.C., 1986. The subaqueous delta of the modern Huanghe (Yellow River). Geo-Mar. Lett. 6 (2), 67–75.

Puga-Bernabéu, Á., Martín, J.M., Braga, J.C., Sánchez-Almazo, I.M., 2010. Downslope-migrating sandwaves and platform-margin clinoforms in a current-dominated, distally steepened temperate-carbonate ramp (Guadix Basin, Southern Spain). Sedimentology 57 (2), 293–311.

Puig, P., Ogston, A.S., Guillén, J., Fain, A.M.V., Palanques, A., 2007. Sediment transport processes from the topset to the foreset of a crenulated clinoform (Adriatic Sea). Cont. Shelf Res. 27 (3), 452–474.

Qiu, J., Liu, J., Saito, Y., Yang, Z., Yue, B., Wang, H., Kong, X., 2014. Sedimentary evolution of the Holocene subaqueous clinoform off the southern Shandong Peninsula in the Western South Yellow Sea. J. Ocean Univ. China 13 (5), 747–760.

Quiquerez, A., Dromart, G., 2006. Environmental control on granular clinoforms of ancient carbonate shelves. Geol. Mag. 143 (3), 343–365.

Rasmussen, E.S., 2009. Detailed mapping of marine erosional surfaces and the geometry of clinoforms on seismic data: a tool to identify the thickest reservoir sand. Basin Res. 21 (5), 721–737.

Reeder, D.B., Ma, B.B., Yang, Y.J., 2011. Very large subaqueous sand dunes on the upper continental slope in the South China Sea generated by episodic, shoaling deep-water internal solitary waves. Mar. Geol. 279 (1), 12–18.

Reeve, M.T., Jackson, C.A.L., Bell, R.E., Magee, C., Bastow, I.D., 2016. The stratigraphic record of prebreakup geodynamics: Evidence from the Barrow Delta, offshore Northwest Australia. Tectonics 35 (8), 1935–1968.

Reid, W., Patruno, S., November 2015. The East Shetland Platform: unlocking the platform potential. With significant advancements in seismic acquisition technology, it is time to re-visit the East Shetland Platform. GeoExpro 12 (6), 41–46.

Rice, P.D., Shade, B.D., 1982. Reflection seismic interpretation and seafloor spreading history of Baffin Bay. In: Embry, A.F., Balkwill, H.R. (Eds.), Arctic Geology and Geophysics, Proceedings of the Third International Symposium on Arctic Geology, pp. 245–265 Canadian Society of Petroleum Geologists Memoir 8.

Rich, J.L., 1951. Three critical environments of deposition and criteria for recognition of rocks deposited in each of them. GSA Bull. 62, 1–20.

Ritchie, B.D., Gawthorpe, R.L., Hardy, S., 2004a. Three-dimensional numerical modeling of deltaic depositional sequences 1: Influence of the rate and magnitude of sea-level change. J. Sediment. Res. 74 (2), 203–220.

Ritchie, B.D., Gawthorpe, R.L., Hardy, S., 2004b. Three-dimensional numerical modeling of deltaic depositional sequences 2: influence of local controls. J. Sediment. Res. 74 (2), 221–238.

Roberts, H.H., Sydow, J., 2003. Late Quaternary Stratigraphy and Sedimentology of the Offshore Mahakam Delta, East Kalimantan (Indonesia).

Roberts, H.H., Adams, R.D., Cunningham, R.H.W., 1980. Evolution of sand-dominant subaerial phase, Atchafalaya Delta, Louisiana. AAPG Bull. 64 (2), 264–279.

Rodger, M., Watts, A.B., Greenroyd, C.J., Peirce, C., Hobbs, R.W., 2006. Evidence for unusually thin oceanic crust and strong mantle beneath the Amazon Fan. Geology 34 (12), 1081–1084.

Ross, W.C., Halliwell, B.A., May, J.A., Watts, D.E., Syvitski, J.P.M., 1994. Slope readjustment; a new model for the development of submarine fans and aprons. Geology 22, 511–514.

Ryan, M.C., Helland-Hansen, W., Johannessen, E.P., Steel, R.J., 2009a. Erosional vs. accretionary shelf margins: the influence of margin type on deepwater sedimentation: an example from the Porcupine Basin, offshore western Ireland. Basin Res. 21 (5), 676–703.

Ryan, W.B.F., Carbotte, S.M., Coplan, J.O., O'Hara, S., Melonian, A., Arko, R., Weissel, R.A., Ferrini, V., Goodwillie, A., Nitsche, F., Bonczkowski, J., Zemsky, R., 2009b. Global multi-resolution topography synthesis. Geochem. Geophys. Geosyst. 10 (3), 1–9. http://dx.doi.org/10.1029/2008GC002332.

Sadler, P.M., 1981. Sediment accumulation rates and the completeness of stratigraphic sections. The Journal of Geology 89 (5), 569–584.

Saito, Y., Wei, H., Zhou, Y., Nishimura, A., Sato, Y., Yokota, S., 2000. Delta progradation and chenier formation in the Huanghe (Yellow River) delta, China. J. Asian Earth Sci. 18 (4), 489–497.

Savrda, C.E., Browning, J.V., Krawinkel, H., Hesselbo, S.P., 2001. Firmground ichnofabrics in deep-water sequence stratigraphy, Tertiary clinoform-toe deposits, New Jersey slope. Palaios 16 (3), 294–305.

Schlee, J.S., Dillon, W.P., Grow, J.A., 1979. Structure of the continental slope off the eastern United States. In: Doyle, L.J., Pilkey, O.H. (Eds.), Geology of Continental Slopes. vol. 27. Society of Economic Paleontologists and Mineralogists, Special Publications, pp. 95–117.

Scisciani, V., Patruno, S., Tavarnelli, E., Calamita, F., Pace, P., Iacopini, D., in review. Modes of reactivation of Late Paleozoic-Mesozoic extensional basins during the Wilson Cycle: case studies from the North Sea (UK) and central Apennines (Italy). In: Tectonic Evolution: 50 Years of the Wilson Cycle Concept. Geological Society Special Publications, The Geological Society, London, United Kingdom.

Sheremet, A., Jaramillo, S., Su, S.F., Allison, M.A., Holland, K.T., 2011. Wave-mud interaction over the muddy Atchafalaya subaqueous clinoform, Louisiana, United States: Wave processes. J. Geophys. Res. 116, C6.

Shipley, T.H., Buffler, R.T., Watkins, J.S., 1978. Seismic stratigraphy and geologic history of Blake Plateau and adjacent western Atlantic continental margin. AAPG Bull. 62 (5), 792–812.

Short, K.C., Stauble, A.J., 1967. Outline of geology of Niger Delta. AAPG Bull. 51 (5), 761–779.

Siringan, F.P., Anderson, J.B., 1993. Seismic facies, architecture, and evolution of the Bolivar Roads tidal inlet/delta complex, east Texas Gulf Coast. J. Sediment. Res. 63 (5).

Smith, D.G., Jol, H.M., 1997. Radar structure of a Gilbert-type delta, Peyto Lake, Banff National Park, Canada. Sediment. Geol. 113 (3-4), 195–209.

Sornoza, L., Barnolas, A., Arasa, A., Maestro, A., Rees, J.G., Hernandez-Molina, F.J., 1998. Architectural stacking patterns of the Ebro delta controlled by Holocene high-frequency eustatic fluctuations, delta-lobe switching and subsidence processes. Sediment. Geol. 117 (1-2), 11–32.

Stanley, D.J., Chen, Z., 1996. Neolithic settlement distributions as a function of sea level–controlled topography in the Yangtze delta, China. Geology 24 (12), 1083–1086.

Steckler, M.S., Mountain, G.S., Miller, K.G., Christie-Blick, N., 1999. Reconstruction of Tertiary progradation and clinoform development on the New Jersey passive margin by 2-D backstripping. Mar. Geol. 154 (1), 399–420.

Steel, R.J., Olsen, T., 2002. Clinoforms, clinoform trajectory and deepwater sands. In: Armentrout, J.M., Rosen, N.C. (Eds.), Sequence Stratigraphic Models for Exploration and Production: Evolving Methodology, Emerging Models and Application Histories. GCS-SEPM Special Publication, pp. 367–381.

Steel, R.J., Crabaugh, J., Schellpeper, M., Mellere, D., Plink-Björklund, P., Deibert, J., Loeseth, T., 2000. Deltas vs. rivers on the shelf edge: their relative contributions to the growth of shelf-margins and basin-floor fans (Barremian and Eocene, Spitsbergen). Deepwater Reserv. World 15 (1), 981–1009.

Steel, R.J., Porebski, S.J., Plink-Bjorklund, P., Mellere, D., Schellpeper, M., 2003. Shelf-Edge Delta Types and their Sequence-Stratigraphic Relationships. Shelf Margin Deltas and Linked Down Slope Petroleum Systems. pp. 205–230.

Steel, R.J., Carvajal, C., Petter, A.L., Uroza, C., 2008. Shelf and shelf-margin growth in scenarios of rising and falling sea level. In: Hampson, G.J., Steel, R.J., Burgess, P.M., Dalrymple, R.W. (Eds.), Recent Advances in Models of Siliciclastic Shallow-Marine. vol. 90. SEPM Special Publications, pp. 47–71.

Stive, M.J., Aarninkhof, S.G., Hamm, L., Hanson, H., Larson, M., Wijnberg, K.M., Nicholls, R.J., Capobianco, M., 2002. Variability of shore and shoreline evolution. Coast. Eng. 47 (2), 211–235.

Stouthamer, E., Berendsen, H.J., 2000. Factors controlling the Holocene avulsion history of the Rhine-Meuse delta (The Netherlands). J. Sediment. Res. 70 (5), 1051–1064.

Stow, D.A.V., Faugères, J.-C., Howe, J.A., Pudsey, C.J., Viana, A.R., 2002. Bottom currents, contourites and deep-sea sediment drifts: current state-of-the-art. Geol. Soc. Lond. Mem. 22, 7–20. http://dx.doi.org/10.1144/GSL.MEM.2002.022.01.02.

Summerhayes, C.P., Sestini, G., Misdorp, R., Marks, N., 1978. Nile Delta: nature and evolution of continental shelf sediments. Mar. Geol. 27 (1–2), 43–65.

Suter, J.R., Berryhill Jr., H.L., 1985. Late Quaternary shelf-margin deltas, Northwest Gulf of Mexico. AAPG Bull. 69 (1), 77–91.

Sweet, M.L., Blum, M.D., 2016. Connections between fluvial to shallow marine environments and submarine canyons: implications for sediment transfer to deep water. J. Sediment. Res. 86 (10), 1147–1162.

Swenson, J.B., Paola, C., Pratson, L., Voller, V.R., Murray, A.B., 2005. Fluvial and marine controls on combined subaerial and subaqueous delta progradation: morphodynamic modeling of compound-clinoform development. J. Geophys. Res. Earth Surf. (F2), 110.

Sydow, J., Roberts, H.H., 1994. Stratigraphic framework of a late Pleistocene shelf-edge delta, northeast Gulf of Mexico. AAPG Bull. 78 (8), 1276–1312.

Sydow, J., Finneran, J., Bowman, A.P., Rosen, H., Fillon, R., Anderson, J., 2003. Stacked shelf-edge delta reservoirs of the Columbus Basin, Trinidad, West Indies. Shelf-Margin Deltas and Linked Downslope Petroleum Systems. pp. 441–465.

Sztanó, P., Szafián, P., Magyar, I., Horányi, A., Bada, G., Hughes, D.W., Hoyer, D.L., Wallis, R.J., 2013. Aggradation and progradation controlled clinothems and deep-water sand delivery model in the Neogene Lake Pannon, Makó Trough, Pannonian Basin, SE Hungary. Glob. Planet. Chang. 103, 149–167.

Ta, T.K.O., Nguyen, V.L., Tateishi, M., Kobayashi, I., Tanabe, S., Saito, Y., 2002. Holocene delta evolution and sediment discharge of the Mekong River, southern Vietnam. Quat. Sci. Rev. 21 (16), 1807–1819.

Tamura, T., Saito, Y., Masuda, F., 2008. Variation in architecture of the Holocene to modern prograding shoreface along the Pacific coast of eastern Japan. In: Hampson, G.J., Steel, R.J., Burgess, P.M., Dalrymple, R.W. (Eds.), Recent Advances in Models of Siliciclastic Shallow-Marine Stratigraphy. vol. 90. SEPM Special Publication, pp. 191–205.

Tesson, M., Gensous, B., Allen, G.P., Ravenne, C., 1990. Late Quaternary deltaic lowstand wedges on the Rhône continental shelf, France. Mar. Geol. 91 (4), 325–332.

Tesson, M., Posamentier, H.W., Gensous, B., 2000. Stratigraphic organization of late pleistocene deposits of the Western Part Of The Golfe du Lion Shelf (Languedoc Shelf), Western Mediterranean Sea, using high-resolution seismic and core data. AAPG Bull. 84 (1), 119–150.

Thorne, J., 1995. On the scale independent shape of prograding stratigraphic units. In: Barton, C., La Pointe, P. (Eds.), Fractals in Petroleum Geology and Earth Processes. Springer US, pp. 97–112.

Törnqvist, T.E., 1994. Middle and late Holocene avulsion history of the River Rhine (Rhine-Meuse delta, Netherlands). Geology 22 (8), 711–714.

Tucker, M.E., 1991. Sequence stratigraphy of carbonate-evaporite basins: models and application to the Upper Permian (Zechstein) of northeast England and adjoining North Sea. J. Geol. Soc. Lond. 148, 1019–1036.

Turner, C.C., Cronin, B.T., Riley, L.A., Patruno, S., Reid, W.T.L., Hoth, S., Knaust, D., Allerton, S., Jones, M.A., and Jackson, C.A-L., in press. The South Viking Graben: overview of Upper Jurassic rift geometry, biostratigraphy and extent of Brae Play submarine fan systems. In: Turner, C.C. & Cronin, B.T. (eds.), Rift-Related Coarse-Grained Submarine Fan Reservoirs: The Brae Play, South Viking Graben, North Sea. American Association of Petroleum Geologists, AAPG Mem 115, DOI:https://doi.org/10.1306/13652177M1153807

Uchupi, E., 1968. Atlantic Continental Shelf and Slope of the United States: Physiography. US Government Printing Office, pp. 30.

Unida, S., Patruno, S., 2016. The palynostratigraphy of the upper Maiolica, Selli Level and the lower Marne a Fucoidi units in the proposed Barremian/Aptian (Lower Cretaceous) GSSP stratotype at Gorgo a Cerbara, Umbria-Marche Basin, Italy. Palynology 40 (2), 230–246.

Uroza, C.A., Steel, R.J., 2008. A highstand shelf-margin delta system from the Eocene of West Spitsbergen, Norway. Sediment. Geol. 203 (3), 229–245.

Van Wagoner, J.C., Mitchum, R.M., Campion, K.M., Rahmanian, V.D., 1990. Siliciclastic Sequence stratigraphy in well logs, cores, and outcrops: concepts for high resolution correlation of time and facies. AAPG Methods Exploration 7 (55 pp.).

Vanney, J.R., Stanley, D.J., 1983. Shelfbreak physiography: an overview. In: Stanley, D.J., Moore, G.T. (Eds.), The Shelf Break: Critical Interface on Continental Margins. vol. 33. SEPM Special Publicaltion, pp. 1–24.

Viana, A.R., Faugères, J.C., Kowsmann, R.O., Lima, J.A.M., Caddah, L.F.G., Rizzo, J.G., 1998. Hydrology, morphology and sedimentology of the Campos continental margin, offshore Brazil. Sediment. Geol. 115 (1-4), 133–157.

Walsh, J.P., Nittrouer, C.A., 2003. Contrasting styles of off-shelf sediment accumulation in New Guinea. Mar. Geol. 196 (3), 105–125.

Walsh, J.P., Nittrouer, C.A., Palinkas, C.M., Ogston, A.S., Sternberg, R.W., Brunskill, G.J., 2004. Clinoform mechanics in the Gulf of Papua, New Guinea. Cont. Shelf Res. 24 (19), 2487–2510.

Wessel, P., Smith, W.H., 1996. A global, self-consistent, hierarchical, high-resolution shoreline database. J. Geophys. Res. Solid Earth 101 (B4), 8741–8743.

Wolinsky, M.A., Pratson, L.F., 2007. Overpressure and slope stability in prograding clinoforms: Implications for marine morphodynamics. J. Geophys. Res. Earth Surf. (F4), 112.

Wood, S.E., Gorin, G.E., 1998. Sedimentary organic matter in distal clinoforms of Miocene slope sediments: Site 903 of ODP Leg 150, offshore New Jersey (USA). J. Sediment. Res. 68 (5).

Xue, Z., Liu, J.P., DeMaster, D., Van Nguyen, L., Ta, T.K.O., 2010. Late Holocene evolution of the Mekong subaqueous delta, southern Vietnam. Mar. Geol. 269 (1), 46–60.

Yang, C.S., Nio, S.D., 1989. An ebb-tide delta depositional model—A comparison between the modern eastern Scheldt tidal basin (southwest Netherlands) and the lower Eocene Roda Sandstone in the southern Pyrenees (Spain). Sediment. Geol. 64 (1), 175–196.

Zecchin, M., Catuneanu, O., 2013. High-resolution sequence stratigraphy of clastic shelves I: units and bounding surfaces. Mar. Pet. Geol. 39 (1), 1–25.

Zhou, L., Liu, J., Saito, Y., Liu, J.P., Li, G., Liu, Q., Gao, M., Qiu, J., 2014. Fluvial system development and subsequent marine transgression in Yellow River (Huanghe) delta and its adjacent sea regions during last glacial maximum to early Holocene. Cont. Shelf Res. 90, 117–132.